OFFICIAL JOURNAL OF THE SCIENTIFIC SOCIETY OF ANATOMISTS, HISTOLOGISTS, EMBRYOLOGISTS AND TOPOGRAPHIC ANATOMISTS OF UKRAINE

DOI: 10.31393
ISSN 1818-1295
eISSN 2616-6194

ВІСНИК МОРФОЛОГІЇ
REPORTS OF MORPHOLOGY

Vol. 28, №3, 2022

Scientific peer-reviewed journal in the fields of normal and pathological anatomy, histology, cytology and embryology, topographical anatomy and operative surgery, biomedical anthropology, ecology, molecular biology, biology of development

Published since 1993
Periodicity: 4 times a year

Vinnytsya · 2022

ВІСНИК МОРФОЛОГІЇ - REPORTS OF MORPHOLOGY

Founded by the "Scientific Society of Anatomists, Histologists, Embryologists, and Topographic Anatomists of Ukraine" and National Pyrogov Memorial Medical University, Vinnytsya in 1993

Certificate of state registration КВ №9310 from 02.11.2004

Professional scientific publication of Ukraine in the field of medical sciences in specialties 221, 222, 228, 229
According to the list of professional scientific publications of Ukraine, approved by the order of the Ministry of Education and Science of Ukraine No. 1188 of 24.09.2020
Professional scientific publication of Ukraine in the field of biological sciences in specialty 091
According to the list of professional scientific publications of Ukraine, approved by the order of the Ministry of Education and Science of Ukraine No. 1471 of 26.11.2020

Approved by the Academic Council of National Pyrogov Memorial Medical University, Vinnytsya, protocol №1 from 02.09.2022.

Indexation: CrossRef, Index Copernicus, Google Schoolar Metrics, National Library of Ukraine Vernadsky

Address editors and publisher:
Pyrogov Str. 56,
Vinnytsya, Ukraine - 21018
Tel.: +38 (0432) 553959
E-mail: nila@vnmu.edu.ua

Computer page-proofs - Klopotovska L.O.
Translator - Gunas V.I.
Technical support - Levenchuk S.S.
Scientific editing - editorship

The site of the magazine - https://morphology-journal.com

CONTENT

DOI: 10.31393/morphology-journal-2022-28(3)-01 Reports of Morphology, Vol. 28, №3, Pages 5-13

ISSN 1818-1295 eISSN 2616-6194

REPORTS OF MORPHOLOGY

Official Journal of the Scientific Society of Anatomists, Histologists, Embryologists and Topographic Anatomists of Ukraine

journal homepage: https://morphology-journal.com

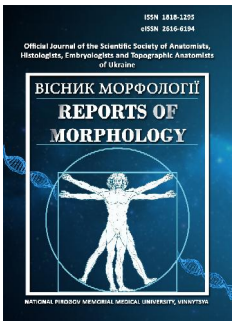

Radiological psoas muscle parameters as a reliable tool for detection of sarcopenia and prediction of short-term survival in liver cirrhosis

Motsiuk V. M., Pentiuk N. O.
National Pirogov Memorial Medical University, Vinnytsya, Ukraine

ARTICLE INFO
Received: 18 May 2022
Accepted: 20 June 2022

UDC: 616.74:616.36-004:621.3.088.6

CORRESPONDING AUTHOR
e-mail: pentiuk.na@gmail.com
Pentiuk N. O.

CONFLICT OF INTEREST
The authors have no conflicts of interest to declare.

FUNDING
Not applicable.

Loss of skeletal muscle mass or sarcopenia is associated with the development of complications and mortality in patients with liver cirrhosis (LC). Skeletal muscle index (SMI) is the most validated parameter of sarcopenia in clinical studies, but its evaluation is difficult in routine clinical practice. The purpose of the study was to assess the diagnostic concordance between different radiologic skeletal muscle parameters and their relationship with a short-term survival of LC patients. The study involved 147 LC patients, including 90 males and 57 females (55.51±0.97). Child-Turcotte-Pugh (CTP) class A was diagnosed in 23 patients, class B in 51 patients, and class C in 73 patients. 50 patients died from LC complications during the follow-up period (489 (306 - 637) days). Skeletal muscle index (SMI), psoas muscle mass index (PMI), and transversal psoas muscle thickness (TPMT) were calculated using the computed tomography at L3 level. The statistical data was processed using the SPSS22 software (© SPSS Inc.). PMI and TPMT were found to be objective parameters of sarcopenia in LC patients having stable diagnostic concordance with SMI (r Spearman's 0.734, 0.649, p<0.001; k Cohen's 0.727, 0.643, p<0.001, respectively). The use of all three parameters allowed to reveal more patients with a reduced skeletal muscle mass. Sarcopenia was diagnosed in 54.9 % of CTP B patients, 86.3 % of CTP C patients, and was associated with an elevated incidence of ascites, hydrothorax, hepatic encephalopathy, and hypoalbuminemia. Sarcopenic patients were found more likely to have an alcohol-related etiology than viral one (HBV, HCV). The overall survival of patients with low SMI, PMI and TPMT was significantly lower according to Kaplan-Meier analysis. SMI, PMI, and TPMT were independent predictors of LC-associated mortality (HR 2.66, 2.19, 2.21, respectively, p<0.05) in Cox proportional hazards regression. At least one of the three decreased radiologic skeletal muscle mass parameters was associated with the highest risk of fatal LC complications (HR 3.65, p=0.021). Therefore, the psoas muscle dimensions were considered a reliable tool for detection of sarcopenia and prediction of short-term survival in LC.

Keywords: *psoas muscle, sarcopenia, liver cirrhosis, hepatitis C, hepatitis B, alcohol-related liver disease.*

Introduction

Liver cirrhosis (LC) is the final stage of chronic liver disease that causes more than 1.03 million deaths worldwide each year [30]. Today, LC is considered as a dynamic process of liver function deterioration, worsening of portal hypertension, associated complications, such as jaundice, ascites, bleeding, encephalopathy, kidney injury, and infectious complications. One-year LC mortality varies from 1 to 3.4 % in compensated patients to 67 % in decompensated patients [30]. Recent studies have shown that malnutrition and its main clinical manifestation sarcopenia are common LC complications associated with unfavorable prognosis [26]. Decreased skeletal muscle mass is associated with hepatic encephalopathy, spontaneous bacterial peritonitis, sepsis, longer hospital stays, higher treatment costs, decreased pre- and post-transplant survival [3, 13, 14, 27, 31, 34].

Computed tomography (CT) is the basic method of skeletal muscle mass assessment. It has been found that

the cross-sectional skeletal muscles area at L3 level strongly reflects the total skeletal muscles mass [19]. The Skeletal Muscle Index (SMI), a height-normalized cross-sectional skeletal muscle area, is the most studied sarcopenia parameter, which has proven its prognostic reliability in LC patients [4, 13]. However, SMI evaluation in clinical practice is associated with certain limitations, as it requires special software, qualified radiologist expertise and significant time [16]. Isolated psoas muscle visualization is technically simpler, and calculating the area or thickness is not so time-consuming process depending on special software. Today, the diagnostic and prognostic importance of psoas muscle parameters for LC patients is still unclear [26].

The purpose of the study was to evaluate the diagnostic concordance between different radiologic skeletal muscle mass parameters and their relationship with short-term survival of LC patients.

Materials and methods

Between 2018 and 2020, 147 LC patients, including 90 males and 57 females (mean age 55.51±0.97) were involved in the study. All participants were informed about the purpose of the study and provided their written consent. Committee on Bioethics of National Pirogov Memorial Medical University, Vinnytsya (protocol № 8 From 17.10.2019) found that the studies do not contradict the basic bioethical standards of the Declaration of Helsinki, the Council of Europe Convention on Human Rights and Biomedicine (1977), the relevant WHO regulations and laws of Ukraine.

Child-Turcotte-Pugh (CTP) Class A was diagnosed in 23 patients, Class B - in 51, and class C - in 73 patients. Viral (HBV, HCV) aetiology was confirmed in 26, alcohol-related - in 85, and viral-alcohol-related - in 36 patients. At baseline, 107 patients had $\geq$ 20 MELD. The patients were followed-up until 2022. During this time, 50 patients died from LC complications.

The skeletal muscle indexes were assessed using CT (Fig. 1). The skeletal muscle cross-sectional area measured at L3 level was normalized to height and the SMI was calculated [24]. Total psoas muscle (right and left) area was normalized to height, and the psoas muscle mass index (PMI) was calculated. The muscle area was visualized and measured using NIH ImageJ version 1.52a software package (https://imagej.nih.gov/ij/download.html) within the range -29 +150 HU [9, 19]. Psoas muscle thickness (mean right and left muscle thickness) was determined using MicroDicom viewer version 2.2.5 as the largest transversal dimension perpendicular to the longitudinal axis of the muscle [29]. The value was normalized to height and the transversal psoas muscle thickness (TPMT) was calculated. The reference values were considered SMI>52.2 and >39.3 cm^2/m^2, PMI>6.44 and >3.49 cm^2/m^2, TPMT>11.1 and >7.42 mm/m in males and females, respectively [18]. A decrease of at least one of the parameters was regarded as sarcopenia.

The statistical data was processed using the SPSS22 software package (© SPSS Inc.). The mean, standard deviation, and standard error of the mean were calculated.

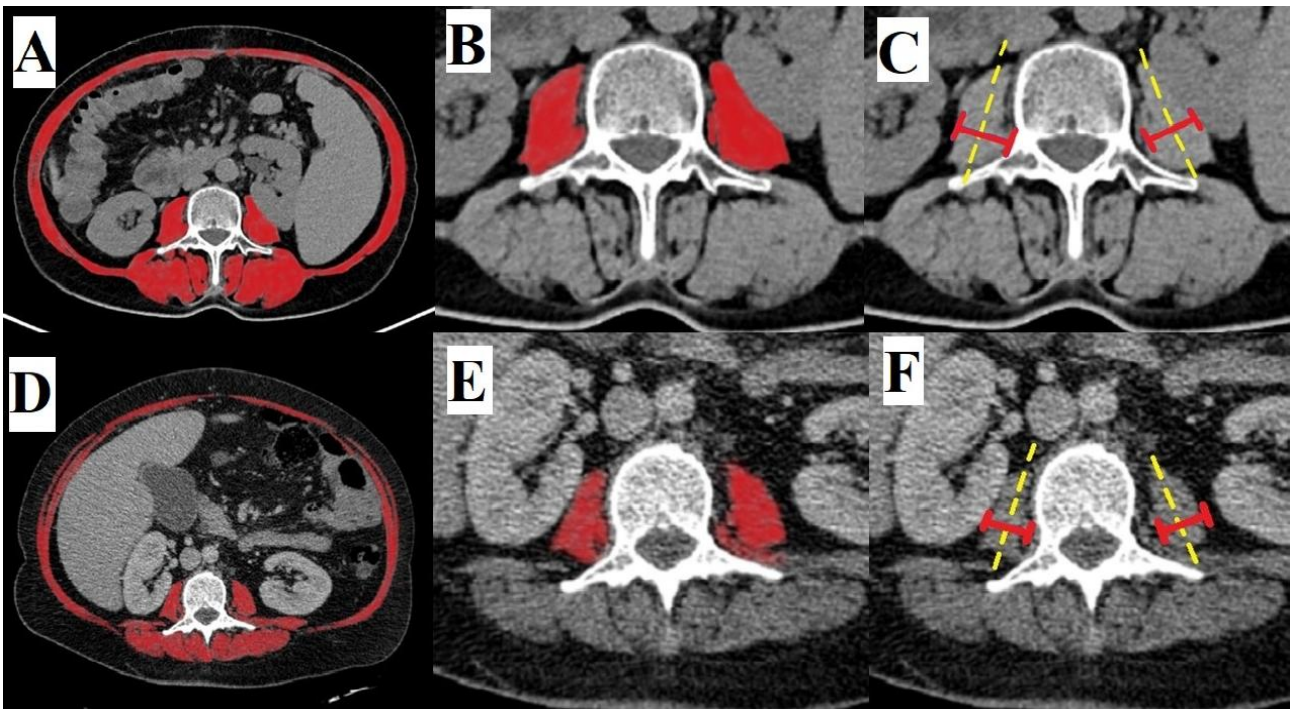

Fig. 1. Abdominal CT images at the third lumbar vertebra level; A, B, C: Non-sarcopenic female patient with SMI 42.0 cm^2/m^2; PMI 5.79 cm^2/m^2; TPMT 12.4 mm/m. D, E, F - sarcopenic female patient with SMI 36.7 cm^2/m^2; PMI 3.31 cm^2/m^2; TPMT 5.09 mm/m.

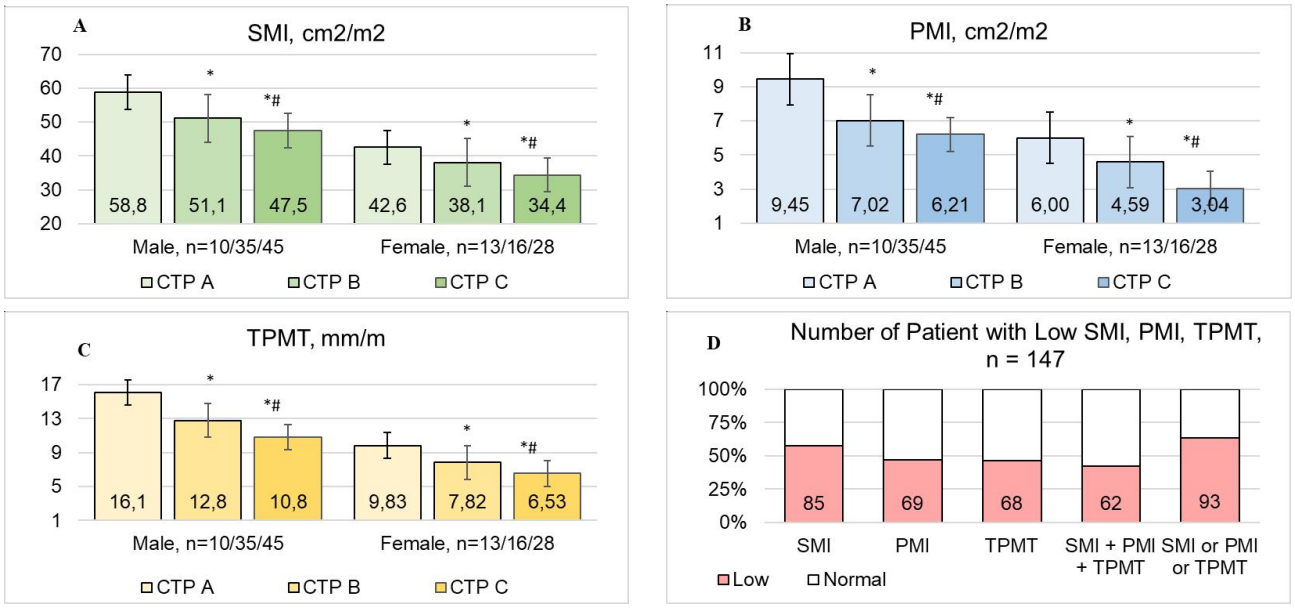

Fig. 2. Muscularity variables in LC patients (M ± SD).
Note: * - p value <0.05 between CTP A and CTP B; # - p value <0.05 between CTP B and CTP C.

Parametric Student's t-test and non-parametric Mann-Whitney U test were used to evaluate the intergroup difference, while Fisher's exact test was used to compare the frequency of changes, and Spearman's rank correlation coefficient was used to determine the relationships between values. The diagnostic concordance between parameters was assessed using Cohen`s kappa statistic and ROC analysis. The patient survival was analyzed using the Kaplan-Meier method, while survival curves were compared using the Logrank test. The Cox regression method was used to assess the mortality predictors. The difference at $p<0.05$ was considered statistically significant. The results were presented as M±SD, M±m, and Me (P_{25} - P_{75}).

Results

LC progression was accompanied by loss of skeletal muscle mass (Fig. 2). The most pronounced decrease of the cross-sectional skeletal muscle area, psoas muscle area and psoas muscle thickness occurred in CTP C patients. The sarcopenia incidence significantly increased with higher CTP class and reached 4.35 % in CTP A patients, 54.9 % - in CTP B, and 86.3 % in CTP C patients ($p<0.05$).

PMI and TPMT significantly correlated with SMI (r Spearman's 0.734, 0.649, respectively, $p<0.001$). ROC analysis showed that low PMI and TPMT values could be a reliable predictor of SMI-established sarcopenia (AUC 0.870, 0.828, respectively, $p<0.001$). 127 of 147 patients were equally assessed using SMI and PMI (i.e., as patients with normal or low muscle mass), while 120 of 147 patients were equally assessed using SMI and TPMT. Cohen's kappa for SMI and PMI was 0.727, for SMI and TPMT was 0.643 ($p<0.001$), which represented a moderate diagnostic agreement between indexes. Worthy to note that simultaneous decrease of PMI, SMI and TPMT was observed in only 42.2 % of patients, while the decrease of at least one of the parameters was observed in 63.3 % of patients.

Table 1. Baseline characteristics of the study population according to sarcopenia.

Characteristics	Sarcopenia absent, n=53	Sarcopenia present, n=94
Age (years), M ± SD	58.13±11.54	53.98±11.82*
Male, n (%) Female, n (%)	24 (45.3) 29 (54.7)	33 (35.1) 61 (64.9)
Viral (HBV, HCV) etiology, n (%) Alcohol-related etiology, n (%) Mixed (viral, alcohol-related) etiology, n (%)	17 (32.1) 19 (35.8) 17 (32.1)	9 (9.57) * 66 (70.2) * 19 (20.2)
Ascites 1 degree, n (%) Ascites 2 - 3-degree, n (%)	25 (47.2) 18 (33.9)	24 (25.5) * 60 (63.8) *
Platelets (*109/L), M ± SD	181.8±77.4	134.6±65.5*
Serum creatinine, (?mol/L), Me (P_{25}- P_{75})	76.0 (69.5 - 92.5)	76.5 (69.0 - 117)
Hepatorenal syndrome, n (%)	7 (13.2)	18 (19.1)
Hydrothorax, n (%)	5 (9.43)	24 (25.5)*
Hepatic encephalopathy I stage, n (%) Hepatic encephalopathy II - III stage, n (%)	10 (18.9) 1 (1.89)	34 (36.2)* 37 (39.4)*
Total bilirubin (mmol/L), Me (P_{25}- P_{75})	24,1 (17,1 - 43,7)	60,0 (36,0 - 98,0)*
Prothrombin time (INR), Me (P_{25}- P_{75})	2.18 (1.60 - 2.57)	2.91 (2.30 - 3.30)*
Albumin (g/L), M ± SD	37.31±5.34	30.77±4.93*
Albumin < 30 g/L, n (%)	6 (11.3)	42 (44.6)*
CTP, M ± SD	7.585±1.965	10.37±1.884*
MELD, M ± SD	19.01±8.50	29.09±7.08*

Note: * - p value <0.05.

Table 2. Muscularity variables in LC patients according to the survival status (M ± SD, %).

Variables	Men		Women	
	Survivors, n=71	Non-survivors, n=31	Survivors, n=40	Non-survivors, n=19
SMI, cm^2/m^2	52.27±6.86	45.99±5.60*	38.96±5.19	33.92±5.04*
PMI, cm^2/m^2	7.291±1.890	6.102±1.466*	4.660±1.724	3.134±1.307*
TPMT, mm/m	12.83±2.82	10.96±2.65*	8.411±1.775	6.122±1.600*
Sarcopenia, n (%)	34 (47.8)	27 (87.1)*	16 (40.0)	15 (78.9)*

Note: * - p value <0.01

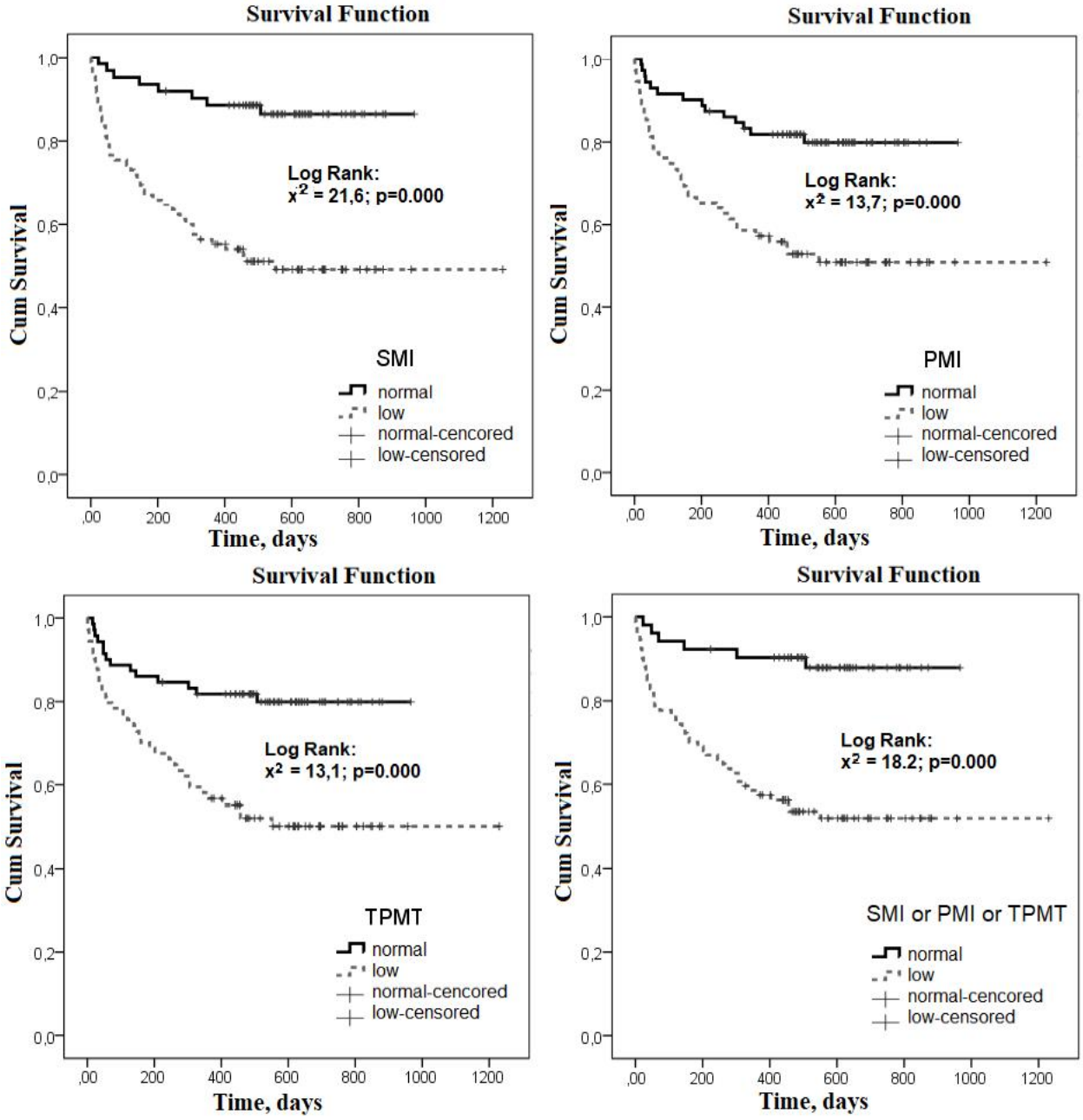

Fig. 3. Kaplan-Meier analysis for survival according to the presence of sarcopenia.

Sarcopenic patients had more severe manifestations of portal hypertension and liver failure (Table 1). The proportion of individuals with overt ascites, hydrothorax, hepatic encephalopathy, and hypoalbuminemia in

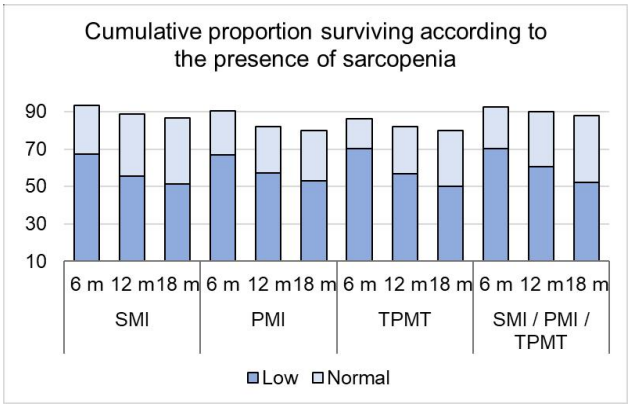

Fig. 4. Cumulative Proportion Surviving according to the presence of sarcopenia.

sarcopenic patients was growing. The mean MELD and CTP score of sarcopenic patients was significantly higher than in patients with normal skeletal muscle mass. SMI, PMI and TPMT were inversely correlated with CTP (r= -0.499/-0.580, -0.502/-0.578 and -0.524/-0.563 in males/females, respectively, p<0.001) and MELD (r= -0.461/-0.391, -0.427/-0.506 and -0.454/-0.512 in males/females, respectively, p<0.001). We noted a trend of higher sarcopenia incidence in males than in females (67.8 vs. 57.9 %, p>0.05, respectively). A decrease of skeletal muscle mass in patients with alcohol-related and viral-alcohol-related etiology was more common than in patients with viral etiology (77.6 and 52.8 vs. 34.6 %, respectively, p<0.05).

The median follow-up period was 489 (306 - 637) days. During this time, no patient was lost to follow-up, and 50 patients (34.0 %) died from LC complications. The deceased patients had significantly lower baseline SMI, PMI, and TPMT, and their sarcopenia incidence was almost twice as high as that of survived patients (Table 2). The overall survival of patients with normal and reduced skeletal muscle mass was significantly different (Fig. 3, Fig. 4). Importantly, low SMI, low PMI, low TPMT were associated with poor survival. The cumulative survival rates in sarcopenic patients (decreased SMI, PMI or T3MT) at Months 6, 12, and 18 were 0.702, 0.606, and 0.520 versus 0.925, 0.905, and 0.880 in non-sarcopenic patients. The mean

Table 3. Univariate Cox regression analysis for mortality.

Variables	HR	95 % CI	p
Sex (male)	0.913	0.516 - 1.616	0.754
Etiology (alcohol-related)	1.428	0.634 - 3.216	0.390
Ascites (2 - 3 degree)	6.246	1.854 - 21.05	0.003
Hydrothorax	4.170	2.361 - 7.367	0.000
Hepatic encephalopathy (II - III stage)	4.216	2.201 - 8.077	0.000
Serum bilirubin (> 50 mmol/L)	2.023	1.153 - 3.550	0.014
Serum albumin (< 30 g/L)	3.980	2.265 - 6.994	0.000
Prothrombin time, INR (> 2)	2.129	0.995 - 4.557	0.052
Platelets (< $100*10^9$/L)	2.154	1.217 - 3.815	0.008
Serum creatinine (> 133 mmol/L)	1.610	0.805 - 3.220	0.178
Sarcopenia (low SMI, ≤ 52.2 / 39.3 cm^2/m^2)	5.040	2.363 - 10.75	0.000
Sarcopenia (low PMI, ≤ 6 .44 / 3.49 cm^2/m^2)	3.039	1.638 - 5.638	0.000
Sarcopenia (low TPMT, ≤ 11.1 / 7.42 mm/m)	2.976	1.604 - 5.522	0.001
Sarcopenia (low SMI, PMI or TPMT)	5.269	2.243 - 12.38	0.000

Table 4. Multivariate Cox regression analysis for mortality.

Variables	Model 1 (low SMI)			Model 2 (low PMI)		
	HR	95% CI	p	HR	95% CI	p
Ascites (2 - 3 degree)	1.145	0.515 - 2.550	0.737	0.805	0.367 - 1.765	0.588
Hydrotorax	1.419	0.649 - 3.100	0.381	1.502	0.698 - 3.230	0.298
Encephalopathy (II - III stage)	2.117	1.000 - 4.497	0.049	2.490	1.176 - 5.275	0.017
Serum bilirubin (> 50 mmol/L)	1.612	0.906 - 2.867	0.104	1.670	0.929 - 3.002	0.086
Serum albumin (< 30 g/L)	2.656	1.440 - 4.897	0.002	2.926	4.605 - 5.333	0.000
Platelets (< $100*10^9$/L)	1.442	0.776 - 2.679	0.246	1.185	0.632 - 2.222	0.597
Sarcopenia	2.664	1.191 - 5.959	0.017	2.193	1.021 - 4.709	0.044
Variables	Model 3 (low TPMT)			Model 4 (low SMI, PMI or TPMT)		
Ascites (2 - 3 degree)	0.768	0.358 - 1.732	0.553	0.909	0.422 - 1.958	0.807
Hydrotorax	1.786	0.822 - 3.881	0.143	1.495	0.699 - 3.197	0.300
Encephalopathy (II - III stage)	2.278	1.069 - 4.854	0.033	2.127	1.009 - 4.489	0.049
Serum bilirubin (> 50 mmol/L)	1.519	0.846 - 2.730	0.162	1.389	0.771 - 2.504	0.274
Serum albumin (< 30 g/L)	2.614	1.416 - 4.825	0.002	2.723	1.497 - 4.953	0.001
Platelets (< $100*10^9$/L)	1.252	0.670 - 2.344	0.479	1.298	0.700 - 2.406	0.408
Sarcopenia	2.214	1.032 - 4.750	0.041	3.653	1.216 - 10.97	0.021

estimate survival time of sarcopenic patients was significantly lower than survival time of patients with normal muscle mass 717.6±43.1 versus 874.1±35.7 days (M±m, p<0.01).

Cox's proportional hazards model was used to determine predictors of LC mortality. Grade 2 - 3 ascites, hydrothorax, stage II - III hepatic encephalopathy, total serum bilirubin >50 μmol/L, serum albumin <30 g/L, platelets $<100*10^9$/L, and low skeletal muscle mass parameters (SMI, PMI or TPMT) were significantly associated with the overall mortality of LC patients in univariate regression analysis (Table 3). Multivariate regression analysis showed that only hepatic encephalopathy, hypoalbuminemia, and decreased skeletal muscle mass were independent mortality predictors for LC patients (Table 4). The highest ratio was obtained in a low SMI, PMI or TPMT model (HR 3.65, p=0.021). Such patients had a 78.5 % probability of earlier development of fatal LC complications than patients with normal muscle mass.

Discussion

Assessment of prognosis is critical important to identify high-risk patients and to select optimal treatment regimen. Traditional prognostic tools CTP and MELD have certain limitations. In particular, CTP encephalopathy and ascites are subjective variables, as their severity may change throughout treatment course. Objective CTP values (bilirubin, albumin) are selected empirically and interpreted rather by rank than a linear model [12]. The MELD score involves objective variables (creatinine, bilirubin, prothrombin test) but correctly predicts three-month survival in only 80 % of cases [12, 23]. A significant disadvantage of both systems is an underestimation of other comorbidities or LC complications, in particular, the nutritional status of patients.

Malnutrition is developed in most LC patients. Reduced food intake, impaired digestion, malabsorption, metabolic disorders, endotoxemia, systemic inflammation, and myokine and adipokine systems disturbance in LC patients lead to protein-energy deficiency and skeletal muscles atrophy [7]. Recent studies suggest that malnutrition and sarcopenia are common, prognostic-modifying, but often underestimated LC complications [27, 28]. CT scan at L3 level allows to accurately evaluate skeletal muscle area, which is strongly consistent with total muscle mass [16]. As LC patients require regular screening for hepatocellular carcinoma and other complications, radiologic assessment of skeletal muscle mass may become a routine procedure.

SMI is the most validated parameter of sarcopenia in clinical studies and an independent predictor of mortality in LC patients [16]. In clinical practice, the SMI calculation is a time-consuming procedure, requiring special software and radiologist expertise. Calculation of psoas muscle area and thickness is considered a more available procedure. In practice, psoas muscle is clearly dissociating with retroperitoneal adipose tissue and vertebrae, rarely infiltrated by fat, not compressed by ascitic fluid and enlarged organs; its size does not depend on physical activity [19]. Psoas muscle thickness calculation does not require special software and radiologist`s expertise. The psoas muscle section area calculated using linear dimensions or software are almost the same figure [5]. In the literature, psoas muscle measurement has been mentioned at the umbilicus or L3, L4 levels [15]. The umbilicus may change position in case of ascites or paracentesis, and is not always visible. To calculate the psoas muscle dimensions, we chose the L3 level, which was taken as a fixed reference point. Radiologic muscle mass parameters are known to have significant sex and ethnic variability [15, 16]. We had determined SMI, PMI and TPMT reference values for Ukrainian population earlier [18].

Our data showed that psoas muscle area and thickness were significantly consistent with SMI. Low PMI and TPMT most likely corresponded to low SMI (AUC >0.800), and muscle mass parameters were found comparable in 73 and 65 % of cases, respectively. Diagnostic agreement between TPMT and SMI had been demonstrated in several other studies [10, 20]. In contrast, Ebadi M. et al. [6] showed that PMI and SMI were moderately concordant in females, yet poorly concordant in male LC patients, and of 29 % of patients in this study were misclassified. Despite diagnostic consistency, these parameters were not equal, as some patients with normal SMI showed low PMI and TPMT, and vice versa. Most likely using only one of the parameters may lead to underestimation of sarcopenia in some LC patients.

According to a recent meta-analysis, the prevalence of sarcopenia in LC patients varies from 15.5 to 68.5 % depending on a cohort, severity of the disease, and assessment methods [27]. In our study low muscle mass was present in 63.3 % of patients. Hight prevalence of sarcopenia in our cohort was probably related with LC decompensation in vast majority of patients and $\geq$20 MELD in more than two-thirds of patients at baseline. A number of studies have demonstrated an association between LC severity, alcohol-related etiology, male sex, and sarcopenia incidence [2, 8, 20, 32]. In our cohort, the incidence of sarcopenia increased along with the disease stage and reached 86.3 % in CTP C patients. Decreased skeletal muscle mass was more common in patients with alcohol-related or viral-alcohol-related liver disease than in patients with isolated viral disease. At the same time, we observed only a trend towards higher incidence of sarcopenia in males.

Our prospective study revealed that sarcopenia was associated with poor survival in LC patients. In particular, patients who died during the follow-up had significantly lower SMI, PMI, and TPMT than those survived. The short-term survival of patients with low values of psoas muscle area and thickness was significantly worse than in patients with normal indexes. The cumulative proportion surviving

in patients with low SMI, PMI and TPMT by 18-th follow-up month was comparable, ranging from 50.2 to 52.8 % versus 79.9 to 86.5 % in patients with normal indexes.

It had previously been shown that loss of muscle mass in LC patients was associated with the development of severe or resistant ascites, hepatic encephalopathy, spontaneous bacterial peritonitis, and occurrence of acute-on-chronic liver failure [17, 22, 34]. In our study, sarcopenic patients were more likely to have overt ascites and encephalopathy, hydrothorax, hypoalbuminemia, hyperbilirubinemia, prolonged prothrombin time, and thrombocytopenia. Some of these factors, such as ascites, encephalopathy, jaundice, hypoalbuminemia, prolonged prothrombin time, and high creatinine, are incorporated into CTP or MELD prognostic tools and associated with poor patient survival [12]. Our goal was to find out what causes a poor prognosis: sarcopenia *per se* or other LC complications that accumulate in sarcopenic patients. We have shown that low muscle mass, ascites, encephalopathy, hydrothorax, hypoalbuminemia, hyperbilirubinemia, and thrombocytopenia are significantly associated with patient mortality in a univariate regression analysis. At the same time, creatinine, prothrombin time, male sex, and alcohol etiology were not significantly associated with the survival rate. Multivariate regression analysis showed that only sarcopenia, hypoalbuminemia and hepatic encephalopathy had independently influenced the time of LC patients` death. It should be mentioned that low PMI and TPMT posed a risk comparable to SMI (HR 2.19, 2.21 and 2.66, $p<0.05$). Patients with low level of at least one of the indexes had the greatest risk (HR 3.65, $p<0.05$). A recent meta-analysis of 10 studies, eight of which assessed the prognostic SMI value and two dealt with TPMT in LC patients without hepatocellular carcinoma showed a risk of mortality comparable with our results (HR 2.31, $p<0.05$) [27].

Several other recent retrospective studies have demonstrated the prognostic TPMT value in LC patients [1, 10, 20, 21]. M. Praktiknjo et al. [22] found that psoas muscle thickness was an independent predictor of one-year mortality and the occurrence of acute-on-chronic liver failure after transjugular portosystemic shunt. TPMT was an independent predictor of overall survival for hepatocellular carcinoma patients receiving targeted therapy [33].

Literature data on psoas muscle area are more controversial. Earlier, Ebadi M. et. al. [6] showed that PMI below cut-off points established by the authors, was not a complete and reliable tool for diagnosing sarcopenia and identifying patients at high risk of mortality compared to SMI, especially in male patients. In another study, low PMI values, independent of MELD, were associated with adverse posttransplant results: infectious complications, prolonged ventilation and intensive care, and higher one-year mortality [11]. Three studies published this year show that PMI-assessed sarcopenia is associated with reduced survival of LC patients awaiting transplantation and patients who have already undergone transplantation, as well as survival of hepatocellular carcinoma patients receiving immune and targeted anticancer therapy [2, 25, 35].

Thus, the psoas muscle dimensions were considered a reliable tool for detection of sarcopenia and prediction of short-term survival in LC. It is worthy to note that sarcopenia is a potentially modified factor of adverse LC outcomes, approaches to the treatment of which are intensively studied [26].

As far as loss of skeletal muscle mass in LC patients is a predictor of an unfavorable prognosis, further clinical studies are needed to find out whether sarcopenia correction may contribute to improvement of survival rate.

Conclusions

1. Radiologic psoas muscle area and thickness parameters (PMI and TPMT) at L3 level are objective sarcopenia markers for LC patients, which have stable diagnostic concordance with the cross-sectional skeletal muscle area (SMI). Using all three parameters allows to identify more patients with reduced skeletal muscle mass.

2. Sarcopenia is common for 54.9 % CTP B, 86.3 % CTP C patients, and associated with an elevated incidence of ascites, hydrothorax, hepatic encephalopathy, and hypoalbuminemia. Sarcopenic patients are more likely to have an alcohol-related etiology than viral one (HBV, HCV).

3. Assessment of psoas muscle thickness and area is a reliable tool to identify high-risk patients. The overall survival of patients with low SMI, PMI and TPMT is significantly reduced. SMI, PMI, and TPMT are considered independent predictors of LC mortality (HR 2.66, 2.19, 2.21, respectively, $p<0.05$). A decrease of at least one of the three radiologic skeletal muscle indexes is associated with the highest relative risk of fatal LC complications (HR 3.65, $p=0.021$).

References

[1] Beer, L., Bastati, N., Ba-Ssalamah, A., Potter-Lang, S., Lampichler, K., Bican, Y., … & Reiberger, T. (2020). MRI-defined sarcopenia predicts mortality in patients with chronic liver disease. *Liver international: official journal of the International Association for the Study of the Liver,* 40(11), 2797-2807. doi: 10.1111/liv.14648

[2] Benmassaoud, A., Roccarina, D., Arico, F. M., Marta, C., Donghia, R., Leandro, G., … & Tsochatzis, E. A. (2022). Sex is a major effect modifier between body composition and mortality in patients with cirrhosis assessed for liver transplantation. *Liver international: official journal of the International Association for the Study of the Liver,* 10.1111/liv.15293. Advance online publication. doi: 10.1111/liv.15293

[3] Bhanji, R. A., Moctezuma-Velazquez, C., Duarte-Rojo, A., Ebadi, M., Ghosh, S., Rose, C., & Montano-Loza, A. J. (2018). Myosteatosis and sarcopenia are associated with hepatic encephalopathy in patients with cirrhosis. *Hepatology international,* 12(4), 377-386. doi: 10.1007/s12072-018-9875-9

[4] Carey, E. J., Lai, J. C., Wang, C. W., Dasarathy, S., Lobach, I.,

Montano-Loza, A. J., … & Fitness, Life Enhancement, and Exercise in Liver Transplantation Consortium (2017). A multicenter study to define sarcopenia in patients with end-stage liver disease. *Liver transplantation: official publication of the American Association for the Study of Liver Diseases and the International Liver Transplantation Society,* 23(5), 625-633. doi: 10.1002/lt.24750

[5] Cespedes Feliciano, E. M., Avrutin, E., Caan, B. J., Boroian, A., & Mourtzakis, M. (2018). Screening for low muscularity in colorectal cancer patients: a valid, clinic-friendly approach that predicts mortality. *Journal of cachexia, sarcopenia and muscle,* 9(5), 898-908. doi: 10.1002/jcsm.12317

[6] Ebadi, M., Wang, C. W., Lai, J. C., Dasarathy, S., Kappus, M. R., Dunn, M. A., … & From the Fitness, Life Enhancement, and Exercise in Liver Transplantation (FLEXIT) Consortium (2018). Poor performance of psoas muscle index for identification of patients with higher waitlist mortality risk in cirrhosis. *Journal of cachexia, sarcopenia and muscle,* 9(6), 1053-1062. doi: 10.1002/jcsm.12349

[7] Ebadi, M., Bhanji, R. A., Mazurak, V. C., & Montano-Loza, A. J. (2019). Sarcopenia in cirrhosis: from pathogenesis to interventions. *Journal of gastroenterology,* 54(10), 845-859. doi: 10.1007/s00535-019-01605-6

[8] Ebadi, M., Bhanji, R. A., Dunichand-Hoedl, A. R., Mazurak, V. C., Baracos, V. E., & Montano-Loza, A. J. (2020). Sarcopenia Severity Based on Computed Tomography Image Analysis in Patients with Cirrhosis. *Nutrients,* 12(11), 3463. doi: 10.3390/nu12113463

[9] Gomez-Perez, S. L., Haus, J. M., Sheean, P., Patel, B., Mar, W., Chaudhry, V., … & Braunschweig, C. (2016). Measuring Abdominal Circumference and Skeletal Muscle From a Single Cross-Sectional Computed Tomography Image: A Step-by-Step Guide for Clinicians Using National Institutes of Health ImageJ. JPEN. *Journal of parenteral and enteral nutrition,* 40(3), 308-318. doi: 10.1177/0148607115604149

[10] Gu, D. H., Kim, M. Y., Seo, Y. S., Kim, S. G., Lee, H. A., Kim, T. H., … & Um, S. H. (2018). Clinical usefulness of psoas muscle thickness for the diagnosis of sarcopenia in patients with liver cirrhosis. *Clinical and molecular hepatology,* 24(3), 319-330. doi: 10.3350/cmh.2017.0077

[11] Kalafateli, M., Mantzoukis, K., Choi Yau, Y., Mohammad, A. O., Arora, S., Rodrigues, S., … & Tsochatzis, E. A. (2017). Malnutrition and sarcopenia predict post-liver transplantation outcomes independently of the Model for End-stage Liver Disease score. *Journal of cachexia, sarcopenia and muscle,* 8(1), 113-121. doi: 10.1002/jcsm.12095

[12] Kim, H. J., & Lee, H. W. (2013). Important predictor of mortality in patients with end-stage liver disease. *Clinical and molecular hepatology,* 19(2), 105-115. doi: 10.3350/cmh.2013.19.2.105

[13] Kim, G., Kang, S. H., Kim, M. Y., & Baik, S. K. (2017). Prognostic value of sarcopenia in patients with liver cirrhosis: A systematic review and meta-analysis. *PloS one*, 12(10), e0186990. doi: 10.1371/journal.pone.0186990

[14] Kumar, V., Benjamin, J., Shasthry, V., Subramanya Bharathy, K. G., Sinha, P. K., Kumar, G., & Pamecha, V. (2020). Sarcopenia in Cirrhosis: Fallout on Liver Transplantation. *Journal of clinical and experimental hepatology,* 10(5), 467-476. doi: 10.1016/j.jceh.2019.12.003

[15] Lee, C. M., Kang, B. K., & Kim, M. (2021). Radiologic Definition of Sarcopenia in Chronic Liver Disease. *Life* (Basel, Switzerland), 11(2), 86. doi: 10.3390/life11020086

[16] Marasco, G., Sadalla, S., Vara, G., Golfieri, R., Festi, D., Colecchia, A., & Renzulli, M. (2021). Imaging Software-Based Sarcopenia Assessment in Gastroenterology: Evolution and Clinical Meaning. *Canadian journal of gastroenterology & hepatology,* 2021, 6669480. doi: 10.1155/2021/6669480

[17] Montano-Loza, A. J., Duarte-Rojo, A., Meza-Junco, J., Baracos, V. E., Sawyer, M. B., Pang, J. X., … & Myers, R. P. (2015). Inclusion of Sarcopenia Within MELD (MELD-Sarcopenia) and the Prediction of Mortality in Patients With Cirrhosis. *Clinical and translational gastroenterology,* 6(7), e102. doi: 10.1038/ctg.2015.31

[18] Motsiuk, V. M., & Pentiuk, N. O. (2021). Діагностичне та прогностичне значення показників товщини та площі поперекового м'язу у хворих на цироз печінки, ускладений саркопенією [Diagnostic and prognostic value of psoas muscle thickness and area in patients with liver cirrhosis and sarcopenia]. *Вісник Вінницького національного медичного університету - Reports of Vinnytsia National Medical University,* 25(4), 551-558. doi: 10.31393/reports-vnmedical-2021-25(4)-06

[19] Mourtzakis, M., Prado, C. M., Lieffers, J. R., Reiman, T., McCargar, L. J., & Baracos, V. E. (2008). A practical and precise approach to quantification of body composition in cancer patients using computed tomography images acquired during routine care. *Applied physiology, nutrition, and metabolism = Physiologie appliquee, nutrition et metabolisme*, 33(5), 997-1006. doi: 10.1139/H08-075

[20] Paternostro, R., Lampichler, K., Bardach, C., Asenbaum, U., Landler, C., Bauer, D., … & Ferlitsch, A. (2019). The value of different CT-based methods for diagnosing low muscle mass and predicting mortality in patients with cirrhosis. *Liver international: official journal of the International Association for the Study of the Liver,* 39(12), 2374-2385. doi: 10.1111/liv.14217

[21] Paternostro, R., Bardach, C., Hofer, B. S., Scheiner, B., Schwabl, P., Asenbaum, U., … & Lampichler, K. (2021). Prognostic impact of sarcopenia in cirrhotic patients stratified by different severity of portal hypertension. *Liver international: official journal of the International Association for the Study of the Liver,* 41(4), 799-809. doi: 10.1111/liv.14758

[22] Praktiknjo, M., Clees, C., Pigliacelli, A., Fischer, S., Jansen, C., Lehmann, J., … & Trebicka, J. (2019). Sarcopenia Is Associated With Development of Acute-on-Chronic Liver Failure in Decompensated Liver Cirrhosis Receiving Transjugular Intrahepatic Portosystemic Shunt. *Clinical and translational gastroenterology,* 10(4), e00025. doi: 10.14309/ctg.0000000000000025

[23] Sacleux, S. C., & Samuel, D. (2019). A Critical Review of MELD as a Reliable Tool for Transplant Prioritization. *Seminars in liver disease,* 39(4), 403-413. doi: 10.1055/s-0039-1688750

[24] Shen, W., Punyanitya, M., Wang, Z., Gallagher, D., St.-Onge, M.-P., Albu, J., … & Heshka, S. (2004) Total body skeletal muscle and adipose tissue volumes: Estimation from a single abdominal cross-sectional image. *J. Appl. Physiol,* 97, 2333-2338. doi: 10.1152/japplphysiol.00744.2004

[25] Tan, Y., Duan, T., Li, B., Zhang, B., Zhu, Y., Yan, K., … & Yan, L. (2022). Sarcopenia defined by psoas muscle index independently predicts long-term survival after living donor liver transplantation in male recipients. *Quantitative imaging in medicine and surgery,* 12(1), 215-228. doi: 10.21037/qims-21-314

[26] Tandon, P., Montano-Loza, A. J., Lai, J. C., Dasarathy, S., & Merli, M. (2021). Sarcopenia and frailty in decompensated cirrhosis. *Journal of hepatology*, 75(Suppl 1), S147-S162. doi:

10.1016/j.jhep.2021.01.025
[27] Tantai, X., Liu, Y., Yeo, Y. H., Praktiknjo, M., Mauro, E., Hamaguchi, Y., … & Nguyen, M. H. (2022). Effect of sarcopenia on survival in patients with cirrhosis: A meta-analysis. *Journal of hepatology,* 76(3), 588-599. doi: 10.1016/j.jhep.2021.11.006
[28] Traub, J., Reiss, L., Aliwa, B., & Stadlbauer, V. (2021). Malnutrition in Patients with Liver Cirrhosis. *Nutrients,* 13(2), 540. doi: 10.3390/nu13020540
[29] Tsien, C., Garber, A., Narayanan, A., Shah, S. N., Barnes, D., Eghtesad, B., … & Dasarathy, S. (2014). Post-liver transplantation sarcopenia in cirrhosis: a prospective evaluation. *Journal of gastroenterology and hepatology,* 29(6), 1250-1257. doi: 10.1111/jgh.12524
[30] Tsochatzis, E. A., Bosch, J., & Burroughs, A. K. (2014). Liver cirrhosis. *Lancet* (London, England), 383(9930), 1749-1761. doi: 10.1016/S0140-6736(14)60121-5
[31] van Vugt, J., Buettner, S., Alferink, L., Bossche, N., de Bruin, R., Darwish Murad, S., … & IJzermans, J. (2018). Low skeletal muscle mass is associated with increased hospital costs in patients with cirrhosis listed for liver transplantation-a retrospective study. *Transplant international: official journal of the European Society for Organ Transplantation*, 31(2), 165-174. doi: 10.1111/tri.13048
[32] Welch, N., Dasarathy, J., Runkana, A., Penumatsa, R., Bellar, A., Reen, J., … & Dasarathy, S. (2020). Continued muscle loss increases mortality in cirrhosis: Impact of aetiology of liver disease. *Liver international: official journal of the International Association for the Study of the Liver*, 40(5), 1178-1188. doi: 10.1111/liv.14358
[33] Yamashima, M., Miyaaki, H., Honda, T., Shibata, H., Miuma, S., Taura, N., & Nakao, K. (2017). Significance of psoas muscle thickness as an indicator of muscle atrophy in patients with hepatocellular carcinoma treated with sorafenib. *Molecular and clinical oncology,* 7(3), 449-453. doi: 10.3892/mco.2017.1321
[34] Zeng, X., Shi, Z. W., Yu, J. J., Wang, L. F., Luo, Y. Y., Jin, S. M., … & Xie, W. F. (2021). Sarcopenia as a prognostic predictor of liver cirrhosis: a multicentre study in China. *Journal of cachexia, sarcopenia and muscle,* 12(6), 1948-1958. doi: 10.1002/jcsm.12797
[35] Zhao, M., Duan, X., Han, X., Wang, J., Han, G., Mi, L., … & Yin, F. (2022). Sarcopenia and Systemic Inflammation Response Index Predict Response to Systemic Therapy for Hepatocellular Carcinoma and Are Associated With Immune Cells. *Frontiers in oncology,* 12, 854096. doi: 10.3389/fonc.2022.854096

РАДІОЛОГІЧНІ ПОКАЗНИКИ ПОПЕРЕКОВОГО М'ЯЗА ЯК НАДІЙНИЙ ІНСТРУМЕНТ ВИЯВЛЕННЯ САРКОПЕНІЇ ТА ПРОГНОЗУВАННЯ КОРОТКОСТРОКОВОГО ВИЖИВАННЯ ПРИ ЦИРОЗІ ПЕЧІНКИ

Моцюк В. М., Пентюк Н. О.

Втрата маси скелетних м'язів або саркопенія асоціюється з розвитком ускладнень та смертністю у хворих на цироз печінки (ЦП). Індекс скелетних м'язів (SMI) є найбільш валідизованим в клінічних дослідженнях показником саркопенії, але його визначення є складним в рутинній клінічній практиці. Мета дослідження: оцінити діагностичну узгодженість між різними радіологічними показниками маси скелетних м'язів та їх зв'язок з короткостроковою виживаністю хворих на ЦП. У дослідження було залучено 147 хворих на ЦП, 90 чоловіків та 57 жінок (55,51±0,97 років). ЦП класу А за Child-Turcotte-Pugh (CTP) був діагностований у 23, класу В - у 51, класу С - у 73 хворих. 50 пацієнтів померли від ускладнень ЦП протягом періоду подальшого спостереження (Me 489 (306 - 637) днів). Методом комп'ютерної томографії визначали нормалізовані до зросту площу поперечного зрізу скелетних м'язів (SMI), площу поперекового м'яза (PMI), товщину поперекового м'яза (TPMT) на рівні L3. Статистичну обробку даних проводили у програмному забезпеченні SPSS22 (©SPSS Inc.). Встановлено, що PMI та TPMT є об'єктивними маркерами саркопенії у хворих на ЦП та мають стійку діагностичну узгодженість з SMI (r Spearman's 0,734, 0,649, p<0,001; k Cohen's 0,727, 0,643, p<0,001, відповідно). Застосування усіх трьох індексів дозволяє виявляти більшу кількість хворих із зниженою масою скелетних м'язів. Саркопенія присутня у 54,9 % у хворих на ЦП класу В, 86,3 % у хворих на ЦП класу С та асоціюється із збільшенням частоти асциту, гідротораксу, печінкової енцефалопатії, гіпоальбумінемії. Пацієнти із саркопенією частіше мають алкогольну етіологію захворювання, ніж вірусну (HBV, HCV). В аналізі Каплана-Мейєра загальна виживаність пацієнтів з низькими значеннями SMI, PMI та TPMT є достовірно меншою. В багатомірному регресійному аналізі Кокса SMI, PMI та TPMT є незалежними предикторами пов'язаної з ЦП смертності (HR 2,66, 2,19, 2,21, відповідно, p<0,05). Зниження хоча б одного із трьох радіологічних показників маси скелетних м'язів асоціюється з найбільшим ризиком фатальних ускладнень ЦП (HR 3,65, p=0,021). Таким чином, розміри поперекового м'яза є надійним маркером саркопенії та можуть прогнозувати короткострокову виживаність хворих на ЦП.

Ключові слова: *поперековий м'яз, саркопенія, цироз печінки, гепатит С, гепатит В, алкогольна хвороба печінки.*

DOI: 10.31393/morphology-journal-2022-28(3)-02 Reports of Morphology, Vol. 28, №3, Pages 14-20

ISSN 1818-1295 eISSN 2616-6194

REPORTS OF MORPHOLOGY

Official Journal of the Scientific Society of Anatomists, Histologists, Embryologists and Topographic Anatomists of Ukraine

journal homepage: https://morphology-journal.com

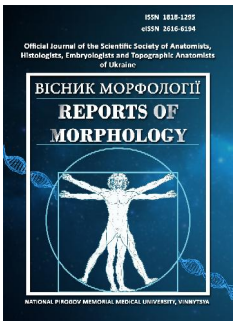

Correlation between aortic root dimensions and biometric indicators in coronary heart disease

Pidvalna U. Ye.

Danylo Halytsky Lviv National Medical University, Lviv, Ukraine

ARTICLE INFO

Received: 16 May 2022

Accepted: 21 June 2022

UDC: 616.132.11:616.12-005.4]-055.1-073.756.8

CORRESPONDING AUTHOR

e-mail: Uljaska.p@gmail.com

Pidvalna U. Ye.

CONFLICT OF INTEREST

The authors have no conflicts of interest to declare.

FUNDING

The work was financially supported by the Danylo Halytsky Lviv National Medical University, Ministry of Health of Ukraine (No state registration: 0120U002129)

Aortic root requires preliminary preoperative analysis for coronary artery bypass graft (CABG) in coronary heart disease (CHD). The dimensions of the aorta correlate with anthropometric indicators. The purpose of the study: to establish the relationship between sinuses of Valsalva height, coronary artery ostia height and biometric parameters (age, height, weight, body surface area and body mass index) in men with CHD using computed tomography. Research materials and methods include contrast-enhanced computed tomography images of the aorta of men with verified CHD. According to growth parameters, division into 2 groups was made. The sinuses of Valsalva height and right and left coronary artery ostia height were measured. Clinical data were analyzed: age, height, body weight, body surface area (BSA) and body mass index (BMI). Statistical analysis: Student's t-test, Kendall's rank correlation method, Pearson's linear correlation, Fisher's multifactorial regression analysis. Analysis of the results of computed tomography of 30 men with CHD (average age 60.80±10.63 years) showed that the average values of the three sinuses of Valsalva height were approximately at the same level. The results of the Pearson linear correlation evaluation showed the absence of a proven relationship between biometric indicators and morphometric data according to CT in men with CHD (p>0.05). Multifactor regression analysis proved the inverse significant influence of weight and the direct significant influence of BMI and BSA on the dependence of left coronary artery ostia height. The multiple correlation coefficient was R=+0.55, with p=0.023, SEE=2.74. Prediction of the level of left coronary artery ostia height in men with CHD was carried out with confirmation of the constructed model. In the first group of short men (n=11) with CHD (average age 60.11±12.63 years, height 1.677±0.023 m), an inverse correlation between height and left coronary artery ostia height (tb=-0.56, p=0.034). Reliable direct relationships between the left coronary artery ostia height parameter and several anthropometric indicators were established: with weight - a direct strong relationship (tb=+0.72, p=0.007), with BMI - a direct relationship of medium strength (tb=+ 0.67, p=0.008), with BSA - average strength direct connection (tb=+0.58, p=0.023). The relationship between the value of the right coronary artery ostia height and the BSA indicator - the inverse of the average strength correlation (tb=-0.51, p=0.046) was proved. Relationships between morphometric parameters and age were not proven. Thus, in men with CHD, left coronary artery ostia height correlates with weight, BMI, and BSA. In short men with CHD, there is an inverse relationship between left coronary artery height and height; direct relationships with weight, BMI and BSA.

Keywords: *aorta, coronary artery, anatomy, computed tomography, sinus of Valsalva.*

Introduction

Structural changes in the coronary arteries are a prerequisite for the development of coronary heart disease (CHD). One of the treatment options for CHD is cardiac surgery - coronary artery bypass graft (CABG). Aortic root, in particular the sinuses of Valsalva and coronary artery ostia, require careful preoperative analysis to avoid intraoperative complications (air embolism during deaeration, conduction disturbances during interventions at the aortic-mitral junction, etc.).

The dimensions of the aorta correlate with anthropometric indicators [4, 6]. The widespread implementation of transcatheter aortic valve replacement (TAVI) contributes to

the intravital study of aortic root morphology in valvular heart disease [7, 15]. Studies indicate different relationships between sex, age, height, body surface area (BSA) and body mass index (BMI) in severe aortic stenosis [1, 3]. On the other hand, the morphometric parameters of sinuses of Valsalva and coronary artery ostia in CHD have not been sufficiently covered. Although a direct association has been established between the risk of coronary heart disease and human height [12, 13].

Contrast-enhanced computed tomography (CT) is considered the "golden" standard for intravital analysis of aortic anatomy [2, 11]. Measurement of the sizes of aortic root structures, taking into account anthropometric indicators in CHD, is important in the context of preoperative analysis.

The purpose of the study: to establish the relationship between sinuses of Valsalva height, coronary artery ostia height and biometric parameters (age, height, weight, body surface area and body mass index) in men with coronary heart disease using computed tomography.

Materials and methods

The study was approved by the Bioethics Commission of the Danylo Halytsky Lviv National Medical University (protocol № 10 dated 12/20/2022).

Study population. The study included male patients of the cardiac surgery department who underwent planned preoperative CT of the aorta. Inclusion criteria: patients referred for coronary artery bypass grafting for CHD. Exclusion criteria: patients with CHD and combined pathology of the heart or aorta; chest injuries or thoracic interventions in the anamnesis; insufficient visualization of the studied structures. It is important to emphasize that patients with CHD and valvular defects were not included in the study. Clinical data, which were considered independent variables, were analyzed: age, height, body weight, BMI and BSA were calculated. BSA was calculated according to Mosteller's formula [9]. Out of the analyzed 168 examinations, 30 people met the specified criteria. According to growth parameters, they are divided into 2 groups: 1st group - with a height of less than 1.7 m (n=11), 2nd group - with a height of 1.71-1.8 m (n=19).

CT assessment. CT was performed on a LightSpeed 64 VCT XT scanner, GE (General Electric) using Ultravist 470 contrast enhancement (Bayer Healthcare). Image analysis and measurements were carried out according to step-by-step recommendations [2].

Statistical analysis. The average values of the basic characteristics of the patients (biometric parameters) were compared according to the Student's t-test. Calculation of interrelationships in small samples of patients was carried out by the method of Kendall's rank correlation, namely, using tb-Kendall's coefficients (Kendall's tau-b), which do not depend on the presence or absence of relationships in ranks. Pearson's linear correlation analysis was conducted between the studied parameters. The relationship between independent variables (biometric indicators) and dependent variables (morphometric indicators of the aorta) was carried out using multivariate regression analysis. When detecting dependencies, the Durbin-Watson autocorrelation criterion checked the correctness of the proposed model ($p<0.05$ was considered reliable). Calculations were performed in R Commander (version 2.7-2, GNU General Public License) and SPSS (version 22.0, IBM Corp., Armonk).

Results

The analysis of the results of computed tomography of 30 men with CHD (average age 60.80±10.63 years) showed that the average values of the three sinuses of Valsalva height were approximately at the same level: the height of the posterior sinus of Valsalva - 22.71±2.07 mm, the height of the left sinus of Valsalva - 21.84±2.69 mm and height of right sinus of Valsalva - 22.21±2.38 mm. The average levels of the departure height of the coronary arteries were: 13.97±3.10 mm for the left coronary artery and 13.81±3.40 mm for the right coronary artery. The level of departure of the coronary artery was considered to be the lower edge of the coronary artery ostia. The left coronary artery ostia height was 18.27±3.13 mm and 17.98±2.95 mm for the right one.

The results of the Pearson linear correlation evaluation showed the absence of a proven relationship between biometric indicators and morphometric data according to CT in men with CHD ($p>0.05$) (Table 1).

A proven direct correlation of medium strength was established between the three sinuses of Valsalva height, namely: left sinus of Valsalva height is interconnected with the height of the posterior and right sinus of Valsalva ($r=+0.39$, $p=0.031$). The interdependence (direct strong relationship) between the left sinus of Valsalva height and the left coronary artery ostia height is also proven: for the lower edge of the ostia ($r=+0.74$, $p=0.000$) and the upper edge of the ostia ($r=+0.78$, $p=0.000$). The level of the right coronary artery ostia height was directly related to the value of the right sinus of Valsalva height ($r=+0.58$, $p=0.001$). The relationship between the values of the sinuses of Valsalva height indicators is visualized (Fig. 1).

Considering the above, it was considered appropriate to conduct a multifactorial regression analysis of the influence of anthropometric parameters on the morphometric parameters of the studied structures in men with CHD. As a result of the study, the dependence of the left coronary artery ostia height on a complex of anthropometric indicators was proven, namely: the inverse significant influence of weight and the direct significant influence of BMI and BSA. The multiple correlation coefficient was $R=+0.55$, with $p=0.023$, SEE=2.74. The adjusted coefficient of multiple determination ($R^2_{adj}=+0.22$) confirmed the dependence of the value of the left coronary artery ostia height in 22.3 % of cases on the specified anthropometric indicators in men with CHD. The Durbin-Watson autocorrelation criterion (1.66) confirmed the correctness of the constructed model (Table 2).

Entering the obtained data into the model, we get the

Table 1. Correlation data (r) between vascular indicators and biometric indicators in men with CHD.

Parameters		Posterior SoV height	Left SoV height	Right SoV height	LCA height (lower)	RCA height (lower)	LCA height (upper)	RCA height (upper)
age	r	-0.11	-0.17	0.21	-0.02	0.03	-0.17	0.03
	p	*0.573*	*0.380*	*0.262*	*0.897*	*0.892*	*0.368*	*0.867*
height	r	-0.02	-0.11	-0.03	-0.30	0.03	-0.16	-0.11
	p	*0.898*	*0.553*	*0.873*	*0.106*	*0.858*	*0.387*	*0.546*
weight	r	0.07	-0.11	0.22	-0.10	0.24	-0.05	0.06
	p	*0.732*	*0.577*	*0.248*	*0.595*	*0.210*	*0.784*	*0.770*
BMI	r	0.10	-0.06	0.28	0.04	0.25	0.02	0.11
	p	*0.597*	*0.766*	*0.140*	*0.836*	*0.181*	*0.900*	*0.557*
BSA	r	0.05	-0.10	0.19	-0.13	0.21	-0.06	0.02
	p	*0.792*	*0.593*	*0.325*	*0.494*	*0.270*	*0.742*	*0.909*
Posterior SoV height	r		0.39*	0.34	0.21	0.05	0.16	0.03
	p		*0.031*	*0.064*	*0.273*	*0.799*	*0.397*	*0.874*
Left SoV height	r	0.39*		0.39*	0.74**	0.03	0.78**	0.19
	p	*0.031*		*0.032*	*0.000*	*0.875*	*0.000*	*0.304*
Right SoV height	r	0.34	0.39*		0.20	0.58**	0.28	0.67**
	p	*0.064*	*0.032*		*0.288*	*0.001*	*0.139*	*0.000*
LCA height (lower)	r	0.21	0.74**	0.20		0.00	0.77**	0.13
	p	*0.273*	*0.000*	*0.288*		*0.997*	*0.000*	*0.487*
RCA height (lower)	r	0.05	0.03	0.58**	0.00		0.17	0.86**
	p	*0.799*	*0.875*	*0.001*	*0.997*		*0.357*	*0.000*
LCA height (upper)	r	0.16	0.78**	0.28	0.77**	0.17		0.28
	p	*0.397*	*0.000*	*0.139*	*0.000*	*0.357*		*0.134*
RCA height (upper)	r	0.03	0.19	0.67**	0.13	0.86**	0.28	
	p	*0.874*	*0.304*	*0.000*	*0.487*	*0.000*	*0.134*	

Notes: BMI - body mass index; BSA - body surface area; SoV - sinus of Valsalva; LCA height (upper) - left coronary artery, upper edge; RCA height (upper) - right coronary artery, upper edge; LCA height (lower) - left coronary artery, lower edge; RCA height (lower) - right coronary artery, lower edge; * - the correlation is significant at $p<0.05$; ** - the correlation is significant at $p<0.001$.

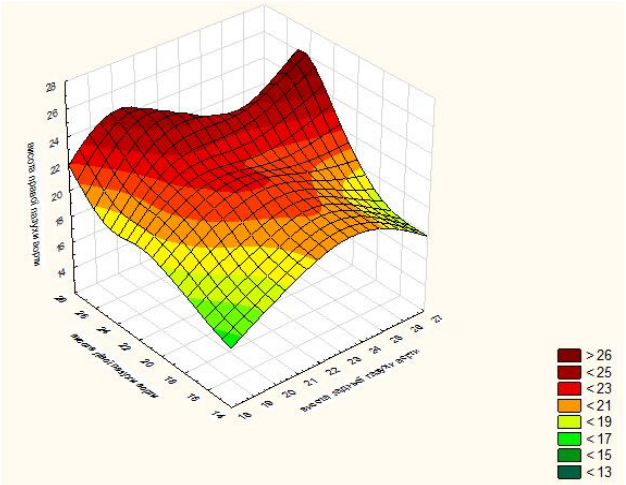

Fig. 1. The relationship between the height indicators of the right, left and posterior sinus of Valsalva in men with CHD.

following linear equation of the model:

the level of the left coronary artery ostia height = -3.676 x A1 + 4.144 x A2 + 194.5 x A3 - 183.05.

As a result of the calculations, the average predicted value of the left coronary artery ostia height in men with CHD is 13.97±1.69 mm (minimum value 9.77 mm, maximum 18.18 mm), which completely coincides with the actual average value, according to CT data, in men with this pathology: 13.97±3.10 mm.

Figure 2 graphically shows the normal probability of the influence of independent anthropometric predictors on the predicted value of left coronary artery ostia height in men with CHD.

For the purpose of practical development of the obtained model, we present two examples of calculations for different anthropometric parameters of studied patients with CHD.

Example № 1. Patient № 7 from the database: male, 54 years old, height 1.75 m, weight 72.0 kg, BMI 23.51 kg/m^2,

Table 2. Results of logistic regression calculations for predicting the level of left coronary artery ostia height in men with CHD.

Indicators	Conventional designation	b- coefficients	p
Constant		-183.05	0.022
Weight	A1	-3.676	0.011
BMI	A2	4.144	0.005
BSA	A3	194.5	0.015

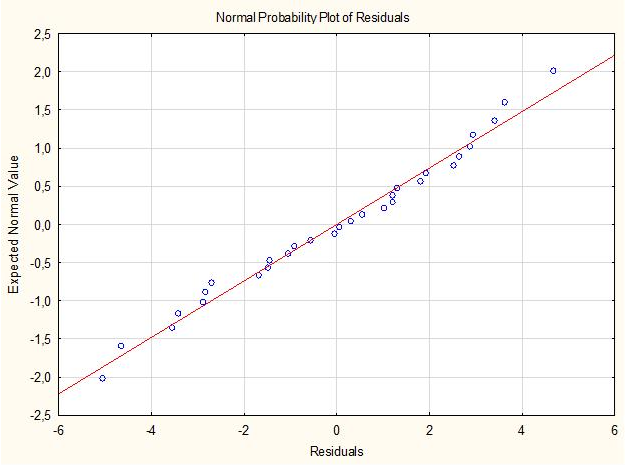

Fig. 2. Normal probability of influence of predictors on the predicted value of left coronary artery ostia height in men with CHD.

BSA 1.870 m^2, left coronary artery ostia height 13.50 mm.

By substituting the given patient data into the presented linear logistic regression equation, we get the result: *level of the left coronary artery ostia height* = -3.676 x 72 + 4.144 x 23.51 + 194.5 x 1.870 - 183.05 = 13.53 mm.

Therefore, the difference between the actual and calculated value is 0.030 mm, which is within the permissible error of 5 %.

Example № 2. Patient № 23 from the database: male, 59 years old, height 1.62 м, weight 80.0 кг, BMI 30.48 kg/m^2, BSA 1.900 m^2, left coronary artery ostia height 18.50 mm.

Table 3. Distribution of vascular parameters (according to CT data) in groups of men with CHD by height (M±SD, mm).

Indicators	Group 1 (1.6-1.7 m) n=11	Group 2 (1.71-1.8 m) n=19	p
Posterior SoV heigh	22.86±2.58	22.48±1.88	*0.683*
Left SoV height	21.90±1.84	21.49±3.08	*0.666*
Right SoV height	22.07±2.22	22.08±2.57	*0.993*
LCA height (lower)	14.98±2.39	13.41±3.50	*0.172*
RCA height (lower)	13.99±2.59	13.42±3.85	*0.645*
LCA height (upper)	18.22±2.93	18.27±3.49	*0.970*
RCA height (upper)	18.39±2.71	17.47±3.14	*0.424*

By substituting the patient's data into the given linear logistic regression equation, we get the result: *level of the left coronary artery ostia height* = -3.676 x 80 + 4.144 x 30.48 + 194.5 x 1.900 - 183.05 = 18.18 mm.

Thus, the obtained calculated value of the left coronary artery ostia height of 18.18 mm practically does not differ (by 0.320 mm) from the one obtained at CT 18.50 mm, which proves the effectiveness of this model in practice.

A comparison of blood vessel data obtained on CT by height in men with CHD showed almost the same parameters of almost all studied indicators (Table 3).

To establish relationships between age-anthropometric data and vessel parameters obtained during CT diagnosis, in 11 short men with CHD (average age 60.11±12.63 years, height 1.677±0.002 m) it was considered appropriate to conduct a correlation analysis using correlation coefficients tb-Kendal (Table 4).

An inverse correlation between height and the value of the upper edge of the left coronary artery ostia height (tb= -0.56, p=0.034) was proved (Fig. 3). Reliable direct relationships were established between the left coronary artery ostia height parameter and several anthropometric

Table 4. Correlation relationships (tb-Kendall) between age and anthropometric data and vascular parameters in short stature person with CHD (n=11).

Parameters		Posterior SoV height	Left SoV height	Right SoV height	LCA height (lower)	RCA height (lower)	LCA height (upper)	RCA height (upper)
age	tb	-0.14	-0.25	0.18	0.16	0.37	0.00	0.13
	p	*0.577*	*0.32*	*0.469*	*0.528*	*0.148*	*1.000*	*0.590*
height	tb	0.16	-0.41	-0.24	-0.39	-0.18	-0.56	-0.10
	p	*0.549*	*0.121*	*0.382*	*0.146*	*0.496*	*0.034*	*0.699*
weight	tb	0.30	0.47	0.10	0.72	-0.26	0.41	-0.41
	p	*0.272*	*0.081*	*0.697*	*0.007*	*0.331*	*0.122*	*0.122*
BMI	tb	0.17	0.42	0.24	0.67	-0.05	0.41	-0.18
	p	*0.510*	*0.101*	*0.360*	*0.008*	*0.855*	*0.102*	*0.468*
BSA	tb	0.42	0.37	0.00	0.58	-0.38	0.28	-0.51
	p	*0.110*	*0.145*	*1.000*	*0.023*	*0.143*	*0.276*	*0.046*

Continuation of table 4.

Parameters		Posterior SoV height	Left SoV height	Right SoV height	LCA height (lower)	RCA height (lower)	LCA height (upper)	RCA height (upper)
Posterior SoV height	tb	-	0.31	0.39	0.29	-0.20	0.12	-0.02
	p	-	*0.226*	*0.135*	*0.264*	*0.455*	*0.643*	*0.926*
Left SoV height	tb	0.31	-	0.41	0.52	-0.28	0.72	-0.09
	p	*0.226*	-	*0.103*	*0.038*	*0.277*	*0.004*	*0.719*
Right SoV height	tb	0.39	0.41	-	0.23	0.30	0.20	0.39
	p	*0.135*	*0.103*	-	*0.365*	*0.237*	*0.417*	*0.125*
LCA height (lower)	tb	0.29	0.52	0.23	-	-0.18	0.63	-0.22
	p	*0.264*	*0.038*	*0.365*	-	*0.469*	*0.012*	*0.369*
RCA height (lower)	tb	-0.20	-0.28	0.30	-0.18	-	-0.11	0.80
	p	*0.455*	*0.277*	*0.237*	*0.469*	-	*0.652*	*0.002*
LCA height (upper)	tb	0.12	0.72	0.20	0.63	-0.11	-	-0.02
	p	*0.643*	*0.004*	*0.417*	*0.012*	*0.652*	-	*0.929*
RCA height (upper)	tb	-0.02	-0.09	0.39	-0.22	0.80	-0.02	-
	p	*0.929*	*0.719*	*0.125*	*0.369*	*0.002*	*0.926*	-

Notes: BMI - body mass index; BSA - body surface area; SoV - sinus of Valsalva; LCA height (upper) - left coronary artery, upper edge; RCA height (upper) - right coronary artery, upper edge; LCA height (lower) - left coronary artery, lower edge; RCA height (lower) - right coronary artery, lower edge.

indicators: with weight - a direct strong relationship (tb=+0.72, p=0.007), with BMI - a medium strength direct relationship (tb=+ 0.67, p=0.008), direct relationship with BSA - medium strength (tb=+0.58, p=0.023) (Fig. 4). Also proven the relationship between the value of the right coronary artery upper edge ostia height and the BSA indicator - the inverse of the average strength correlation (tb=-0.51, p=0.046). Relationships between morphometric parameters and age were not proven.

Average strength correlation was established without validation. Among the most pronounced are: the correlation between the left sinus of Valsalva height and all biometric

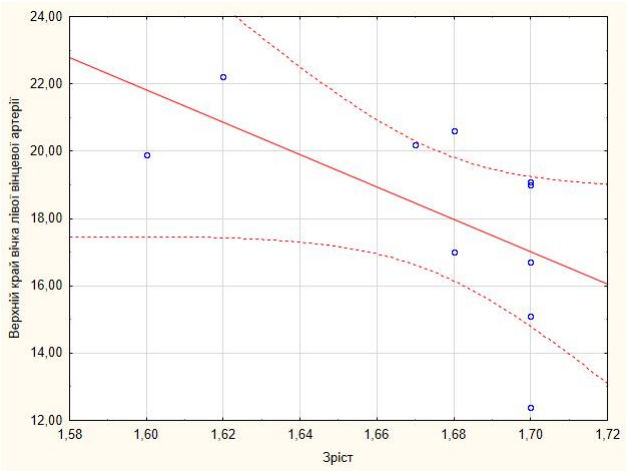

Fig. 3. Correlation between the height indicator and the value of the left coronary artery upper edge ostia height in short men with CHD.

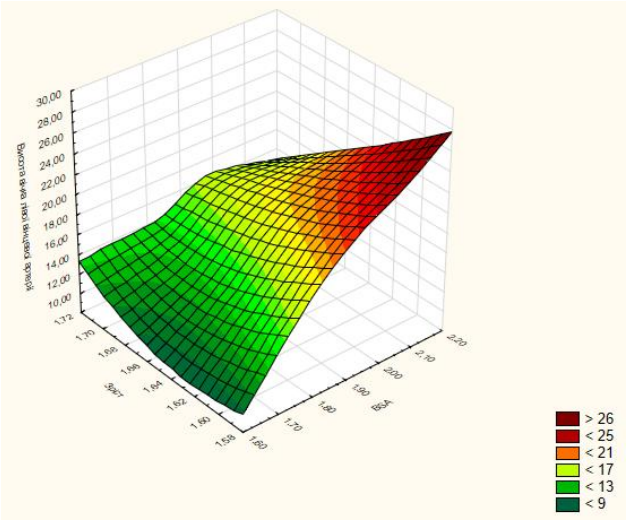

Fig. 4. The relationship between height indicators, BSA and the value of left coronary artery ostia height in a short person with CHD.

parameters (tb from -0.41 (with height) p=0.121 to +0.47 (with weight), p=0.081); between the left coronary artery upper edge ostia height indicator and weight and BMI (tb=+0.41, p=0.122 and p=0.102); between the right coronary artery upper edge ostia height parameter and weight (tb=-0.41, p=0.122).

Also, as a result of the conducted analysis, direct correlations between the values of certain morphometric parameters in short men with CHD were proven. In particular, the indicator of left sinus of Valsalva height was directly related to the parameters of the left coronary artery height: the lower

edge of the ostia (medium strength direct connection tb=+0.52, p=0.038) and the upper edge of the ostia (strong direct connection tb =+0.72, p=0.004). No proven correlations were found for the posterior sinus of Valsalva and right sinus of Valsalva height parameters, which again we attribute to the small sample of patients.

Discussion

CT measurement of sinuses of Valsalva height and coronary artery ostia height taking into account age, sex, height, weight, BMI and BSA in men with CHD results in a proven direct correlation of average strength between the three sinuses of Valsalva height. The relationship between the sinuses of Valsalva height and the corresponding coronary artery ostia height is logical [10]. According to the multifactorial regression analysis, there is a dependence of the left coronary artery ostia height on a complex of anthropometric indicators, namely: the inverse significant influence of weight and the direct significant influence of BMI and BSA. As a result, the prediction of the level of the left coronary artery ostia height in men with CHD was confirmed using the constructed model.

In the group of people of short stature, the inverse correlation between height and the height of the left coronary artery was proven. The smaller the height of a patient with CHD, the greater left coronary artery upper edge ostia height. The parameter of the left coronary artery ostia height has reliable direct relationships with weight (strong direct), with BMI (medium strong direct) with BSA (medium strong direct). Right coronary artery upper edge ostia height with BSA (reverse average force). It should be noted that a number of average strength relationships between other morphometric parameters and biometric data were established, which did not have confirmation of reliability due to a small sample (n=11).

It is important to emphasize that all patients were less than 1.80 m tall, which confirms the data that short people suffer from CHD more often [12, 13]. The relationship between the morphometric parameters of the aorta and biometric parameters taking into account body weight in men of group 1 (short stature) is consistent with previously published data [14, 16]. However, the previous studies concerned aortic stenosis. Relationships between morphometric parameters and age were not proven. Although a positive correlation between age and aortic root parameters has been described in men [16].

The issue of correlation of morphometric indicators is still debatable [5]. Obviously, this is due to the different groups of individuals included in the study. This includes racial, ethnic, and social affiliation [8]. According to the analysis of the literature, similar studies have not been published in Ukraine. The obtained results are particularly important in the context of aortic analysis for individuals with CHD who are candidates for CABG.

Conclusions

In men with CHD, left coronary artery ostia height correlates with weight, BMI, and BSA. In short men with CHD, there is an inverse relationship between left coronary artery height and height; direct relationships with weight, BMI and BSA.

References

[1] Bahlmann, E., Nienaber, C. A., Cramariuc, D., Gohlke-Baerwolf, C., Ray, S., Devereux, R. B., … & Gerdts, E. (2011). Aortic root geometry in aortic stenosis patients (a SEAS substudy). *European Journal of Echocardiography,* 12(8), 585-590. doi: 10.1093/ejechocard/jer037

[2] Blanke, P., Weir-McCall, J. R., Achenbach, S., Delgado, V., Hausleiter, J., Jilaihawi, H., … & Leipsic, J. A. (2019). Computed tomography imaging in the context of transcatheter aortic valve implantation (TAVI) / transcatheter aortic valve replacement (TAVR): An expert consensus document of the Society of Cardiovascular Computed Tomography. *Journal of Cardiovascular Computed Tomography,* 13(1), 1-20. doi: 10.1016/j.jcct.2018.11.008

[3] Buellesfeld, L., Stortecky, S., Kalesan, B., Gloekler, S., Khattab, A. A., Nietlispach, F., … & Windecker, S. (2013). Aortic Root Dimensions Among Patients With Severe Aortic Stenosis Undergoing Transcatheter Aortic Valve Replacement. *JACC: Cardiovascular Interventions*, 6(1), 72-83. doi: 10.1016/j.jcin.2012.09.007

[4] Devereux, R. B., de Simone, G., Arnett, D. K., Best, L. G., Boerwinkle, E., Howard, B. V., … & Roman, M. J. (2012). Normal Limits in Relation to Age, Body Size and Gender of Two-Dimensional Echocardiographic Aortic Root Dimensions in Persons ≥15 Years of Age. *The American Journal of Cardiology,* 110(8), 1189-1194. doi: 10.1016/j.amjcard.2012.05.063

[5] Forte, E., Punzo, B., Salvatore, M., Maffei, E., Nistri, S., Cavaliere, C., & Cademartiri, F. (2020). Low correlation between biometric parameters, cardiovascular risk factors and aortic dimensions by computed tomography coronary angiography. *Medicine,* 99(35), e21891. doi: 10.1097/MD.0000000000021891

[6] Komutrattananont, P., Mahakkanukrauh, P., & Das, S. (2019). Morphology of the human aorta and age-related changes: anatomical facts. *Anatomy & Cell Biology,* 52(2), 109-114. doi: 10.5115/acb.2019.52.2.109

[7] Madukauwa-David, I. D., Midha, P. A., Sharma, R., McLain, K., Mitra, R., Crawford, K., … & Yoganathan, A. P. (2019). Characterization of aortic root geometry in transcatheter aortic valve replacement patients. *Catheterization and Cardiovascular Interventions,* 93(1), 134-140. doi: 10.1002/ccd.27805

[8] Merz, A. A., & Cheng, S. (2016). Sex differences in cardiovascular ageing. I*n Heart,* 102(11), 825-831. doi: 10.1136/heartjnl-2015-308769

[9] Mosteller, R. D. (1987). Simplified Calculation of Body-Surface Area. *New England Journal of Medicine*, 317(17). doi: 10.1056/NEJM198710223171717

[10] Nasr, A. Y., & El Tahlawi, M. (2018). Anatomical and radiological angiographic study of the coronary ostia in the adult human hearts and their clinical significance. *Anatomy & Cell Biology,* 51(3), 164-173. doi: 10.5115/acb.2018.51.3.164

[11] Otto, C. M., Nishimura, R. A. W., Bonow, R. O., Carabello, B. A., Erwin, J. P., Gentile, F., … & Toly, C. (2021). 2020 ACC/AHA Guideline for the Management of Patients/American Heart

Association Joint Committee on Clinical Practice Guidelines. *Circulation,* 143(5), e72-e227. doi: 10.1161/CIR.0000000000000923

[12] Paajanen, T. A., Oksala, N. K. J., Kuukasjarvi, P., & Karhunen, P. J. (2010). Short stature is associated with coronary heart disease: a systematic review of the literature and a meta-analysis. *European Heart Journal*, 31(14), 1802-1809. doi: 10.1093/eurheartj/ehq155

[13] Silventoinen, K., Zdravkovic, S., Skytthe, A., McCarron, P., Herskind, A. M., Koskenvuo, M., … & Project for the G. (2006). Association between Height and Coronary Heart Disease Mortality: A Prospective Study of 35,000 Twin Pairs. *American Journal of Epidemiology,* 163(7), 615-621. doi: 10.1093/aje/kwj081

[14] Stolzmann, P., Knight, J., Desbiolles, L., Maier, W., Scheffel, H., Plass, A., … & Alkadhi, H. (2009). Remodelling of the aortic root in severe tricuspid aortic stenosis: implications for transcatheter aortic valve implantation. *European Radiology,* 19(6), 1316-1323. doi: 10.1007/s00330-009-1302-0

[15] Tomii, D., Okuno, T., Heg, D., Grani, C., Lanz, J., Praz, F., … & Reineke, D. (2022). Sinus of Valsalva Dimension and Clinical Outcomes in Patients Undergoing Transcatheter Aortic Valve Implantation. *American Heart Journal,* 244, 94-106. doi: 10.1016/j.ahj.2021.11.004

[16] Wang, X., Ren, X.-S., An, Y.-Q., Hou, Z.-H., Yu, Y.-T., Lu, B., & Wang, F. (2021). A Specific Assessment of the Normal Anatomy of the Aortic Root in Relation to Age and Gender. *International Journal of General Medicine*, Volume 14, 2827-2837. doi: 10.2147/IJGM.S312439

КОРЕЛЯЦІЯ МІЖ РОЗМІРАМИ ЦИБУЛИНИ АОРТИ ТА БІОМЕТРИЧНИМИ ПОКАЗНИКАМИ ПРИ ІШЕМІЧНІЙ ХВОРОБІ СЕРЦЯ

Підвальна У. Є.

Цибулина аорти вимагає прецензійного доопераційного аналізу для проведення аорто-коронарного шунтування при ішемічній хворобі серця. Розміри аорти корелюють з антропометричними показниками. Мета дослідження: встановити взаємозв'язок між висотою пазух аорти, висотою відходження вічок вінцевих артерій та біометричними показниками (віком, зростом, масою, площею поверхні тіла та індексом маси тіла) у чоловіків із ішемічною хворобою серця за допомогою комп'ютерної томографії. Матеріали та методи дослідження включають зображення комп'ютерної томографії з контрастуванням аорти чоловіків із верифікованою ішемічною хворобою серця. Згідно параметрів росту здійснено поділ на 2 групи. Проведено вимірювання висоти пазух аорти та висоти відходження вічок правої та лівої вінцевих артерій. Проаналізовані клінічні дані: вік, зріст, маса тіла, індекс маси тіла (ІМТ) та площа поверхні тіла (ППТ). Статистичний аналіз: t-критерій Стьюдента, методом рангової кореляції Кендала, лінійна кореляція Пірсона, мультифакторний регресійний аналіз Фішера. Аналіз результатів комп'ютерної томографії 30 хворих на ІХС чоловіків (середній вік 60,8±10,63 років) показав, що середні значення висоти трьох пазух аорти були приблизно на одному рівні. Результати оцінки проведеного лінійного кореляційного зв'язку за Пірсоном показали відсутність доведеного взаємозв'язку між біометричними показниками та морфометричними даними згідно КТ у хворих на ІХС чоловіків (p>0,05). Мультифакторний регресійний аналіз довів зворотній суттєвий вплив ваги та прямий суттєвий вплив ІМТ і ППТ на залежність висоти відходження вічка лівої вінцевої артерії. Коефіцієнт множинної кореляції становив R=+0,55, при p=0,023, SEE=2,74. Проведено прогнозування рівня висоти відходження вічка лівої вінцевої артерії у хворих на ІХС чоловіків із підтвердженням побудованої моделі. У першій групі чоловіків невисокого зросту (n=11) із ІХС (середній вік 60,11±12,63 років, зріст 1.677±0.023 м) доведено зворотній середньої сили кореляційний зв'язок між зростом та значенням висоти відходження верхнього краю вічка лівої вінцевої артерії (tb=-0,56, p=0,034). Встановлено достовірні прямі взаємозв'язки між параметром висоти вічка лівої вінцевої артерії та кількома антропометричними показниками: із вагою - прямий сильний зв'язок (tb=+0,72, p=0,007), із ІМТ - середньої сили прямий зв'язок (tb=+0,67, p=0,008), із ППТ - середньої сили прямий зв'язок (tb=+0,58, p=0,023). Доведено взаємозв'язок між значенням висоти відходження верхнього краю вічка правої вінцевої артерії та показником ППТ - зворотній середньої сили зв'язок (tb =-0,51, p=0,046). Не було доведено зв'язків між морфометричними параметрами та віком. Таким чином, у чоловіків із ішемічною хворобою серця висота відходження вічка лівої вінцевої артерії корелює з вагою, ІМТ і ППТ. У чоловіків невисокого зросту з ІХС існує зворотній зв'язок між висотою лівої вінцевої артерії та зростом; прямі взаємозв'язки з вагою, ІМТ і ППТ.

Ключові слова: *аорта, вінцева артерія, анатомія, комп'ютерна томографія, пазуха аорти.*

DOI: 10.31393/morphology-journal-2022-28(3)-03 Reports of Morphology, Vol. 28, №3, Pages 21-25

ISSN 1818-1295 eISSN 2616-6194

REPORTS OF MORPHOLOGY

Official Journal of the Scientific Society of Anatomists, Histologists, Embryologists and Topographic Anatomists of Ukraine

journal homepage: https://morphology-journal.com

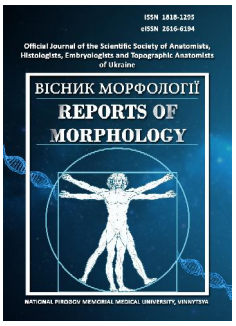

Submicroscopic changes in the heart of adult rats under conditions of persistent hyperhomocystemia

Kaminsky R. F.[1], Dzevulska I. V.[1], Yanchyshyn A. Ya.[1], Matkivska R. M.[1], Samborska I.A.[2]

[1]Bogomolets National Medical University, Kyiv, Ukraine
[2]National Pirogov Memorial Medical University, Vinnytsya, Ukraine

ARTICLE INFO
Received: 20 May 2022
Accepted: 24 June 2022

UDC: 616-001.17:615.451.3

CORRESPONDING AUTHOR
e-mail: anatomynmu@gmail.com
Yanchyshyn A. Ya.

CONFLICT OF INTEREST
The authors have no conflicts of interest to declare.

FUNDING
Not applicable.

Cardiovascular diseases are the leading cause of death and disability worldwide. It has been established that in recent years there has been a significant increase in the number of patients with this pathology, forcing researchers, scientists and physicians to look for risk factors of cardiovascular diseases, one of which is hyperhomocysteinemia (HHCys). The aim of the research is to study the features of submicroscopic changes in the heart of adult rats under conditions of HHCys. Experimental studies were performed on 22 white nonlinear adult (6-8 months) male rats in accordance with the principles of bioethics (Strasbourg, 1986; Kyiv, 2001). During the experiment, the animals were divided into two groups - control and experimental. Simulation of persistent HHCys was achieved by administering to rats the experimental group thiolactone homocysteine (HCys) at a dose of 200 mg/kg body weight intragastrally for 60 days. Ultrathin sections were studied in the PEM - 125K electron microscope. It was found that the introduction of thiolactone HCys to adult rats at a dose of 200 mg/kg causes the development of dystrophic and destructive changes in the heart of animals. Significant connective tissue edema was observed in the endocardium, and disturbances in the components of the microcirculatory tract were detected in the myocardium. Local enlightenment, cytoplasmic edema and local condensation of heterochromatin in hypertrophied nuclei were detected in hemocapillary endothelial cells. In cardiomyocytes, myofibrils are thickened, mitochondria are swollen with partial destruction of the cristae, tubules of smooth endoplasmic reticulum and T-tubules are dilated. These findings indicate that in adult rats HHCys caused the development of pathological changes in the endocardium, myocardium of experimental animals and in the microcirculatory tract.

Keywords: *hyperhomocysteinemia, heart, muscle fibers, cardiomyocytes, mitochondria, sarcomeres, rats.*

Introduction

Cardiovascular diseases are the leading cause of death and disability worldwide. It has been established that in recent years there has been a significant increase in the number of patients with this pathology, forcing researchers, scientists and doctors to look for risk factors of cardiovascular diseases in order to diagnose them in the early stages of development and prevention [18, 19].

Over the last decade, scientists' interest in the problem of HHCys has increased significantly, as an increase in plasma of this sulfur-containing amino acid leads to the emergence, progression and development of complications of cardiovascular diseases [2, 7, 17].

A significant amount of scientific works is devoted to the study of the main mechanisms of pathological action of elevated HCys levels on the human body, but the most studied today is hypomethylation and homocysteinylation of proteins. Hypomethylation causes a violation of the expression of a number of genes, which in turn is reflected in severe endothelial dysfunction, inhibition of its regeneration, vascular damage, excessive accumulation of lipids in the vascular wall, increased thrombosis. Homocysteinylation of proteins under conditions of HHCys is characterized by changes in their structure and functions. By homocysteinylation, important protein molecules lose their activity, for example, proaccelerin, fibrinogen, endothelial cell apoptosis factors, and so on [3, 4, 5, 13].

The above pathological changes that occur under

HHCys conditions contribute to the development of endothelial dysfunction. Prolonged negative effects of HCys on the vascular wall lead to the release of cytokines, chemokines (MCP-1, IL-8), the expression of adhesion molecules (VCAM-1), the initiation of platelet and coagulation hemostasis, activation of thrombin synthesis, and inhibition of anticoagulation and fibrinolysis. In addition, HCys affects all pathological processes leading to the formation of atherosclerotic plaques [6, 9, 11, 21].

Thus, increasing the concentration of HCys in blood plasma is a predictor of the development of pathologies of the cardiovascular system, and the study of its impact on structural changes in the heart and blood vessels is relevant today.

The aim of the research is to study the features of submicroscopic changes in the heart of adult rats under conditions of HHCys.

Materials and methods

The studies were performed on 22 white nonlinear adult (6-8 months) male rats. During the experiment, the animals were divided into two groups - control and experimental (11 animals in each group). Simulation of the state of hyperhomocysteinemia was achieved by administering to rats of the experimental group thiolactone HCys at a dose of 200 mg/kg body weight intragastrally for 60 days. Animals were decontaminated by decapitation under thiopental anesthesia.

The provisions of the "European Convention for the Protection of Vertebrate Animals Used for Experimental and Scientific Purposes" (Strasbourg, 1985) and the "General Ethical Principles for Animal Experiments", approved by the First National Congress on Bioethics, were followed in keeping, caring for and manipulating all animals (Kyiv, 2001).

Small pieces of rat heart were selected for ultrastructural study. They were fixed in 2.5-3.0 % solution of glutaraldehyde and and postfixed in 1 % osmium tetraoxide solution on the pH 7.2-7.4 phosphate buffer, followed by dehydration in alcohol and propylene oxide and then embedded into mixture of epoxy resins. Ultrathin sections were contrasted with uraniacetate and lead citrate according to Reynolds and studied in the PEM - 125K electron microscope [8, 12].

Results

Submicroscopic studies of the heart of adult animals in experimental HHCys revealed damage to the organ wall in the form of dystrophic and destructive changes. Thickening of collagen fibers and pronounced edema of the main substance of the endocardium were revealed. Partial stratification of muscle fibers has been identified. In the intercalated discs, the integrity of intercellular contacts was violated (Fig. 1).

The nuclei of cardiomyocytes changed their shape due to increased invagination of the karyolemma. The amount

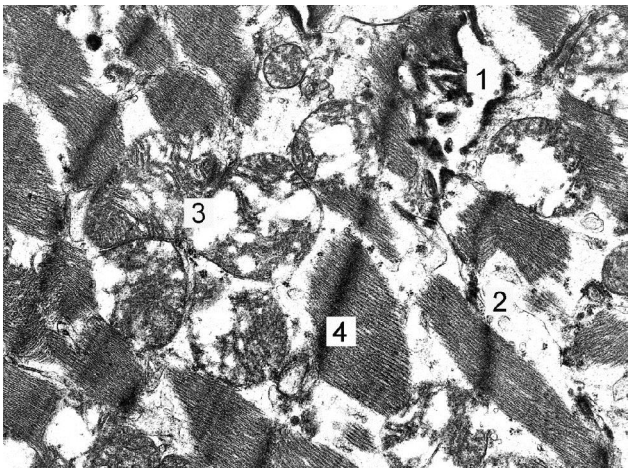

Fig. 1. Electronogram of cardiomyocytes of the myocardium of a mature rat with hyperhomocysteinemia: 1 - intercalated disc; 2 - cytoplasm of the cardiomyocyte; 3 - mitochondria; 4 - myofibrils. x14 000 magnification.

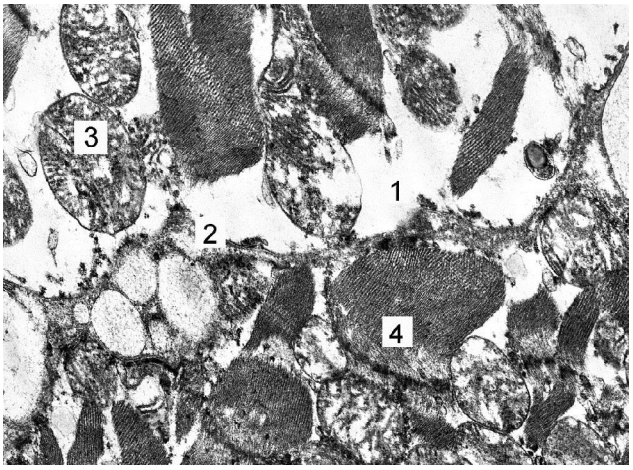

Fig. 2. Electrogram of myocardial cardiomyocyte of mature rat in hyperhomocysteinemia: 1 - cytoplasm of the cardiomyocyte; 2 - plasmalemma; 3 - mitochondria; 4 - myofibrils. x14 000 magnification.

of condensed chromatin increased compared to the intact group of adult animals. Karyoplasm is heterochromic, perinuclear spaces are partially expanded. Significant ultrastructural changes were found in the cytoplasmic organelles of cardiomyocytes. Thickening and partial loosening of myofibrils were detected. Thinning and partial lysis of myofilaments in myofibrils were determined. Locally, the sarcomeres were placed in a disordered manner, areas of myofibril overexpansion were detected. Mitochondria are swollen, the matrix is enlightened, cristae are destructured (Fig. 2). The expansion of the tubules of the smooth endoplasmic reticulum and T-tubes was revealed.

An increase in the relative volume of myocardial connective tissue was found. The thickness of collagen fibers increased, they often formed thick bundles. The blood vessels were full-blooded. Violation of the structural organization of the hemocapillary wall was revealed. Local

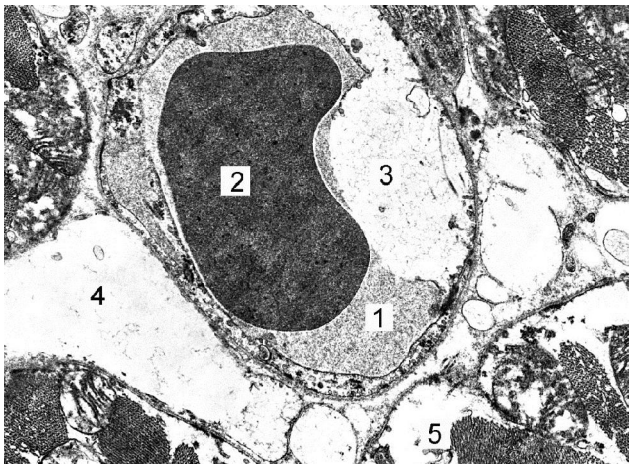

Fig. 3. Electronogram of hemocapillaries of the myocardium of a mature rat with hyperhomocysteinemia: 1 - hemocapillary lumen; 2 - erythrocyte; 3 - edema of the cytoplasm of the endothelial cell; 4 - perivascular space; 5 - cytoplasm of the cardiomyocyte. x8 000 magnification.

edema and cytoplasmic enlightenment were found in endotheliocytes. Endothelial cell nuclei were enlarged, heterochromatin became more condensed, and localized to the inner membrane of the karyolemma. The basement membrane is characterized by compaction, in some areas it was swollen, homogeneous (Fig. 3).

Discussion

According to research in recent years, HHCys causes the development of a wide range of disorders of the cardiovascular system. In particular, it is known that HHCys is a potential initiator of the development of an imbalance of prooxidant and antioxidant enzymes in the myocardium of rats, especially in males. It is also proved that under the conditions of administration of thiolactone HCys to rats, the activity of lipid peroxidation and oxidative modification of myocardial proteins increases. This fact is confirmed by the increase in the content of malonic dialdehyde and carbonyl groups of proteins in the myocardium. At the same time, the levels of these compounds were directly related to the concentration of HCys in the plasma of experimental animals. According to biochemical studies, HHCys also causes the development of cardiomyocyte cytolysis, as evidenced by the probable increase in AST and CPK activity in experimental rats [15].

The results of clinical studies show that in patients after coronary artery bypass grafting an increase in the concentration of plasma HCys has a negative impact on the state of the structural components of the aortic walls. Thus, histological examination of aortic fragments in this category of patients with a HCys plasma level of 15.72± 6.03 μmol/l in 29.69 % of individuals noted thickening of the tunica media with diffuse lymphocytic infiltration. Signs of tunica media hypertrophy and sclerosis, lymphocytic infiltration were observed in 51.85% of patients. In the subendothelial layer there was a decrease in the number of elastic fibers. Elastic membranes showed signs of partial destruction. The inner elastic membrane had areas of single ruptures [16].

It is a well-known fact that elevated HCys level is associated with a risk of cardiovascular disease. A large number of experimental studies show that HHCys causes the development of oxidative stress and ER stress, which are the causes of endothelial dysfunction. In addition, this amino acid under certain conditions causes a violation of the stability of atherosclerotic plaque and increases the degree of thrombotic complications. W. K. C. Lai and M. Y. Kan note that HCys disrupts the transport of nitric oxide (NO) precursor - L-arginine to endothelial cells, enhances the production of reactive oxygen species (ROS) with NADPH oxidase, which causes disorders of NO synthesis and its bioavailability. HCys also destroys the enzyme dimethylaminohydrolase and leads to the accumulation of NO synthase inhibitor - asymmetric dimethylarginine. It is also known that thiolactone HCys is able to interact with lysine-rich proteins, act as a trigger of ER stress and apoptosis of vascular wall endothelial cells [14].

Scientists note that HCys affects all pathological processes leading to the formation of atherosclerotic plaque. According to them, the mechanism is triggered by the production of significant amounts of ROS, reduced activity of the antioxidant system, increased levels of NADPH oxidase. ROS causes not only damage of endothelial cells, but also a decrease in the number of endothelial progenitors. Blood monocytes, replacing endothelial cells of the vascular wall, later turn into macrophages. The last are able to transform into so-called foam cells due to the absorption of oxidized VLDL. Under conditions of HHCys, their content increases due to inhibition of the synthesis of alipoprotein A-1 and disruption of the reverse transport of cholesterol to the liver. The gradual increase in the subendothelial space of foam cells under these conditions creates a vicious circle, causing a progressive increase in the number of atherosclerotic plaques [1, 10, 20].

Conclusion

Studies of the heart of adult animals in experimental HHCys have established dystrophic and destructive changes in the wall of the organ. Connective tissue edema was found in the endocardium. Violation of the components of the microcirculatory tract was detected in the myocardium. Local enlightenment, cytoplasmic edema and local condensation of heterochromatin in hypertrophied nuclei were detected in hemocapillary endothelial cells. In cardiomyocytes, myofibrils are thickened, mitochondria are swollen with partial destruction of the cristae, tubules of smooth endoplasmic reticulum and T-tubules are dilated. These findings indicate that in adult rats HHCys caused the development of pathological changes in the endocardium, myocardium of experimental animals and in the microcirculatory channel.

References

[1] Amodio, G., Moltedo, O., Faraonio, R., & Remondelli, P. (2018). Targeting the Endoplasmic Reticulum Unfolded Protein Response to Counteract the Oxidative Stress-Induced Endothelial Dysfunction. *Oxid Med Cell Longev,* 2018, 4946289. doi: 10.1155/2018/4946289

[2] Azzini, E., Ruggeri, S., & Polito, A. (2020). Homocysteine: Its Possible Emerging Role in At-Risk Population Groups. I*nt J Mol Sci,* 21(4), 1421. doi: 10.3390/ijms21041421

[3] Barroso, M., Handy, D. E., & Castro, R. (2017). The Link Between Hyperhomocysteinemia and Hypomethylation: Implications for Cardiovascular Disease. *Journal of Inborn Errors of Metabolism & Screening*, 5, 1-15. doi: 10.1177/2326409817698994

[4] Behera, J., Tyagi, S. C., & Tyagi, N. (2019). Hyperhomocysteinemia induced endothelial progenitor cells dysfunction through hypermethylation of CBS promoter. *Biochem Biophys Res Commun,* 510(1), 135-141. doi: 10.1016/j.bbrc.2019.01.066

[5] Bhattacharya, R., & Singh, L. R. (2020). Protein S-homocysteinylation: Identification of S-linked Protein Targets in the Blood Based on I-silico Srudy and Investigation of the Effect of Homocysteine on the Structural and Functional Interrity of the Potential Target Proteins. *Biochem Mol Biol,* 34(1), 1. doi: 10.1096/fasebj.2020.34.s1.03852

[6] Chernyavskiy, I., Veeranki, S., Sen, U., & Tyagi, S. C. (2016). Atherogenesis: hyperhomocysteinemia interactions with LDL, macrophage function, paraoxonase1, and exercise. *Ann NY Acad Sci,* 1363(1), 138-154. doi: 10.1111/nyas.13009

[7] Chrysant, S. G., & Chrysant, G. S. (2018). The current status of homocysteine as a risk factor for cardiovascular disease: a mini review. *Expert Rev Cardiovasc Ther,* 16(8), 559-565. doi: 10.1080/14779072.2018.1497974

[8] Dobrelia, N. V., Boitsova, L. V. & Danova, I. V. (2015). Legal basis for ethical examination of preclinical studies of drugs using laboratory animals. *Pharmacology and drug toxicology,* (2), 95-100.

[9] Esse, R., Barroso, M., de Almeida, I. D., & Castro, R. (2019). The Contribution of Homocysteine Metabolism Disruption Endothelial Dysfunction: State-of-the-Art. *International Journal of Molecular Sciences,* 20(4), 867. doi: 10.3390/ijms20040867

[10] Fang, K., Chen, Z., & Liu, M. (2015). Apoptosis and calcification of vascular endothelial cell under hyperhomocysteinemia. *Med Oncol,* 32(1), 403-405. doi: 10.1007/s12032-014-0403-z

[11] Hassan, E. A. (2019). The Relation between Homocysteine, Oxidative Stress and Atherosclerosis Disease. *Indian Journal of Public Health Research & Development,* 10(7), 537-542. doi: 10.5958/0976-5506.2019.01626.7

[12] Horalskyi, L. P., Khomych, V. T., & Kononskyi, O. I. (2011). *Fundamentals of histological technique and morphofunctional research methods in normal and pathology.* Zhytomyr: Polissya.

[13] Jakubowski, H. (2019). Homocysteine modification in protein structure / function and human disease. *Physiol Rev,* 99, 555-604. doi: 10.1152/physrev.00003.2018

[14] Lai, W. K. C. & Kan, M. Y. (2015). Homocysteine-induced endothelial dysfunction. *Ann Nutr Metab,* 67, 1-12. doi: 10.1159/000437098

[15] Melnik, A. V. (2017). Sex differences in pro-antioxidant system indicators in myocardium of rats under the conditions of hyperhomocysteinemia. *Achievements of Clinical and Experimental Medicine*, 1, 47-52.

[16] Nikonenko, O. S., Nikonenko, A. O., Chmul, K. O. & Osaulenko, V. V. (2020). Study of the influence of homocysteine and vitamin D metabolism on the development of destructive vascular wall processes. *Ukrainian Journal of Cardiovascular Surgery*, 3(40), 22-27. doi: 10.30702/ujcvs/20.4009/05002-027/11.9

[17] Rehman, T., Shabbir, M. A., Inam-Ur-Roheem, M., Manzoor, M. F., Ahmad, N., Liu, Z. W., … & Aadil, R. M. (2020). Cysteine and homocysteine as biomarker of various diseases. *Food Sci Nutr*, 8(9), 4696-4707. doi: 10.1002/fsn3.1818

[18] Spiteri, J., & von Brockdorff, P. (2019). Economic development and health outcomes: Evidence from cardiovascular disease mortality in Europe. *Soc Sci Med*, 224, 37-44. doi: 10.1016/j.socscimed.2019.01.050

[19] Timmis, A., Townsend, N., Gale, C. P., Torbica, A., Lettino, M., Petersen, S. E., … & Vardas, P. (2020). European Society of Cardiology: Cardiovascular Disease Statistics 2019. *European Heart Journal,* 41(1), 12-85. doi: 10.1093/eurheartj/ehz859

[20] Wang, X. C., Sun, W. T., Yu, C. V., Pun, S. H., Underwood, M. J., He, G. W., … & Yang, Q. (2015). ER stress mediates homocysteine-induced endothelial dysfunction: Modulation of IK Ca and SK Ca channels. *Atherosclerosis,* 242(1), 191-198. doi: 10.1016/j.atherosclerosis.2015.07.021

[21] Wu, X., Zhang, L., Miao, Y., Yang, J., Wang, X., Wang, C. C., … & Wang, L. (2019). Homocysteine causes vascular endothelial dysfunction by disrupting endoplasmic reticulum redox homeostasis. *Redox Biol,* 20, 46-59. doi: 10.1016/j.redox.2018.09.021

СУБМІКРОСКОПІЧНІ ЗМІНИ В СЕРЦІ ДОРОСЛИХ ЩУРІВ ЗА УМОВ СТІЙКОЇ ГІПЕРГОМОЦИСТЕЇНЕМІЇ

Камінський Р. Ф., Дзевульська І. В., Янчишин А. Я., Матківська Р. М., Самборська І. А.

Захворювання серцево-судинної системи є провідною причиною смертності та інвалідності населення у всьому світі. Встановлено, що протягом останніх років реєструють значне зростання чисельності хворих з даною патологією, що змушує дослідників, науковців та лікарів до пошуку факторів ризику хвороб серцево-судинної системи, одним з яких є гіпергомоцистеїнемія (ГГц). Метою дослідження є вивчення особливостей субмікроскопічних змін в серці дорослих щурів за умов ГГц. Експериментальні дослідження проведені на 22 білих нелінійних дорослих (6-8 місяців) щурах-самцях з дотриманням принципів біоетики (Страсбург, 1986; Київ, 2001). Протягом дослідження тварин поділено на дві групи - контрольну та дослідну. Моделювання стану стійкої ГГц досягали шляхом введення щурам дослідної групи тіолактону гомоцистеїну (Гц) в дозі 200 мг/кг маси тіла інтрагастрально протягом 60 днів. Ультратонкі зрізи досліджували за допомогою електронного мікроскопу РЕМ - 125К. Встановлено, що введення дорослим щурам тіолактону Гц в дозі 200 мг/кг спричиняє розвиток дистрофічних та деструктивних змін в серці тварин. В ендокарді виявлений значний набряк сполучної тканини. У міокарді визначалося порушення компонентів мікроциркуляторного русла. В ендотеліоцитах гемокапілярів виявлено локальне просвітлення та набряк цитоплазми та локальна конденсація гетерохроматину в гіпертрофованих ядрах. У кардіоміоцитах міофібрили потовщені, мітохондрії набряклі з частковою деструкцією крист,

канальці гладкої ендоплазматичної сітки та Т-трубочки розширені. Дані знахідки свідчать, що в дорослих щурів ГГц зумовлювала розвиток патологічних змін в ендокарді, міокарді дослідних тварин та в мікроциркуляторному руслі.
Ключові слова: *гіпергомоцистеїнемія, серце, м'язові волокна, кардіоміоцити, мітохондрії, саркомери, щури.*

DOI: 10.31393/morphology-journal-2022-28(3)-04 Reports of Morphology, Vol. 28, №3, Pages 26-31

ISSN 1818-1295 eISSN 2616-6194

REPORTS OF MORPHOLOGY

Official Journal of the Scientific Society of Anatomists, Histologists, Embryologists and Topographic Anatomists of Ukraine

journal homepage: https://morphology-journal.com

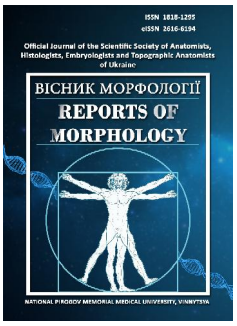

Peculiarities of indicators of the respiratory system in women at rest and their changes during the burning of the next cigarette

Shevchuk T. Ya., Aponchuk L. S., Pikalyuk V. S., Olishkevich O. O.
Lesya Ukrainka Volyn National University, Lutsk, Ukraine

ARTICLE INFO
Received: 24 May 2022
Accepted: 28 June 2022

UDC: 612.2-055.2:613.81/.84

CORRESPONDING AUTHOR
e-mail: tetyana_shevchuk_2013@ukr.net
Shevchuk T. Ya.

CONFLICT OF INTEREST
The authors have no conflicts of interest to declare.

FUNDING
Not applicable.

One of the important problems facing modern society is the increase in the number of people with various types of addictions, the most common of which is smoking. Smoking and its medical-demographic and economic consequences are in the circle of scientific interests of many domestic and foreign scientists. That is why the aim of the scientific article is to study the peculiarities of the state of the respiratory system in women at rest and during the burning of another cigarette. The study was conducted in the Laboratory of Medical and Biological Monitoring and Public Health at the Department of Human and Animal Physiology, Faculty of Biology and Forestry, Lesya Ukrainka Volyn National University for 60 women aged 17-21. At the first stage of the study, absolute anthropometric indicators were measured, such as height, weight, chest circumference. In the second stage women were interviewed on the Fagerström test. According to its results, the study is divided into 3 groups: Group I - women who have a history of smoking more than 3 years, burn more than 10 cigarettes per day and have a high level of dependence, Group II - women who have a history of smoking 1-3 years, up to 10 cigarettes are smoked per day and have a low and medium level of dependence, Group III - (control) women who do not smoke. The next stage of the study involved a functional diagnosis of the external respiratory system in women at rest and 15 minutes after smoking a cigarette using the functional method of pneumotachography (PTG). Registration and analysis of relevant indicators was carried out using a diagnostic automated complex "Cardio+". Statistical data processing was performed using generally accepted methods of variation statistics (because the distribution of the results was normal) using MS Excel 2007 software. This article presents a study of the state of external respiration at rest and 15 minutes after burning another cigarette, which revealed the negative effects of smoking on the respiratory system of women who smoke. The study made it possible to make a detailed analysis of indicators of respiratory function in women aged 17-21 years, smokers and compare them with non-smokers. Based on the obtained results, it was found that in women smokers (groups I and II) there is a significant decrease in volume (FVC, VC, FEV1) indicators of external respiration, as well as the Tiffeneau-Pinelli test at $p<0.05$, compared with the group of women control group both at rest and 15 minutes after firing the next cigarette. Analysis of velocity (MEF at the level of exhalation 25 %, 50 %, 75 %, PEF) of airflow through the bronchi to the lungs indicates a gradual decrease from MEF 25 % to MEF 75 % in women of the experimental groups, but a significant decrease is observed only at the level sight of 75 % in 15 min after burning of the next cigarette between I and III groups (at $p<0.05$). A statistically significant difference between the values of the calculated Tiffeneau-Pinelli index, which characterizes the presence of obstructive respiratory failure, in women of groups II and III both at rest and 15 minutes after burning another cigarette. Thus, a decrease in these indicators indicates the presence of bronchial obstruction of the middle and small bronchi, as well as a violation of respiratory muscle strength and bronchial patency. It has also been shown that the reactivity (reduction) of volumetric and velocity indicators of external respiration to cigarette burning was higher in the group of women who do not smoke (control).

Keywords: *smoking, women-smokers, external respiration, cigarettes, reactivity.*

Introduction

Smoking is one of the most urgent problems of our time, especially young girls and women increasingly become addicted to smoking, which is characterized by a negative impact on their somatic and mental health [5, 8, 9, 11]. Today, there are many preventive types of smoking that can be used to get rid of this bad habit, one of them is social advertising, but it is only gaining its relevance [1, 5, 10, 15, 16].

According to scientific research [10], the age of the first attempt to smoke falls on 12-13 years, which is an unfavorable prognostic sign, on the one hand, from the point of view of the formation of children's health, and on the other hand, an increase in the smoking frequency of persons of working age in the future. In particular, the tobacco industry uses various manipulative tools to attract young people to smoking [6, 9]. One of the many techniques is the use of colorful logos on cigarette packs, which further encourage the purchase [2, 14, 23, 25].

Since today's teenagers are poorly informed about the impact of tobacco smoking on all organs and systems of our body [12, 13, 16, 19], there is a need for a theoretical and empirical study of the peculiarities of the state of respiratory system indicators at rest and during the smoking of the next cigarette, which on today's time is quite relevant.

The purpose of the work is to study the peculiarities of the condition of the respiratory system indicators in women at rest and during the smoking of the next cigarette.

Materials and methods

The study was conducted in the laboratory of medical and biological monitoring and public health at the Department of Human and Animal Physiology, Faculty of Biology and Forestry, Lesya Ukrainka Volyn National University. The study used a functional research method - pneumotachography and a method of statistical analysis of experimental data. Compliance of the research procedure with the legislation of Ukraine on health protection and the Declaration of Helsinki 2000, the directive of the European Society 86/609 regarding the participation of people in medical and biological research was confirmed by the commission on bioethics of the Faculty of Biology and Forestry of Volyn National University named after Lesya Ukrainka (protocol № 1 from 21.10.2016). All subjects were familiarized with the conditions of the examination and before the start of work gave written voluntary consent to participate in the study.

According to the outpatient cards, all women belonged to the group of practically healthy people. The studied women smoked Winston street light (light) cigarettes. There are 10 packs of cigarettes in the block. There are 20 pieces in a pack. The length of each cigarette is 8 cm. The nicotine content is 0.5 mg, tar - 0.6 mg. The filter is normal. 60 women aged 17-21 took part in the study, who were interviewed according to the Fagerström test. According to its results, the following groups were distinguished: Group I - women who have smoked for more than 3 years, smoke more than 10 cigarettes per day and have a high level of addiction (20 people), Group II - women who have smoked for 1-3 years, smoke up to 10 cigarettes per day and have a low and medium level of addiction (20 people), III group - (control) women who do not smoke (20 people).

To write the work, such indicators of pneumotachography as forced vital capacity (FVC, l), vital capacity (VC, l), forced expiratory volume in 1 second (FEV1, l), Tiffeneau-Pinelli index (%), maximal expiratory flow were used 25 % FVC (MEF 25 %, l/s), maximal expiratory flow 50 % FVC (MEF 50 %, l/s), maximal expiratory flow 75 % FVC (MEF 75 %, l/s), peak expiratory flow (PEF, s).

Statistical data processing was carried out using parametric methods of variational statistics using MS Excel 2007 software. Arithmetic mean (M), standard error of the arithmetic mean (m), Student's reliability criterion (t) were calculated (reliability level p?0.05).

Results

Analyzing the data obtained during the study of external breathing parameters at rest and after 15 min after smoking the next cigarette, we noted that most indicators have statistically significant differences (at $p \leq 0.05$) in representatives of all three groups (Table 1).

During the study, it was found that the reactivity (decrease) of external breathing indicators to smoking another cigarette was higher in representatives of the control group who do not smoke (see Table 1).

The analysis of the volumetric indicators of the respiratory system in women showed that they differ significantly in all three studied groups (Figs. 1-2, see Table 1).

In women of group I (smoking experience more than 3 years), the FVC indicator is significantly lower than in non-smokers (group III), both at rest and after 15 minutes after smoking another cigarette ($p<0.05$). Among representatives

Table 1. Indicators of external breathing of female smokers at rest and those who do not smoke, and their changes during the smoking of the next cigarette (M±m, n=60).

Indicators	Smoking experience >3 y.		Control group	
	rest	reactivity	rest	reactivity
FVC, l	2.403±0.296*	-0.301±0.442	3.26±0.122	-0.710±0.255
VC, l	2.786±0.302*	-0.262±0.405	3.22±0.110	-0.691±0.265
FEV1, l	2.390±0.284*	-0.332±0.410	3.166±0.120	-0.41±0.201
Tiffeneau-Pinelli index,%	83.69±8.73*	12.13±0.21	98.06±0.37	-15.98±0.92
MEF 25%, l/s	5.298±0.367*	0.089±0.465	6.398±0.200*	-1.345±0.299
MEF 50%, l/s	5.001±0.321*	-0.189±0.478	6.599±0.166	-0.903±0.491
MEF 75%, l/s	4.189±0.365*	-0.022±0.399	5.501±0.220*	-1.111±0.512
PEF, s	5.899±0.376*	0.289±0.522	8.154±0.289*	-2.390±0.401

Note: * - the data are significantly different at $p \leq 0.05$.

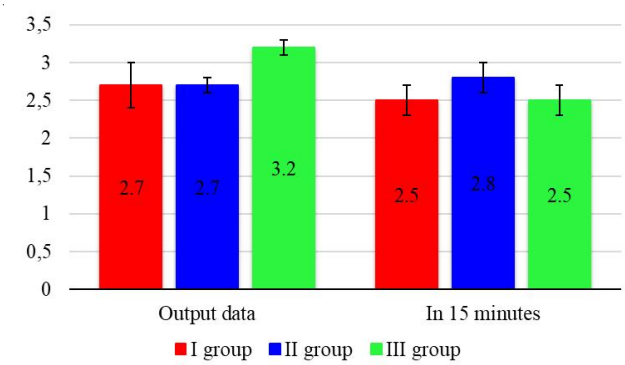

Fig. 1. Comparative analysis of the VC indicator in women of the I, II and III groups and their changes during the smoking of the next cigarette.

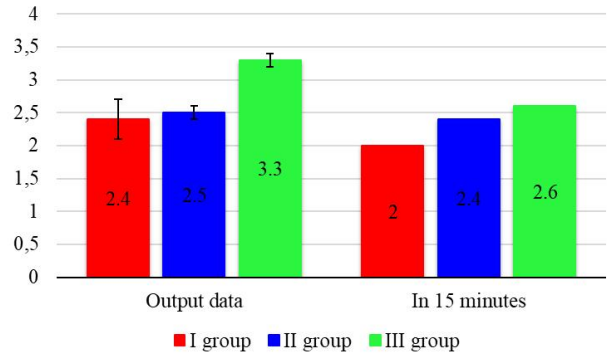

Fig. 2. Comparative analysis of the FVC indicator in women of the I, II and III groups and their changes during the smoking of the next cigarette.

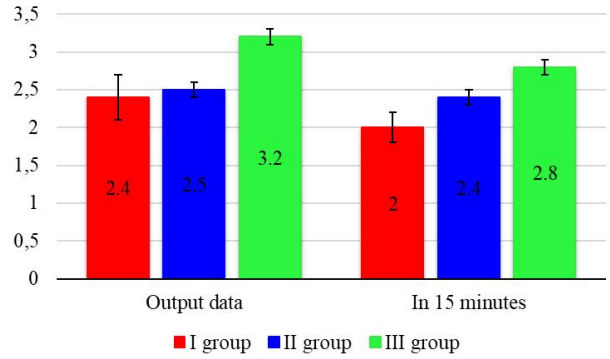

Fig. 3. Comparative analysis of the FEV1 index in women of groups I, II and III and their changes during smoking the next cigarette.

of II (smoking experience from 1 to 3 years) and III groups, significant differences in this indicator were observed only in a state of rest. This indicator decreased in all three groups, but it was significantly lower in the group I. We observe a similar trend when analyzing changes in the VC indicator (see Figs. 1-2).

The FEV1 indicator in female smokers of both groups is lower than in the control group, at $p<0.05$ in a state of rest (Fig. 3). After smoking the next cigarette, the indicator significantly decreases in all groups, however, significant differences were established only between I (smoking experience over 3 years) and III groups of women.

The Tiffeneau-Pinelli sample calculation indicators (the ratio of FEV to FVC) make it possible to dynamically assess the efficiency of external breathing of the examinees. In this study, we observed significant differences between the indicators of II (smoking experience from 1 to 3 years) and III groups both at the initial data and after 15 minutes after smoking another cigarette (Fig. 4).

The analysis of the speed indicators of the respiratory system indicates their gradual decrease from the maximum volumetric speed at the level of 25 % to the maximum volumetric speed at the level of 75 % in women of all three groups (Figs. 5-7, see Table 1). Moreover, MEF indicators

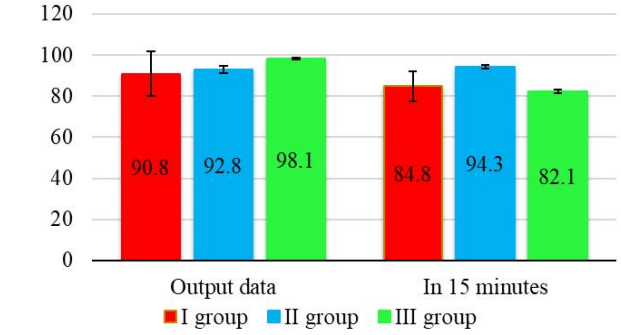

Fig. 4. Comparative analysis of the Tiffeneau-Pinelli test in women of groups I, II and III and their changes during smoking the next cigarette.

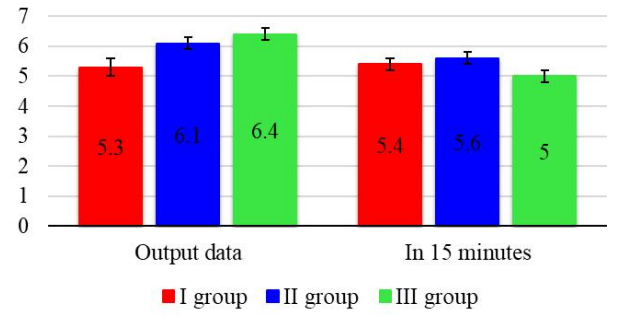

Fig. 5. Comparative analysis of the MEF indicator at the level of 25 % in women of the I, II and III groups and their changes during the smoking of the next cigarette.

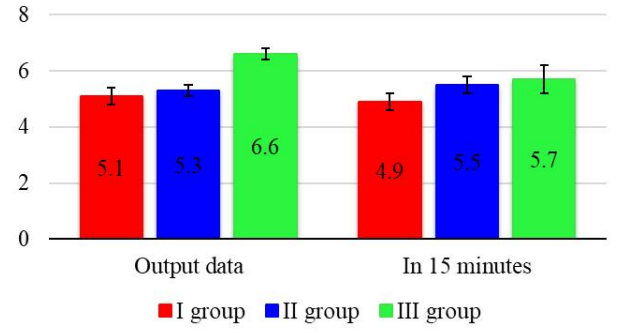

Fig. 6. Comparative analysis of the MEF indicator at the level of 50 % in women of the I, II and III groups and their changes during the smoking of the next cigarette.

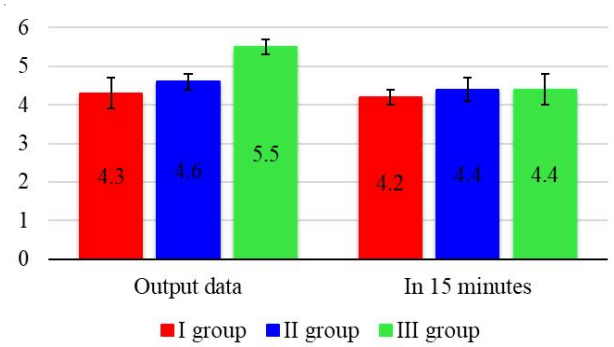

Fig. 7. Comparative analysis of the MEF indicator at the level of 75% in women of groups I, II and III and their changes during smoking the next cigarette.

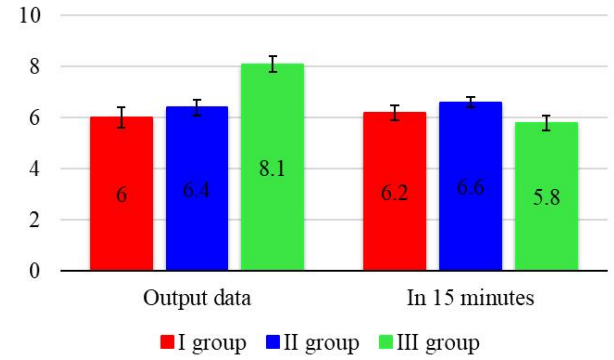

Fig. 8. Comparative analysis of the PEF indicator in women of groups I, II and III and their changes during smoking the next cigarette.

are at the level of 25 %; 50 %; 75 % higher in the control group (at $p<0.05$), which indicates better pulmonary ventilation.

However, a decrease in the value of the MEF indicator at the level of 25% is observed in the I (smoking experience over 3 years) and II (smoking experience from 1 to 3 years) groups, and in the I group it slightly increases after smoking another cigarette.

During MEF at the level of 75 %, a reliable decrease in the value of this indicator was established after 15 minutes between I (smoking experience over 3 years) and III groups (at $p<0.05$).

Initial data of PEF in female smokers (I and II groups) are significantly lower, compared to individuals of the control group (Fig. 8, see Table 1).

The value of this indicator is especially low in women who have been smoking for more than 3 years and smoke more than 10 cigarettes per day and have a high level of addiction (Group I - 103 %). After smoking another cigarette in 15 minutes we note a significant decrease in the values of the indicator between I (smoking experience over 3 years) and III groups.

Discussion

An analysis of the indicators of the respiratory system in young women at rest and their changes during the smoking of the next cigarette was revealed, which indicates that most of the speed and volume indicators have a reliable difference between the comparison groups in representatives of all three groups.

It was investigated that in women who smoke (I and II groups) at rest and 15 minutes after smoking the next cigarette there is a decrease in the Tiffeneau-Pinelli test, as well as volume and speed indicators of external breathing, which indicates a slight violation of bronchial patency, since the smoking experience is 3 - 5 years. Also, smoking causes spasm of blood vessels, to which the body responds by increasing pressure and heart rate, resulting in rapid breathing, shortness of breath, and coughing.

It is worth noting that a large number of scientists who study the impact of smoking on the functional state of a young organism claim that teenagers are sufficiently aware of the harmful effects of smoking on health. As the literature analysis showed, the prevalence of smoking among young people varies from 25 % to 50 % [15]. According to Pasko K. A. et al. [15], up to 92 % of the interviewed teenagers answered that smoking harms health and is the cause of many diseases. The obtained results indicate the presence of moderate tobacco addiction in a significant number of teenagers. One of the reasons for the fact that attempts to quit smoking turned out to be useless or with a temporary effect in 29 % of the interviewed teenagers. Apparently, the main reason for failure is weak motivation and tobacco addiction [4, 6, 15, 16].

A significant number of scientific works are devoted to the study of functional changes in the body of male adolescents and young adults during smoking [5, 7, 17, 22, 25].

It should be noted that there are quite a number of works devoted to the study of the impact of tobacco products on the respiratory system, in particular of men (with accompanying diseases), in which the negative impact of the components of tobacco smoke on the state of individual organs and systems is noted [3, 6, 7, 12, 13, 17-19, 21-25].

However, studies of the impact of tobacco smoking on the functional state of the respiratory system in healthy young women aged 17-21 years with different smoking experience and the manifestation of reactivity in response to smoking another cigarette are relevant and less studied [20]. However, the analysis of literary sources in recent years indicates that, against the background of the reduction in the prevalence of smoking of ordinary cigarettes, electronic cigarettes are becoming more and more popular, in particular, among teenagers and young people, which is a reason for further research into their effects on the body in comparison with ordinary cigarettes [4, 10, 11]. Therefore, further research on this topic, in our opinion, should be directed to the study of the effects of smoking electronic cigarettes or vapes on the respiratory system.

Conclusion

Based on the studies of external breathing at rest (initial data) and after smoking another cigarette, it was

established that female smokers (I and II groups) have a decrease in volume and speed indicators of external breathing, as well as the Tiffeneau-Pinelli test. This indicates a violation of bronchial patency and strength of respiratory muscles - bronchial obstruction of medium and small bronchi. At the same time, the reactivity (decrease) of external breathing indicators to smoking another cigarette was higher in the representatives of the control group.

References

[1] Aksenova, A. V., Oshchepkova, E. V., Orlovsky, A. A., & Chazova, I. E. (2020). Gender-age peculiarities of smoking and diabetes mellitus role in the development of myocardial infarction in patients with arterial hypertension. *Systemic Hypertension,* 17(4), 24-31. doi: 10.26442/2075082X.2020.4.200245

[2] Bedzai, A. O., & Shcherbyna, O. M. (2019). Жінки-курці: тенденції, наслідки, та мотивації відмови від куріння [Women smokers: trends, consequences, and motivations for quitting]. *Вісник ЛДУБЖД - Bulletin of the LDUBZHD,* (19), 61-67. doi: 10.32447/20784643.19.2019.06

[3] Davis, K. C., Murphy-Hoefer, R., Levine, B., King, B. A., Hu, S., & Rodes, R. (2019). Peer Reviewed: Evidence of the Impact of the Tips From Former Smokers Campaign: Results From the Behavioral Risk Factor Surveillance System. *Preventing chronic disease*, (16), 1-5. doi: 10.5888/pcd16.190110

[4] Dobrovolska, L. I. (2020). Світовий досвід боротьби з вейпінгом та його наслідки серед дітей та молоді [World experience in combating vaping and its consequences for children and youth]. *Вісник медичних і біологічних досліджень - Bulletin of Medical and Biological Research*, 3(5), 153-160. doi: 10.11603/bmbr.2706-6290.2020.3.11297

[5] Halimov, A., & Kovalska, I. (2021). Формування культури ведення здорового способу життя майбутніми офіцерами-прикордонниками [Formation of a culture of healthy living by future border guards]. *Збірник наукових праць Національної академії Державної прикордонної служби України - Collection of scientific works of the National Academy of the State Border Guard Service of Ukraine,* 25(2), 17-36. doi: 10.32453/pedzbirnyk.v25i2.779

[6] Hutor, T. H. & Kozii-Bredelieva, S. P. (2020). Поширеність вживання тютюнових виробів серед молодого населення львівської області [Prevalence of tobacco use among the young population of Lviv region]. *Вісник соціальної гігієни та організації охорони здоров'я України - Bulletin of social hygiene and health care organization of Ukraine*, 4(86), 13-18. doi: 10.11603/1681-2786.2020.4.11904

[7] Ilchenko, S. I., Fialkovska, A. O., & Skriabina, K. V. (2021). Взаємозв'язок рівня моноаксиду азоту з активністю фіброгенного цитокіну TGF-β1 та їхня роль у діагностиці розвитку незворотних морфофункціональних змін бронхів у підлітків, які курять [Relationship between nitric oxide levels and fibrogenic cytokine TGF-β1 activity and their role in diagnosing the development of irreversible bronchofunctional changes in the bronchi in adolescents who smoke]. *Палотогія - Palotology,* 18(2), 189-195. doi: 10.14739/2310-1237.2021.2.225193

[8] Kashuba, V. O., & Maslova, O. V. (2015). Поширеність шкідливих звичок серед підлітків із вадами слуху як додатковий фактор ризику погіршення стану їхнього здоров'я [Prevalence of bad habits among adolescents with hearing impairments as an additional risk factor for deteriorating health]. *Фізичне виховання, спорт і культура здоров'я у сучасному суспільстві - Physical education, sports and health culture in modern society,* 4(32), 175-178.

[9] Kotova, N. V., Starets, O. O., & Kovalenko, D. A. (2021). Вплив вторинного тютюнового диму на респіраторну патологію, сенсибілізацію та розвиток алергічних захворювань у дітей раннього віку (огляд літератури) [The effect of second-hand tobacco smoke on respiratory pathology, sensitization and development of allergic diseases in young children (literature review)]. *Здоров'я дитини - Child health,* 16(5), 368-374. doi: 10.22141/2224-0551.16.5.2021.239717

[10] Latina, H. O., & Zaikina, H. L. (2020). Стан поширення та основні напрями профілактики тютюнопаління у підлітків 11-17 років (реґіонарний аспект) [Status of distribution and main directions of tobacco prevention in adolescents aged 11-17 (regional aspect)]. *Український журнал медицини, біології та спорту - Ukrainian Journal of Medicine, Biology and Sports,* 5, 6(28), 349-354. doi: 10.26693/jmbs05.06.349

[11] Lisetska, I. S. (2021). Види та пристрої для паління та їх шкідливий вплив на організм людини [Types and devices for smoking and their harmful effects on the human body]. *Український журнал Перинатологія і Педіатрія - Ukrainian Journal of Perinatology and Pediatrics,* 1(85), 81-90. doi: 10.15574/PP.2021.85.81

[12] Mostovoi, Yu. M., Slepchenko, N. S., Dmytriiev, K. D., & Sydorov, A. A. (2018). Хронічне обструктивне захворювання легень та серце: здобутки та питання сьогодення [Chronic obstructive pulmonary disease and heart disease: achievements and issues of the present]. *Український пульмонологічний журнал - Ukrainian Pulmonology Journal*, (4), 56-61. doi: 10.31215/2306-4927-2018-102-4-56-61

[13] Ostrovska, S. S. (2016). Ремоделювання дихальної системи при тютюнопалінні (огляд іноземної літератури) [Remodeling of the respiratory system in smoking (review of foreign literature)]. *Вісник морфології - Reports of Morphology,* 2(22), 412-414.

[14] Palamarchuk, O. S. (2021). *Особливості функціонального стану автономної нервової системи під впливом глибокого дихання в режимі біологічного зворотного зв'язку: монографія [Features of the functional state of the autonomic nervous system under the influence of deep breathing in the mode of biological feedback: monograph].* Ужгород: Вид-во УжНУ "Говерла", 128 с. ISBN 978-617-7825-41-7

[15] Pasko, K. A., Luhova, Yu. R., Holovanova, I. A., Pluzhnikova, T. V., & Krasnova, O. I. (2019). Проблема куріння серед сучасної молоді [The problem of smoking among modern youth]. *Українська медична стоматологічна академія - Ukrainian Medical Dental Academy*, 103-104.

[16] Rohach, I. M., Keretsman, A. O., Pohoriliak, R. Yu., & Reho, O. Yu. (2020). Поширення куріння та вживання алкоголю серед школярів м. Ужгорода, як одна із основних медико-соціальних проблем сучасності [The spread of smoking and alcohol consumption among schoolchildren in Uzhgorod, as one of the main medical and social problems of our time], *Вісник проблем біології і медицини - Bulletin of problems of biology and medicine*, 2(156), 324-327. doi: 10.29254/2077-4214-2020-2-156-324-327

[17] Slepchenko, N. S., Dmytriiev, K. D., Cimbalyuk, N. V., & Mostovoi, Yu. M. (2021). Бронхіальна астма та паління [Bronchial asthma and smoking]. *Український пульмонологічний журнал - Ukrainian Pulmonology Journal,* (1), 62-64. doi:

10.31215/2306-4927-2021-29-1-62-64
[18] Slepchenko, N. S. (2013). Паління та кардіопульмональна патологія: вплив на виникнення, перебіг та прогноз [Smoking and cardiopulmonary pathology: impact on the occurrence, course and prognosis]. *Вісник Вінницького національного медичного університету - Reports of Vinnytsia National Medical University,* 17(1), 263-267.
[19] Soldatenko, V. H. (2021). Актуальні питання захворювань органів дихання серед здобувачів вищої освіти [Topical issues of respiratory diseases among higher education students]. *Вісник Луганського національного університету імені Тараса Шевченка - Bulletin of Taras Shevchenko National University of Luhansk*, 2(340), 174-181. doi: 10.12958/2227-2844-2021-2(340)-2-174-181
[20] Shevchuk, T. Ya., Aponchuk, L. S., & Romaniuk, A. P. (2015). Стан показників зовнішнього дихання у жінок, які курять [The state of indicators of external respiration in women who smoke]. *Вісник Харківського національного університету імені В. Н. Каразіна - Bulletin of V. N. Karazin Kharkiv National University,* 24(1153), 163-170.
[21] Shevchuk, T., Pshybelskyj, V., Zhuravlov, O., & Zhuravlova, O. (2021). Особливості показників серцево-судинної системи в осіб зрілого віку залежно від конституції тіла за несприятливих екологічних умов [Features of indicators of the cardiovascular system in adults depending on the constitution of the body under adverse environmental conditions]. *Вісник морфології - Bulletin of morphology,* 27(1), 72-78. doi: 10.31393/morphology-journal-2021-27(1)-10
[22] Tovt-Korshynska, M. I., & Rudakova, S. O. (2011). Особливості психоемоційного стану та схильність до гострих респіраторних захворювань у курців тютюну різної статі [Features of psycho-emotional state and predisposition to acute respiratory diseases in tobacco smokers of different sexes]. *Науковий вісник Ужгородського університету - Scientific Bulletin of Uzhgorod University,* (40), 145-147.
[23] Voloshyna, O. B., & Zbitnieva, V. O. (2017). Частота і ступінь порушень дихальної функції в пацієнтів з артеріальною гіпертензією залежно від стажу куріння [Frequency and degree of respiratory disorders in patients with hypertension depending on smoking history]. *Здоров'я суспільства - Public health*, 6(3), 43-46.
[24] Zanetti, F., Zhao, X., Pan, J., Peitsch, M. C., Hoeng, J., & Ren, Y. (2019). Effects of cigarette smoke and tobacco heating aerosol on color stability of dental enamel, dentin, and composite resin restorations. *Quintessence Int,* 50(2), 156-166. doi: 10.3290/j.qi.a41601
[25] Zieliński, E., Zieliński, M., Motylewski, B., & Skalski, D. (2021). Study of adolescents' awareness of the effects of smoking in order to increase the effectiveness of cancer prevention. *Bulletin of Lviv State University of Life Safety,* (23), 46-52. doi: 10.32447/20784643.23.2021.07

ОСОБЛИВОСТІ ПОКАЗНИКІВ ДИХАЛЬНОЇ СИСТЕМИ В ЖІНОК У СПОКОЇ ТА ЇХ ЗМІНИ ПІД ЧАС ВИПАЛЮВАННЯ ЧЕРГОВОЇ СИГАРЕТИ

Шевчук Т. Я., Апончук Л. С., Пикалюк В. С., Олішкевич О. О.

Однією з важливих проблем, з якими стикається сучасне суспільство, є збільшення кількості людей з різними видами залежності, найпоширенішою з яких є тютюнопаління. Тютюнопаління та його медико-демографічні й економічні наслідки перебувають у колі наукових інтересів багатьох вітчизняних та зарубіжних учених. Саме тому метою наукової статті є дослідження особливостей стану показників дихальної системи в жінок у стані спокою та під час випалювання чергової сигарети. Дослідження проведено в лабораторії медико-біологічного моніторингу та громадського здоров'я на кафедрі фізіології людини і тварин факультету біології та лісового господарства Волинського національного університету імені Лесі Українки на 60 жінках віком 17-21 років. На першому етапі дослідження були виміряні абсолютні антропометричні показники, такі як зріст, маса, окружність грудної клітки. На другому етапі, жінки проходили анкетування за тестом Фагерстрема. За його результатами досліджуваних поділено на 3 групи: I група - жінки, які мають стаж паління понад 3 роки, за добу випалюють понад 10 сигарет і мають високий рівень залежності, II група - жінки, які мають стаж паління 1-3 роки, за добу випалюють до 10 сигарет і мають низький та середній рівень залежності, III група - (контрольна) жінки, які не палять. Наступний етап дослідження передбачав проведення функціональної діагностики системи зовнішнього дихання в жінок у спокої та через 15 хв. після випалювання сигарети з використанням функціонального методу пневмотахографії (ПТГ). Реєстрацію та аналіз відповідних показників здійснювали за допомогою діагностичного атоматизованого комплексу "Кардіо+". Статистична обробка даних проводилася з використанням загальноприйнятих параметричних методів варіаційної статистики (оскільки розподіл отриманих результатів був нормальним) за допомогою програмного забезпечення MS Excel 2007. У даній статті представлене дослідження стану показників зовнішнього дихання в стані спокою та через 15 хв після випалювання чергової сигарети, яке дало змогу виявити негативний вплив тютюнопаління на дихальну систему організму жінок, які палять. Проведене дослідження дало змогу зробити детальний аналіз показників функції зовнішнього дихання, в жінок, віком 17-21 років, що палять та порівняти їх з не курцями. На основі одержаних результатів було встановлено, що у жінок-курців (I та II груп) відбувається достовірне зниження об'ємних (ФЖЄЛ, ЖЄЛ, ОФВ1) показників зовнішнього дихання, а також проби Тіфно при $p<0,05$, порівняно з групою жінок контрольної групи як у стані спокою, так і через 15 хв. після випалювання чергової сигарети. Аналіз швидкісних (МОШ на рівні видиху 25 %, 50 %, 75 %, ПОШ) показників потоку повітря по бронхах до легень вказує на поступове їх зниження з МОШ 25 % до МОШ 75 % у жінок дослідних груп, але достовірне зниження спостерігається лише на рівні видику 75 % через 15 хв. після випалювання чергової сигарети між I і III групами (при $p<0,05$). Досліджено статистично значиму різницю між значеннями розрахункового показника індексу Тіфно, що характеризує наявність обструктивної дихальної недостатності, в жінок II і III груп як у стані спокою, так і через 15 хв після випалювання чергової сигарети. Таким чином, зниження даних показників свідчить про наявність бронхіальної обструкції середніх і дрібних бронхів, а також про порушення сили дихальних м'язів та бронхіальної прохідності. Також доведено, що реактивність (зниження) об'ємних і швидкісних показників зовнішнього дихання на випалювання сигарети була вищою у групи жінок, котрі не палять (контрольна).

Ключові слова: *тютюнопаління, жінки-курці, зовнішнє дихання, сигарети, реактивність.*

DOI: 10.31393/morphology-journal-2022-28(3)-05 Reports of Morphology, Vol. 28, №3, Pages 32-37

ISSN 1818-1295 eISSN 2616-6194

REPORTS OF MORPHOLOGY

Official Journal of the Scientific Society of Anatomists, Histologists, Embryologists and Topographic Anatomists of Ukraine

journal homepage: https://morphology-journal.com

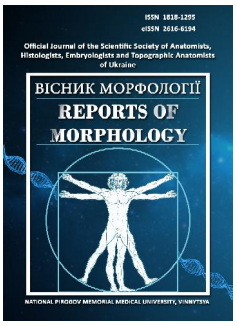

Determination of cephalometric parameters according to the COGS method, which characterize the position of individual teeth relative to cranial structures depending on the types of faces in Ukrainian young men and young women with an orthognathic bite

Nesterenko Ye. A., Shinkaruk-Dykovytska M. M., Chugu T. V., Dudik O. P., Gunas V. I.
National Pirogov Memorial Medical University, Vinnytsya, Ukraine

ARTICLE INFO
Received: 26 May 2022
Accepted: 30 June 2022

UDC: 616.714.1-071.3(477)

CORRESPONDING AUTHOR
e-mail: tikhonova_123@ukr.net
Nesterenko Ye. A.

CONFLICT OF INTEREST
The authors have no conflicts of interest to declare.

FUNDING
Not applicable.

An aesthetically pleasing face is one of the main goals of orthodontic treatment. However, in the case of severe pathology, in order to achieve the harmony of the complex of soft and hard tissues of the face, it is necessary to carry out not only orthodontic but also surgical intervention, i.e. orthognathic surgery. A cephalometric analysis for orthognathic surgery (COGS) is an effective element necessary for planning such treatment. The purpose of the study is to establish the peculiarities of cephalometric parameters that characterize the position of individual teeth relative to cranial structures according to the COGS method in Ukrainian young men and young women with an orthognathic bite, depending on the type of face. 46 young men (aged 17 to 21) and 72 young women (aged 16 to 20) who belonged in three generations to residents of Ukraine of the Caucasian race and had an orthognathic bite, underwent cephalometry according to the COGS method. OnyxCeph^{3}™ software, version 3DPro, Image Instruments GmbH, Germany, was used for cephalometric analysis of indicators characterizing the position of individual teeth relative to cranial structures. According to the value of Garson's morphological index, the type of face was determined. Statistical processing of the obtained results was carried out in the license package "Statistica 6.0" using non-parametric estimation methods. Between young women with different types of face, the following reliable or trends of differences in linear and angular indicators, which characterize the position of individual teeth relative to cranial structures according to the COGS method, were established: in young women with a very wide face type, smaller values of the distances 1u-NF, 1l-MP, 6u-NF and the OP-HP angle (compared to medium and narrow face types), as well as the 6l-MP distance (compared only to the medium face type); young women with an average face type have larger values of the 6l-MP distance (compared to narrow face types), as well as the OP-HP angle (compared to wide and narrow face types). Between young men with different types of faces, there are practically no reliable or trends of differences in linear and angular indicators that characterize the position of individual teeth relative to cranial structures according to the COGS method. Manifestations of sexual dimorphism of linear and angular indicators, which characterize the position of individual teeth relative to cranial structures according to the COGS method, have been established: in young men, the values of most linear dimensions are higher in representatives with very wide, wide and narrow face types; young women with different types of faces have larger values of the OP-HP angle. The obtained results will allow dentists to provide the necessary assistance to the patient at a modern level, taking into account not only the age, sex and ethnic characteristics of a person, but also the type of his face.

Keywords: *cone-beam computed tomography, teleradiography, COGS cephalometry, cephalometry, teeth, young men, young women, orthognathic occlusion, facial types, sex differences.*

Introduction

When it comes to maxillofacial pathology, which disrupts the functioning of not only the speech and chewing apparatus, but also the aesthetic appearance of the face, it is important to carry out correct and consistent treatment.

First of all, in this case, an adequate solution is the use of all possible modern and proven means that can eliminate this pathology.

One of the topical issues that scientists are currently discussing in various publications is the grounds for using orthodontic treatment and orthognathic surgery - which of these methods should be used in which situations? Is it necessary to combine them? Should orthodontic treatment precede orthognathic surgery?

S. Eslami and others [8] tried to identify the most sensitive parameters that can be used as a criterion for choosing which method to use in class III bite pathology - orthognathic surgery or orthodontic treatment. The Holdaway H angle and the assessment of jaw disharmony according to Wits, as it turned out, are critical diagnostic parameters for determining the treatment method for this pathology.

In general, the most generalized assessment of the researchers at the moment allows us to identify both of these methods as powerful tools that strengthen each other when they are combined, especially considering the development of modern digital radiological research methods, which allow to increase the accuracy of treatment prediction and reduce the risk of complications [6, 16]. Performing orthognathic intervention before orthodontic treatment is one of the most modern views on the concept of treatment of dental and jaw pathologies [15].

If we take into account the economic efficiency of orthognathic surgery and orthodontic treatment, no significant difference was found between them (p=0.979) in terms of the time spent on treatment (p=0.003), the duration of the doctor's work (p=0.015), the cost (p=0.924) or quality of life index (p=0.41) [10].

Inadequate and inappropriate planning of orthodontic intervention, in turn, leads to adverse consequences, in particular, discrepancies in expectations and actual results of the treatment [14]. Errors of this kind are divided into 4 categories: complications associated with inadequate decompensation of teeth, complications associated with treatment planning, complications of postoperative orthodontic care, and complications associated with appliances [12]. Some conditions, such as temporomandibular joint pathology, are more common complications than others [25].

Significant improvements in the patient's quality of life and psycho-emotional state can be achieved in the shortest possible time after a successful orthognathic intervention. The data of Emadian Razvadi E. S. with co-authors [7] indicate that the quality of life of patients significantly increased in the period before the start of treatment and 4 months after its start (p<0.013).

However, it should not be forgotten that not all psychological aspects of life can be improved only through orthognathic treatment. Operative intervention first of all eliminates the disturbance of social activity, which was disturbed due to dental and jaw pathology [20].

Thus, the orthognathic method of treatment of maxillofacial pathology occupies a key place in the treatment process of the patient, and affects a number of aspects of his life. One of the elements of this method that requires attention from scientists is the study of cephalometry for orthognathic surgery (COGS). This powerful anthropometric mechanism, created to increase the effectiveness of treatment planning, is quite sensitive to such variables as sex, age, nationality, face type, etc. In turn, this requires conducting clinical studies on the local population, taking into account as many of these variables as possible.

The purpose of the study is to establish the peculiarities of cephalometric parameters that characterize the position of individual teeth relative to cranial structures according to the COGS method in Ukrainian young men and young women with an orthognathic bite, depending on the type of face.

Materials and methods

A cephalometric study of lateral teleroentgenograms obtained with the dental cone-beam tomograph Veraviewepocs 3D Morita was carried out in 46 young men (YM) (aged 17 to 21 years) and 72 young women (YW) (aged 16 to 20 years) taken from the database of the research center and Department of Pediatric Dentistry, National Pirogov Memorial Medical University, Vinnytsya. All young men and young women applied to the private dental clinic "Vinintermed" for a diagnostic examination, belonged in three generations to residents of Ukraine of the Caucasian race and had a physiological bite that was as close as possible to an orthognathic bite (hereinafter referred to as an orthognathic bite). Committee on Bioethics of National Pirogov Memorial Medical University, Vinnytsya (protocol № 8 From 30.09.2021) found that the studies do not contradict the basic bioethical standards of the Declaration of Helsinki, the Council of Europe Convention on Human Rights and Biomedicine (1977), the relevant WHO regulations and laws of Ukraine.

According to the COGS method [1], the OnyxCeph^{3}™ software, version 3DPro, of Image Instruments GmbH, Germany, was used for cephalometric analysis (software license №URSQ-1799 registered to Dmitriev M. O.).

According to the value of Garson's morphological index [19], the face type of YM and YW with an orthognathic bite was determined.

For the convenience of clinical use of a large array of metric characteristics used in the COGS method, we used the distribution of teleradiographic indicators proposed by Dmitriev M. O. [3, 4, 5], according to which the third group includes indicators that actually characterize the position of individual teeth relative to each other and cranial structures. It is this group of indicators that is most often corrected in the process of orthodontic treatment of dento-jaw anomalies.

The main cephalometric points and measurements

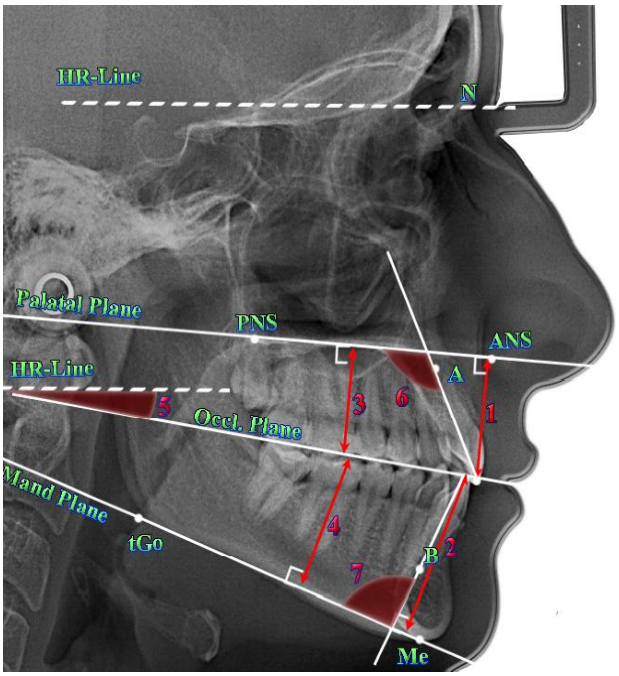

Fig. 1. The main cephalometric points and COGS measurements included in the third group of indicators: 1 - distance **1u-NF**; 2 - distance **1l-MP**; 3 - distance **6u-NF**; 4 - distance **6l-MP**; 5 - angle **OP-HP**; 6 - angle **Max1-NF**; 7 - angle **Mand1-MP**.

characterizing the position of individual teeth relative to cranial structures (included in the third group of indicators) are presented in Figure 1:

distance **1u-NF** (distance of incisal edge of 1u to palatal plane) - characterizes the position of the upper middle incisor relative to the palatal plane; determined by the length of the perpendicular to the line **ANS-PNS**, drawn from the point **Is1u** (mm);

distance **1l-MP** (distance of incisal edge of 1l to mand. plane) - characterizes the position of the lower middle incisor relative to the mandibular plane; determined by the length of the perpendicular to the line **tGo-Me**, omitted from the point **Is1L** (mm);

distance **6u-NF** (distance of mesial cusp of 6u to palatal plane) - characterizes the position of the first molar relative to the palatal plane; determined by the length of the perpendicular to the line **ANS-PNS**, drawn from the point **6u** (mm);

distance **6l-MP** (distance of mesial cusp of 6l to mand. plane) - characterizes the position of the lower first molar relative to the mandibular plane; determined by the length of the perpendicular to the line ***tGo-Me***, omitted from the point **6L** (mm);

angle **OP-HP** (angle of occl. to horizontal plane) - the angle formed by the lines ***apOcP-ppOcP*** та ***HR-Line*** (°);

angle **Max1-NF** (angle of axis of 1u to palatal plane) - the angle formed by the lines **Ap1u-Is1u** та **ANS-PNS** (°);

angle **Mand1-MP** (angle of axis of 1l to mand. plane) - the angle formed by the lines **Is1L-Ap1L** та **tGo-Gn** (°).

The obtained results were statistically processed in the license package "Statistica 6.0" using non-parametric estimation methods. Mean values and standard deviation were determined for each characteristic. The significance of the difference in values between independent quantitative values was determined using the Mann-Whitney U-test.

Results

Tables 1 and 2 present the results of the value of linear and angular indicators, which characterize the position of individual teeth relative to cranial structures according to the COGS method in YM or YW with an orthognathic bite, depending on the type of face.

We have established significantly greater or trends to greater values of the following indicators in YM or YW:

in YM - distance values of 1l-MP (with a very wide, $p<0.05$, wide $p<0.01$ and narrow face, $p=0.064$), 6u-NF (with a wide face, $p<0.01$), 6l-MP (with a very wide, $p<0.01$, wide $p<0.05$ and narrow face, $p<0.05$), as well as the angle Mand1-MP (with a very wide face, $p=0.071$);

in YW - the value of the angle OP-HP (with a very wide, $p=0.075$, wide $p=0.059$, medium, $p<0.05$ and narrow face, $p=0.064$).

Table 1. The value of linear and angular indicators that characterize the position of individual teeth relative to cranial structures according to the COGS method in YM with different types of faces (M±σ).

Indicator	Face type				p_{1-2}	p_{1-2}	p_{1-4}	p_{2-3}	p_{2-4}	p_{3-4}
	Very wide (1)	Wide (2)	Average (3)	Narrow (4)						
Distance 1u-NF	25.24±3.54	27.09±2.63	26.90±2.46	26.50±2.63	>0.05	>0.05	>0.05	>0.05	>0.05	>0.05
Distance 1l-MP	38.52±2.64	39.73±2.17	40.33±3.19	40.09±2.42	>0.05	>0.05	>0.05	>0.05	>0.05	>0.05
Distance 6u-NF	22.54±3.22	23.03±1.87	22.66±1.66	22.10±2.48	>0.05	>0.05	>0.05	>0.05	>0.05	>0.05
Distance 6l-MP	32.54±1.67	32.20±2.19	32.90±3.22	33.44±2.39	>0.05	>0.05	>0.05	>0.05	>0.05	>0.05
Angle OP-HP	0.760±5.819	5.259±5.445	7.409±3.856	4.825±4.720	>0.05	**=0.062**	>0.05	>0.05	>0.05	>0.05
Angle Max1-NF	113.4±8.0	112.2±6.3	109.3±5.0	109.1±2.6	>0.05	>0.05	>0.05	>0.05	>0.05	>0.05
Angle Mand1-MP	103.0±8.0	97.65±7.52	94.68±7.52	95.96±4.84	>0.05	**=0.079**	>0.05	>0.05	>0.05	>0.05

Notes: here and in the following table, M±σ - average sample ± standard deviation; $p_{(1\text{-}2,\ 1\text{-}3,\ 1\text{-}4,\ 2\text{-}3,\ 2\text{-}4,\ 3\text{-}4)}$ - validity of differences in linear or angular scores between YM or between YW with corresponding face types.

Table 2. The value of linear and angular indicators that characterize the position of individual teeth relative to cranial structures according to the COGS method in YW with different types of faces (M±σ).

Indicator	Face type				p_{1-2}	p_{1-2}	p_{1-4}	p_{2-3}	p_{2-4}	p_{3-4}
	Very wide (1)	Wide (2)	Average (3)	Narrow (4)						
Distance 1u-NF	24.62±2.21	26.48±2.16	27.63±2.56	25.99±1.76	>0.05	**<0.05**	**=0.054**	>0.05	>0.05	>0.05
Distance 1l-MP	35.65±1.75	37.60±2.37	38.86±3.20	37.98±1.78	>0.05	**<0.01**	**<0.01**	>0.05	>0.05	>0.05
Distance 6u-NF	20.25±1.44	21.48±1.78	21.89±1.84	21.48±1.36	>0.05	**<0.05**	**<0.05**	>0.05	>0.05	>0.05
Distance 6l-MP	28.94±1.96	30.49±2.24	31.67±2.39	30.15±1.98	>0.05	**<0.01**	>0.05	>0.05	>0.05	**=0.070**
Angle OP-HP	5.856±4.133	7.976±3.976	11.64±3.37	9.017±2.728	>0.05	**<0.001**	**<0.05**	**<0.05**	>0.05	**=0.070**
Angle Max1-NF	112.9±5.9	110.2±5.5	109.6±4.8	110.9±7.3	>0.05	>0.05	>0.05	>0.05	>0.05	>0.05
Angle Mand1-MP	95.60±8.51	96.77±5.38	93.67±5.70	93.46±6.04	>0.05	>0.05	>0.05	>0.05	>0.05	>0.05

Discussion

COGS analysis in a complex application with three-dimensional computer modeling is the most optimal way to obtain satisfactory functional and aesthetic results for both the doctor and the patient in the most complex types of bite pathology [2].

Comparison of cephalometric parameters according to COGS before and after anterior segmental osteotomy using statistical analysis revealed changes in the parameters of both soft and hard tissues in patients. The biggest changes were found in the protrusion of the upper lip and upper incisor [9].

Evaluation of changes in COGS indicators in soft tissues after single-jaw and double-jaw surgery in patients with Class III skeletal pathology found more significant changes in the upper lip in double-jaw surgery. At the same time, during interventions on one jaw, there is a positive correlation between hard and soft tissues of the lower jaw [17].

COGS analysis was used to analyze the effect of chin protrusion on normal facial profile. For this study, 60 people without previous orthodontic treatment were selected. Men and women with class II and class III facial profiles had statistically significant differences in B-Pg values [21].

According to the COGS analysis, cases with cleft palate and cleft lip are at high risk of Le Fort 1 fracture recurrence. Patient follow-up revealed mean linear horizontal advancement achieved along the nose (N) to the anterior nasal spine (ANS) relative to the true vertical plane at 15 months at the level of 5.17 mm, and at 12 months 3.91 mm [13].

As for the ethnic differences in the COGS analysis, the best example to show the diversity of results within even one country is India. Joshi S. with co-authors [11] studied the cephalograms of 100 people, ethnic residents of the state of Maharashtra. Compared to Caucasians norms, men from this state have a straighter profile, less vertical height and less mandibular divergence. At the same time, women have a convex profile, reduced vertical height and less divergence of the lower jaw.

At the same time, the population living in the more southern state of India, Kerala, according to the data analysis of the obtained indicators, compared to Caucasians, have a longer length of the front and back of the skull base, protrusion of the lower jaw, lower front face height, front and back height teeth, inclined upper and lower incisors and a less noticeable chin [18].

The state of Karnataka is located in the middle between the states described in the studies above. G. M. Shashikumar and others [22], after examining the cephalograms of 100 ethnic residents of this state, found that compared to Caucasians, they have larger bulges (men), larger values of the throat angle, lower lip protrusion, and mentolabial furrow; at the same time, smaller values of the nasolabial angle were found.

The population of Northern India (all the previous states were southwestern) has significantly lower values of the proclination of the teeth of the upper and lower jaws, the angle of the occlusal plane, and higher values of the chin protrusion compared to Caucasians. In addition, the authors found pronounced manifestations of sexual dimorphism of most indicators [23, 24].

Between Ukrainian YM or YW with an orthognathic bite with different facial types, when comparing the linear and angular indicators that characterize the position of individual teeth relative to the cranial structures by the COGS method, almost all reliable or trends of discrepancies are established between the YW, namely:

YW with very wide face type have significantly smaller, or trends toward smaller values of 1u-NF, 1l-MP, 6u-NF distances and OP-HP angle (compared to medium and narrow face types), as well as 6l-MP distances (compared to only the average face type);

YW with a medium face type, significantly higher or trends towards greater values of the 6l-MP distance (compared to the narrow face type) and the OP-HP angle (compared to the wide and narrow face types).

Among YM with different face types, only the trends of differences in angle indicators between representatives with very wide and medium face types were established, namely: in young men with a medium face type, larger values of the OP-HP angle and smaller values of the Mand1-MP angle were established.

We also established the manifestations of sexual

dimorphism of linear and angular indicators that characterize the position of individual teeth relative to cranial structures according to the COGS method, namely, reliably greater or trends to greater values:

in YM with very wide, wide and narrow face types - distance values of 1l-MP and 6l-MP; in young men with a wide face type - 6u-NF distance values and in young men with a very wide face type - Mand1-MP angle values;

in YW with very wide, wide, medium and narrow types of face - the magnitude of the angle OP-HP.

The results obtained by us in Ukrainian YM and YW with an orthognathic bite on the characteristics of the magnitude of linear and angular indicators, which characterize the position of individual teeth relative to cranial structures according to the COGS method, will allow dentists to provide the necessary assistance to the patient at a modern level, taking into account the age, sex, ethnic characteristics of the person and the type of her face.

Conclusion

1. Virtually all reliable or trends in the discrepancies of linear and angular indicators that characterize the position of individual teeth relative to cranial structures by the COGS method are established only between YW with orthognathic occlusion (between YW with very wide face type and medium and narrow face types, as well as between YW with medium face type and with wide and narrow face types).

2. Between YM and YW with an orthognathic bite and the corresponding facial types, manifestations of sexual dimorphism of indicators characterizing the position of individual teeth relative to cranial structures according to the COGS method were established: in YM, in most cases, larger values of linear dimensions were found in representatives with very wide, wide and narrow face types; in YW with different types of face - larger values of the angle OP-HP.

References

[1] Burstone, C. J., James, R. B., Legan, H., Murphy, G. A., & Norton, L. A. (1979). Cephalometrics for orthognathic surgery. *J. Oral. Surg,* 36, 269-277. PMID: 273073

[2] Conley, R. S., & Edwards, S. P. (2019). Three-dimensional treatment planning for maxillary and mandibular segmental surgery for an adult Class III: Where old meets new. *The Angle Orthodontist,* 89(1), 138-148. doi: 10.2319/120117-823.1

[3] Dmitriev, M. O. (2016). Кореляції основних краніальних показників з характеристиками верхньої та нижньої щелеп у мешканців України юнацького віку [Correlations of main cranial index with characteristics of upper and lower jaws among residents in Ukraine of adolescent age]. *Світ медицини та біології - World of Medicine and Biology*, 4(58), 24-29.

[4] Dmitriev, M. O. (2017). Зв'язки кутових міжщелепних показників з характеристиками положення зубів та профілем м'яких тканин лиця у мешканців України юнацького віку [Links of angular inter-jaws indices with the characteristics of the closure plane, the position of the teeth and the soft-tissue profile of the face in the youth of Ukraine]. *Світ медицини та біології - World of Medicine and Biology,* 2(60), 51-59.

[5] Dmitriev, M. O. (2017). Зв'язки основних краніальних показників з характеристиками положення зубів верхньої і нижньої щелеп та профілем м'яких тканин лиця у юнаків і дівчат [Relations of key cranial indicators with the characteristics of the teeth of the upper and lower jaws and profile face soft tissue in boys and girls]. *Вісник морфології - Reports of Morphology,* 23(1), 125-131.

[6] Elnagar, M. H., Aronovich, S., & Kusnoto, B. (2020). Digital workflow for combined orthodontics and orthognathic surgery. *Oral and Maxillofacial Surgery Clinics,* 32(1), 1-14. doi: 10.1016/j.coms.2019.08.004

[7] Emadian Razvadi, E. S., Soheilifar, S., Esmaeelinejad, M., & Naghdi, N. (2017). Evaluation of the changes in the quality of life in patients undergoing orthognathic surgery: a multicenter study. *Journal of Craniofacial Surgery, 2*8(8), e739-e743. doi:10.1097/SCS.0000000000003887

[8] Eslami, S., Faber, J., Fateh, A., Sheikholaemmeh, F., Grassia, V., & Jamilian, A. (2018). Treatment decision in adult patients with class III malocclusion: surgery versus orthodontics. Progress in orthodontics, 19(1), 1-6. doi: 10.1186/s40510-018-0218-0

[9] Harshitha, K. R., Srinath, N., Christopher, S., & Kumar, H. N. (2014). Evaluation of soft and hard tissue changes after anterior segmental osteotomy. *Journal of clinical and diagnostic research: JCDR*, 8(9), ZC07-ZC10. doi: 10.7860/JCDR/2014/9409.4791

[10] Hu, J., Jiang, Y., Wang, D., Guo, S., Li, S., Jiang, H., & Cheng, J. (2021). Comparison of cost-effectiveness and benefits of surgery-first versus orthodontics-first orthognathic correction of skeletal class III malocclusion. *International Journal of Oral and Maxillofacial Surgery*, 50(3), 367-372. doi: 10.1016/j.ijom.2020.06.007

[11] Joshi, S., Punamiya, S., Naik, C., Mhatre, B., Garad, A., & Chabalani, D. (2022). A study to evaluate cephalometric hard tissue profile of maharashtrian population for orthognathic surgery. *Indian Journal of Dental Sciences*, 14(2), 68-73. doi: 10.4103/IJDS.IJDS_60_21

[12] Klein, K. P., Kaban, L. B., & Masoud, M. I. (2020). Orthognathic surgery and orthodontics: inadequate planning leading to complications or unfavorable results. *Oral and Maxillofacial Surgery Clinics*, 32(1), 71-82. doi: 10.1016/j.coms.2019.08.008

[13] Kumari, P., Roy, S. K., Roy, I. D., Kumar, P., Datana, S., & Rahman, S. (2013). Stability of cleft maxilla in Le Fort I maxillary advancement. *Annals of Maxillofacial Surgery,* 3(2), 139-143. doi: 10.4103/2231-0746.119223

[14] Moon, W., & Kim, J. (2016, March). Psychological considerations in orthognathic surgery and orthodontics. In Seminars in *Orthodontics* (Vol. 22, No. 1, pp. 12-17). WB Saunders. doi: 10.1053/j.sodo.2015.10.003

[15] Naran, S., Steinbacher, D. M., & Taylor, J. A. (2018). Current concepts in orthognathic surgery. *Plastic and Reconstructive Surgery,* 141(6), 925e-936e. doi: 10.1097/PRS.0000000000004438

[16] Ngan, P., & Moon, W. (2015). Evolution of Class III treatment in orthodontics. *American Journal of Orthodontics and Dentofacial Orthopedics,* 148(1), 22-36. doi: 10.1016/j.ajodo.2015.04.012

[17] Parappallil, C. J., Parameswaran, R., Vijayalakshmi, D., & Mavelil, B. G. T. (2018). A comparative evaluation of changes in soft

tissues after single-jaw surgery and bimaxillary surgery in skeletal class III Patients. *Journal of Maxillofacial and Oral Surgery,* 17(4), 538-546. doi: 10.1007/s12663-017-1079-7

[18] Patla, M., Achalli, S., Saidath, K., Soans, C. R., & Nayak, U. K. (2017). Cephalometric Norms for Orthognathic Surgery in Kerala Population. *Journal of Health and Allied Sciences NU,* 7(1), 45-51. doi: 10.1055/s-0040-1708695

[19] Proffit, U. R., Fildz, G. U., & Saver, D. M. (2006). *Современная ортодонтия (перевод с английского Д. С. Персина) [Modern orthodontics (translation from English by D. S. Persina)]*. М.: МЕДпресс-информ - M.: MEDpress-inform.

[20] Saghafi, H., Benington, P., & Ayoub, A. (2020). Impact of orthognathic surgery on quality of life: a comparison between orthodontics-first and surgery-first approaches. *British Journal of Oral and Maxillofacial Surgery,* 58(3), 341-347. doi: 10.1016/j.bjoms.2020.01.005

[21] Sainath, M. C., & Preeti, R. (2019). Quantitative Eevaluation of Influence of Hard Tissue Chin Prominence on Perceived Normal Soft Tissue Facial Profile. *University Journal of Surgery and Surgical Specialities,* 5(9), 7-9.

[22] Shashikumar, G. M., Naik, D. P., Savakkanavar, M. B., Sreedhara, S., & Reddy, S. R. K. (2015). Hard tissue cephalometric norms for orthognathic surgery in Karnataka population. *Journal of International Oral Health,* 7(11), 28-32.

[23] Singh, G., Agrawal, A., Chaturvedi, T. P., & Naveen, K. P. (2019). A Computer Assisted Comparison of Cephalometric Norms between Caucasians and North Indian Population: An Analytical Study. *Sch Bull,* 5(4), 138-147. doi: 10.21276/sb.2019.5.4.2

[24] Singh, S. P., Utreja, A. K., & Jena, A. K. (2013). Cephalometric norms for orthognathic surgery for North Indian population. *Contemporary clinical dentistry,* 4(4), 460-466. doi: 10.4103/0976-237X.123041

[25] Wolford, L. M. (2020). Comprehensive post orthognathic surgery orthodontics: complications, misconceptions, and management. *Oral and Maxillofacial Surgery Clinics,* 32(1), 135-151. doi: 10.1016/j.coms.2019.09.003

ВИЗНАЧЕННЯ ЦЕФАЛОМЕТРИЧНИХ ПАРАМЕТРІВ ЗА МЕТОДОМ COGS, ЯКІ ХАРАКТЕРИЗУЮТЬ ПОЛОЖЕННЯ ОКРЕМИХ ЗУБІВ ВІДНОСНО ЧЕРЕПНИХ СТРУКТУР У ЗАЛЕЖНОСТІ ВІД ТИПІВ ОБЛИЧЧЯ В УКРАЇНСЬКИХ ЮНАКІВ І ДІВЧАТ ІЗ ОРТОГНАТИЧНИМ ПРИКУСОМ

Нестеренко Є. А., Шінкарук-Диковицька М. М., Чугу Т. В., Дудік О. П., Гунас В. І.

Естетично приємний вигляд обличчя є однією з головних цілей ортодонтичного лікування. Проте, у випадку тяжкої патології, для досягнення гармонійності комплексу м'яких та твердих тканин обличчя необхідно провадити не тільки ортодонтичне але і хірургічне втручання, тобто ортогнатичну хірургію. Ефективним елементом, необхідним для планування такого лікування є цефалометричний аналіз для ортогнатичної хірургії (COGS). Мета дослідження - встановити особливості цефалометричних параметрів, які характеризують положення окремих зубів відносно черепних структур за методом COGS, в українських юнаків і дівчат із ортогнатичним прикусом у залежності від типу обличчя. 46 юнакам (віком від 17 до 21 років) і 72 дівчатам (віком від 16 до 20 років), які належали у трьох колінах до мешканців України європеоїдної раси та мали ортогнатичний прикус, проведено цефалометрію згідно COGS-методу. Для проведення цефалометричного аналізу показників, які характеризують положення окремих зубів відносно черепних структур, використовувалось програмне забезпечення OnyxCeph³™, версії 3DPro, компанії Image Instruments GmbH, Німеччина. Відповідно значенням морфологічного індексу Гарсона проводилося визначення типу обличчя. Статистичну обробку отриманих результатів проводили в ліцензійному пакеті "Statistica 6.0" з використанням непараметричних методів оцінки. Між дівчатами з різними типами обличчя встановлені наступні достовірні або тенденції відмінностей лінійних і кутових показників, які характеризують положення окремих зубів відносно черепних структур за методом COGS: у представниць із дуже широким типом обличчя - менші значення величини відстаней 1u-NF, 1l-MP, 6u-NF і кута OP-HP (порівняно з середнім і вузьким типами обличчя), а також відстані 6l-MP (порівняно лише з середнім типом обличчя); у представниць із середнім типом обличчя - більші значення величини відстані 6l-MP (порівняно з вузьким типом обличчя), а також кута OP-HP (порівняно з широким і вузьким типами обличчя). Між юнаками з різними типами обличчя практично не встановлені достовірні або тенденції відмінностей лінійних і кутових показників, які характеризують положення окремих зубів відносно черепних структур за методом COGS. Встановлені прояви статевого диморфізму лінійних і кутових показників, які характеризують положення окремих зубів відносно черепних структур за методом COGS: в юнаків - більші значення більшості лінійних розмірів у представників із дуже широким, широким і вузьким типами обличчя; у дівчат із різними типами обличчя - більші значення величини кута OP-HP. Отримані результати дозволять лікарям-стоматологам надавати необхідну пацієнту допомогу на сучасному рівні з урахуванням не тільки вікових, статевих та етнічних особливостей людини, але й типу її обличчя.

Ключові слова: *конусно-променева комп'ютерна томографія, телерентенографія, цефалометрія за COGS-методом, кефалометрія, зуби, юнаки, дівчата, ортогнатичний прикус, типи обличчя, статеві розбіжності.*

DOI: 10.31393/morphology-journal-2022-28(3)-06 Reports of Morphology, Vol. 28, №3, Pages 38-44

ISSN 1818-1295 eISSN 2616-6194

REPORTS OF MORPHOLOGY

Official Journal of the Scientific Society of Anatomists, Histologists, Embryologists and Topographic Anatomists of Ukraine

journal homepage: https://morphology-journal.com

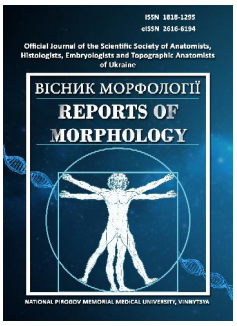

Structural organization of the carotid sinus under the influence of monosodium glutamate in the experiment: analysis of changes in dynamics

Sodomora O. O.
Danylo Halitskiy Lviv National Medical University, Lviv, Ukraine

ARTICLE INFO
Received: 31 May 2022
Accepted: 4 July 2022

UDC:
612.014.46:547.466.64:611.133]-08

CORRESPONDING AUTHOR
e-mail: tikhonova_123@ukr.net
Nesterenko Ye. A.

CONFLICT OF INTEREST
The authors have no conflicts of interest to declare.

FUNDING
Not applicable.

Carotid artery pathology is one of the leading causes of cerebral stroke. Among the pathogenetic factors in the development of carotid artery damage, disorders of lipid metabolism, atherosclerosis, and metabolic syndrome occupy a prominent place. The alimentary factor is extremely important in this context. Monosodium glutamate is one of the most common food additives, which is often used uncontrollably and can cause changes in the structure and functions of organs and tissues. The purpose of the study: to analyze the dynamics of morphological changes in the carotid sinus area under the influence of monosodium glutamate when administered orally in an experiment. The area of the carotid sinus of 20 male laboratory white rats that received sodium glutamate orally at a dose of 10 mg/kg/day for 8 weeks was studied by morphological methods at the macro- and microstructural levels after 6 and 8 weeks of the experiment. The obtained data are compared with the results of a morphological study of the same area in 20 animals of the control group. Statistical processing of animal weight was performed using MS Excel 2007 software. Mean ± standard deviation was determined. After 6 weeks of the experiment, when evaluating the histological structure of the wall of the internal carotid artery in the area located directly above the bifurcation, when compared with the control group, multiplication and folding of the intima were found in the experimental group, presumably associated with the proliferation of endothelial cells under the influence of sodium glutamate, detachment of the endothelium and lysis of individual endotheliocytes, as well as uneven thickening of elastic media fibers and disruption of their structure. Attention was drawn to the accumulation of white fat perivasally and in the zone of the carotid glomus, as well as the disorganization of nerves and the expansion of vessels of the microcirculatory channel. After 8 weeks of the experiment, the negative dynamics of structural changes were noticeable: signs of increased inflammatory infiltration, deformation of the vessels of the microcirculatory bed with thickening of their walls and narrowing of the lumen, stasis, noticeable degranulation of cells of type I carotid glomus cells, the appearance of single labrocytes (mast cells) in the infiltrate. The amount of adipose tissue (white fat) in the area of the carotid sinus and the perivasal bifurcation of the carotid arteries, as well as in the immediate vicinity of the carotid glomus, also increased markedly, and a tendency towards thickening of adipose tissue was noted. Thus, monosodium glutamate with systematic oral use can cause a violation of the structural organization of the carotid sinus, the wall of the carotid arteries and the carotid glomus, and the severity of changes in dynamics increases. Further research is needed to clarify the nature of the structural changes in the carotid sinus under the conditions of withdrawal of monosodium glutamate, as well as to find possible ways of correction.

Keywords: *monosodium glutamate, carotid sinus, carotid glomus, internal carotid artery, carotid bifurcation.*

Introduction

Cardiovascular diseases, in particular myocardial infarction and cerebral stroke, continue to hold the leadership in the structure of the causes of mortality in the whole world, and also occupy a prominent place in the statistics of

premature deaths (up to 70 years of age) according to the data of the World Health Organization [19]. One of the leading causes of cerebral blood circulation disorders, including cerebral strokes, is the pathology of the carotid arteries [5, 8]. An important role in its development is played not only by a family predisposition to dyslipidemia, but also completely controllable factors - a sedentary lifestyle, unhealthy diet, in particular, the consumption of high-calorie foods with a significant fat content, as well as the widespread use in the food industry of additives to improve the organoleptic properties of food [19]. The most common among them is monosodium glutamate, also known as additive E621 or monosodium salt of glutamic acid, which is considered relatively safe and is allowed for use in many countries of the world, in particular in Ukraine. Additive E621 is used to enhance the taste and improve the organoleptic properties of food, which are lost due to long-term storage [15].

Despite numerous studies reporting the harmful effects of monosodium glutamate on the living organism [1], its use continues to be widespread and sometimes uncontrolled due to the fact that the presence of the additive E621 is often not even recorded on food packaging. The monosodium salt of glutamic acid is also present in baby food products. Since it was reported about the effect of the E621 supplement on brain tissue [6], the human psyche [11], as well as the ability to cause changes in eating behavior, manifested in increased appetite and an increase in the amount of food consumed, with the subsequent development of excess body weight and obesity [2, 17], the long-term administration of monosodium glutamate is a cause for concern, given the potential adverse effects that can be expressed in pathological changes in the structure of organs and tissue and subsequently lead to a violation of their functions and the development of a number of pathological conditions.

Oxidative stress is considered one of the important pathogenetic aspects of sodium glutamate's influence on a living organism [6, 7]. An important role is also played by the development of inflammation and fibrosis [7], metabolic disorders [3, 18] and DNA damage - the so-called genotoxic effect [1, 10]. Numerous studies have reported adverse effects of monosodium glutamate on the heart [3] and vessels, including the aorta [3] and thoracic arteries [13], as well as other organs [4]. Given the important role of the morphology of the carotid arteries in the pathogenesis of brain perfusion disorders, the effect of the systematic use of monosodium glutamate on their structure has not been sufficiently studied. Of particular interest is the nature of morphological changes, their dynamics and the degree of irreversibility of possible damage, the reaction of tissues to the withdrawal of monosodium glutamate, as well as the possibility of correction [14].

The purpose of the study is to analyze the dynamics of morphological changes in the carotid sinus area under the influence of monosodium glutamate when administered orally in an experiment.

Materials and methods

40 male white laboratory rats were involved in the study, which were equally divided into experimental and control groups. The animals were kept in cages of 4 individuals each, in a well-ventilated room of the vivarium, and had unlimited access to food corresponding to the standard diet of the vivarium. Animals of the experimental group received 10 mg/kg/day of monosodium glutamate administered orally for 8 weeks, while animals of the control group did not receive food supplements. Throughout the experiment, the principles of the European Convention for the Protection of Vertebrate Animals Used for Experimental and Other Scientific Purposes (Strasbourg, 1986), the norms of Law of Ukraine № 3447-IV "On the Protection of Animals from Cruelty Treatment", general ethical principles of experiments on animals, adopted by the First National Congress of Ukraine on Bioethics (2001), which was confirmed by the Commission on the Ethics of Scientific Research, Experimental Developments and Scientific Works of Danylo Halytsky Lviv National Medical University (protocol № 3 dated 11.3.2022) were strictly observed.

After 6 weeks from the start of the study, half of the animals were removed from the experiment by overdose of ether anesthesia; the rest of the animals were removed from the experiment at the end of the 8th week. The research material is represented by histological preparations of the carotid sinus of white rats, made by making sections of the tissue of the bifurcation of the carotid arteries from previously prepared paraffin blocks. For histological examination, sections were stained with methylene blue. The preparations were studied and photographed at magnifications of the microscope: x200, x400, x1000. The "Aver Media" computer system was used to photograph micropreparations.

Statistical processing of animal weight was performed using MS Excel 2007 software (mean ± standard deviation was determined).

Results

The average weight of animals in the control group after 6 and 8 weeks of the experiment was 276.5±6.3 g and 283.5±5.6 g, in the experimental group this indicator was 337.4±4.3 g and 364.5±6.2 g, respectively.

During the morphological study of the studied area of the carotid sinus of a white rat, it was found that the internal and external carotid arteries originated from the common carotid artery. The bifurcation of the common carotid artery was typically located at the posterior angle (greater horn) of the hyoid bone, 2-4 mm below the latter in animals of both groups. The diameter of the internal carotid artery practically corresponded to that of the external carotid artery. The bifurcation of the carotid arteries in animals of both groups was located below the typical location in 17.5 % of cases (7/40 adult white rats). The location of nerves and sensory nerve endings in the carotid sinus and carotid glomus in rats of both groups was similar to that in humans.

The carotid glomus was located in the carotid sinus, closer to the internal carotid artery, and had a size of 0.6-0.7 mm by 0.5-0.4 mm, and was surrounded by connective tissue. Its vascularization occurred due to a small branch of the external carotid artery - the glomus artery, and venous outflow - into a small vein of the same name, which opened into the internal jugular vein. Sensory innervation was provided by branches of the glossopharyngeal and vagus nerves, autonomic innervation by fibers of parasympathetic nodes, in which the branches of the vagus nerve are interrupted, as well as by the sympathetic plexus, and the sympathetic trunk was located dorsal to the common carotid artery and the vagus nerve. Cervical nodes in this area were grouped into three pairs: upper, middle, and posterior. The upper cervical node lay at the level of the bifurcation of the common carotid artery in close proximity to the internal carotid artery, carotid sinus, and carotid glomus.

During histological examination (staining with methylene blue), the wall of both carotid arteries consisted of clearly defined three layers: inner - intima, middle - media, and outer - adventitia, in which small blood vessels, known as vasa vasorum, were visible.

After 6 weeks of the experiment, when evaluating the histological structure of the wall of the internal carotid artery in the area located directly above the bifurcation, when compared with the control group (Fig. 1), in the experimental group (Fig. 2), multiplication and folding of the intima, presumably associated with proliferation, were found of endothelial cells under the influence of monosodium glutamate, detachment of the endothelium and lysis of single endotheliocytes, as well as uneven thickening of the elastic fibers of the media and disruption of their structure, which causes changes in the intima-media ratio and may ultimately have a negative effect on the perfusion of brain tissues. Attention was drawn to the accumulation of white fat perivasally and in the zone of the carotid glomus, as well as the disorganization of nerves and the expansion of vessels of the microcirculatory channel.

After 8 weeks of the experiment, the histological

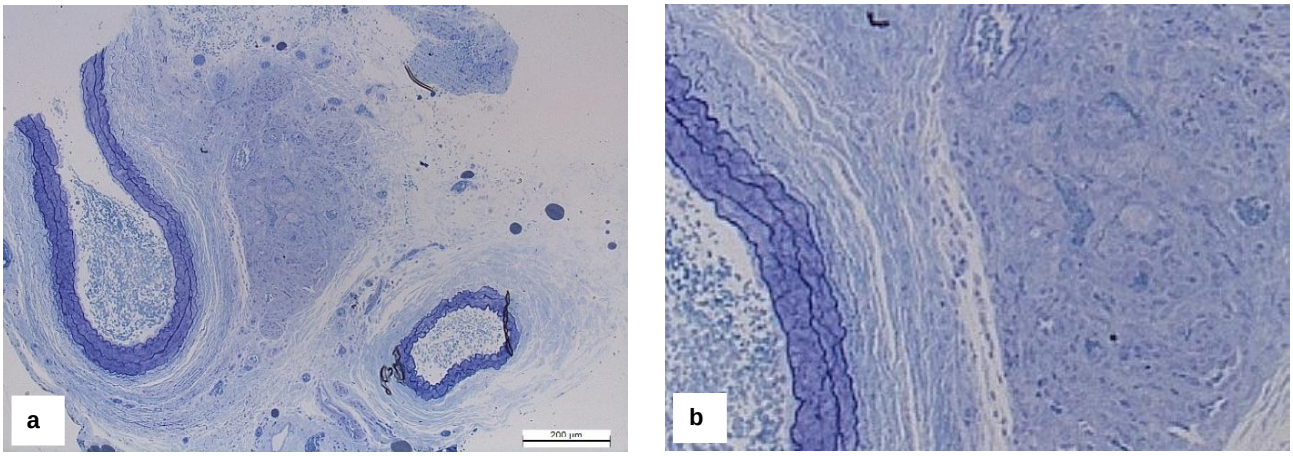

Fig. 1. Carotid artery bifurcation area (a) and a fragment of the internal carotid artery wall in the area immediately above the bifurcation of the common carotid artery of a white rat (b) of the control group. Staining with methylene blue. Photomicrograph. Magnification: x200 (a) and x400 (b).

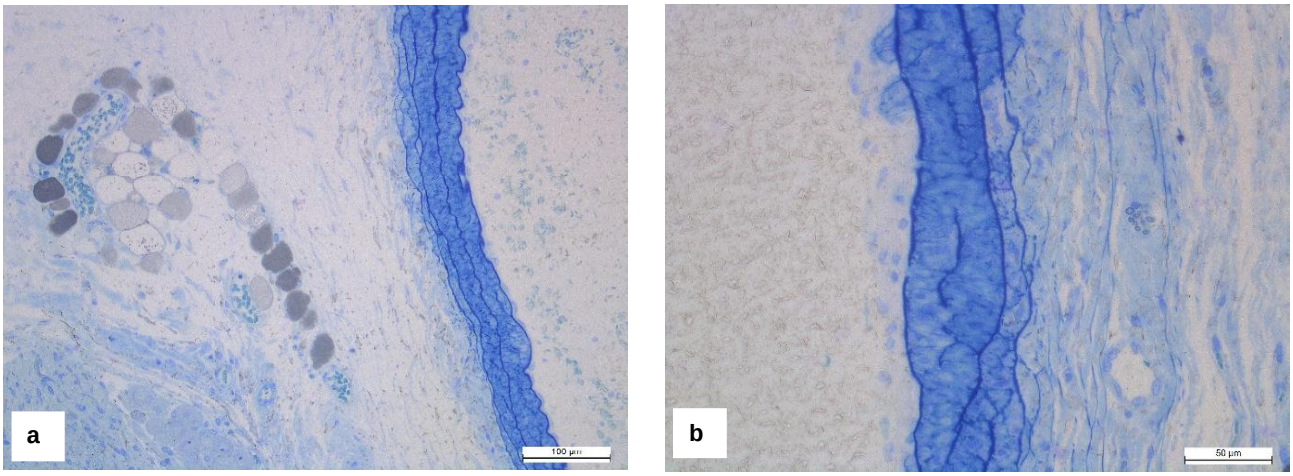

Fig. 2. Bifurcation area of carotid arteries with carotid glomus (a) and a fragment of the wall of the internal carotid artery in the area located directly above the bifurcation of the common carotid artery of a white rat (b) of the experimental group 6 weeks after the start of the experiment. Staining with methylene blue. Photomicrograph. Magnification: x200 (a) and x400 (b).

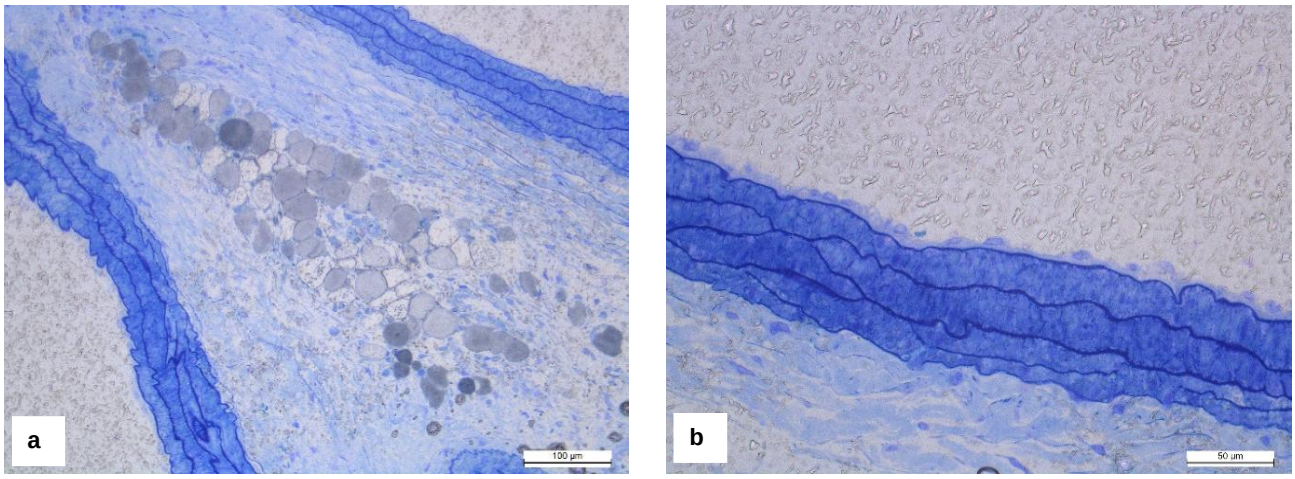

Fig. 3. Carotid artery bifurcation zone (a) and a fragment of the wall of the internal carotid artery in the area located directly above the bifurcation of the common carotid artery of a white rat (b) of the experimental group 8 weeks after the start of the experiment. Staining with methylene blue. Photomicrograph. Magnification: x200 (a) and x400 (b).

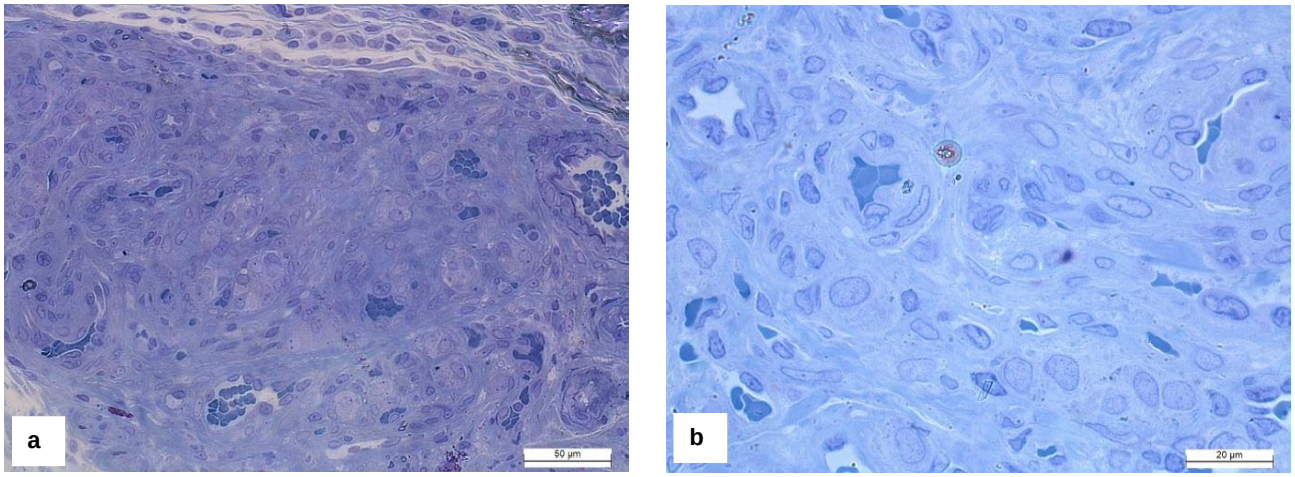

Fig. 4. Fragments of the glomus of a white rat of the control group. Staining with methylene blue. Photomicrograph. Magnification: x200 (a) and x400 (б).

structure of the wall of the carotid artery (Fig. 3) was characterized by an increase in the amount of adipose tissue perivasally and in the bifurcation zone of the carotid artery and the carotid glomus, the appearance of an inflammatory cell infiltrate, proliferation of arterioles, an increase in the irregularity of the vascular wall, especially expressed in the media zone, changes from the side of the connective tissue, in particular its swelling and unclear structure, hyperemia of the vessels of the microcirculatory channel.

Regarding the localization of the carotid glomus, it was located in the area of the internal carotid artery, directly above the bifurcation of the common carotid artery, 1-1.5 mm more cranially than the latter. The presence of the adventitian capillary plexus in the zone of the carotid glomus attracted attention. When staining with methylene blue, baroreceptors were detected in the form of rounded nerve endings. Four main components were identified in the carotid glomus: cells, nerve fibers, vessels and the main substance of connective tissue. A cluster of cells, also called glomeruli, is the main structural element of the carotid glomus and consisted of two types of cells in the white rat: cells of type I (glomus cells) - from 2 to 12 cells in each glomerulus, on average 4, surrounded by cells of type II (supporting) - 1-3 cells in a glomerulus. These two cell types can be clearly distinguished even by light microscopy (Fig. 4). Glomus cells were chemoreceptors and contained secretory granules, had a round or oval shape, and their size varied from 8 to 16 ?m. The nucleus of glomus cells is clearly delineated, oval in shape, the cytoplasm is granular. Type II cells, the number of which was 15-20 % of all glomus cells, were usually visible on the periphery of the clusters, resembled neuroglia cells in structure, had elongated hyperchromic nuclei, a thin cytoplasmic strip, and pronounced processes that surrounded the glomus cells. The carotid glomus also contained autonomous microganglionic cells located on the periphery of the glomus or directly in the latter. Clusters of cells are separated by layers of connective tissue, which, when connected, formed the capsule of the carotid glomus. The

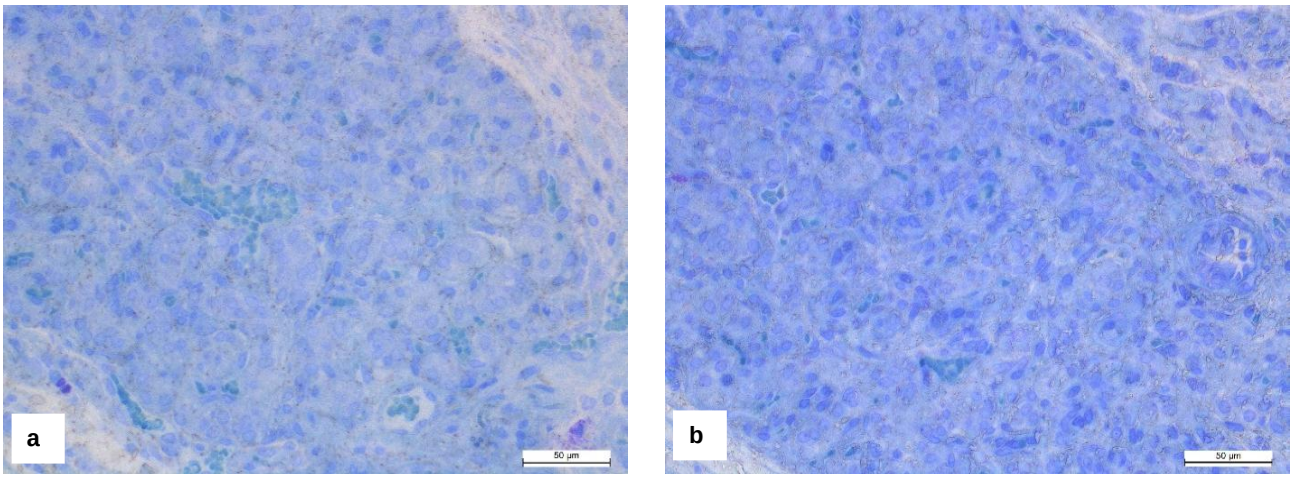

Fig. 5. Fragments of the glomus of a white rat of the experimental group after 6 weeks (a) and 8 weeks (b) of the experiment. Staining with methylene blue. Photomicrograph. Magnification: x400.

stroma around the lobes of the carotid glomus of white rats is rich in blood vessels and nerves.

As for the structural organization of the carotid glomus, after 6 weeks of the experiment, in the control group (see Fig. 4) its typical structure was observed: type I cells were located in the glomeruli and surrounded by type II cells, between the glomeruli there were visible layers of connective tissue, then as in the experimental group, after 6 weeks of the experiment (Fig. 5a), attention was drawn to a decrease in the number of type I cells in some clusters, as well as a pronounced thickening and swelling of the connective tissue layers between them, signs of inflammation, thrombus formation, and hyperemia of the microcirculatory vessels. After 8 weeks of the experiment (Fig. 5b), the negative dynamics of structural changes were noticeable: signs of increased inflammatory infiltration, deformation of vessels of the microcirculatory bed with thickening of their walls and narrowing of the lumen, stasis, noticeable degranulation of type I cells, appearance of single labrocytes (mast cells) in the infiltrate. The amount of adipose tissue (white fat) in the area of the carotid sinus and the perivasal bifurcation of the carotid arteries, as well as in the immediate vicinity of the carotid glomus, also increased markedly, and a tendency towards thickening of adipose tissue was noted.

Discussion

The pathology of the carotid arteries plays a leading role in the pathogenetic mechanisms of the development of cerebrovascular disorders, which lead not only to cerebral strokes, but also to cognitive changes [12]. The determination of risk factors that directly affect the morphology and, as a result, the function of the carotid arteries is of great clinical importance, since the modification of such factors allows to reduce the risks associated with morbidity, immediate and remote negative consequences for patients, loss of their working capacity, and a decrease in quality and a decrease in life expectancy. To study the influence of external factors on the structure and function of the carotid arteries, in particular the carotid sinus, the bifurcation zone and related structures, it is advisable to use experimental models that offer wide opportunities for analyzing processes and changes, as well as factors that can modify their course [10].

This study used a low dose of monosodium glutamate that was approved for use in food in most countries. The oral route of administration followed by free access to food was expedient in order to accurately model the route of entry of monosodium glutamate into the human body during life and consumption of usual food products. It is this fact that allows the extrapolation of the experimental study to the general human population, because parenteral or subcutaneous administration of monosodium glutamate does not occur under normal conditions. An important aspect was the assessment of the morphological changes of the studied area in dynamics, as this indirectly makes it possible to predict the speed and severity of pathological changes of the studied area with systematic consumption of monosodium glutamate.

Therefore, after 6 and 8 weeks of the experiment, histological examination revealed significant changes in the structure of the wall of the carotid arteries in the carotid sinus area at the microscopic level, as well as changes in the morphology of the carotid glomus in the animals of the experimental group, which could be directly caused by the oral administration of monosodium glutamate in comparison with a control group that did not receive a food supplement. The progressive accumulation of adipose tissue perivasally in the area of bifurcation of carotid arteries and carotid glomus attracted special attention. The growth of structural and inflammatory changes in dynamics seems to be important, which may indicate an increase in the toxic effects of monosodium glutamate over time with its systematic use with food [7]. The above-mentioned morphological manifestations could be not only a consequence of the direct toxic effect of monosodium

glutamate, but also the result of its indirect effect, namely the stimulation of the appetite of the animals of the experimental group, which led to an increased feeling of hunger, consumption of more food and, as a result, faster weight gain.

Given the key role of vascular pathology in the development of cerebral stroke, possible violations of the structural organization of blood vessels, in particular, carotid arteries, as well as areas of the carotid sinus should be taken into account in persons who systematically consume monosodium glutamate as a food additive for the possible timely prevention of unfavorable distant consequences for cerebral and systemic blood circulation by modifying risk factors and using appropriate preventive measures [16]. Preventing the development of structural changes in the carotid glomus is also of great practical importance, as a violation of the morphology will inevitably lead to a negative impact on its functions, which can potentially affect not only the quality of brain perfusion, but also the tone of blood vessels, blood pressure, and systemic blood circulation in general. The role of mast cells in conditions of structural disorders of the carotid sinus and carotid glomus requires additional research, since the available data on the influence of the content of their granules on the functions of the body are somewhat contradictory and require clarification. The problem of the dynamics of structural changes in the carotid sinus zone under the conditions of sodium glutamate withdrawal is also of great interest, since their reversible nature can have a beneficial effect on at least partial restoration of the functions of damaged structures.

Further research is needed to clarify the nature of the structural changes in the carotid sinus under the conditions of withdrawal of monosodium glutamate, as well as to find possible ways of correction.

Conclusion

Monosodium glutamate with systematic oral use can cause a violation of the structural organization of the carotid sinus, the wall of the carotid arteries and the carotid glomus, and the severity of the changes in dynamics increases.

References

[1] Abdou, H. M., Hassan, E. H., & Aly, R. G. (2020). Monosodium glutamate (MSG):promoter of neurotoxicity, testicular impairment, inflammation and apoptosis in male rats. *Swed J BioSci Res*, 1(2), 78-90. doi: 10.51136/sjbsr.2020.78.90

[2] Chen, W., Chen, Z., Xue, N., Zheng, Z., Li, S., & Wang, L. (2013). Effects of CB1 receptor blockade on monosodium glutamate induced hypometabolic and hypothalamic obesity in rats. *Naunyn-Schmiedeberg's Archives of Pharmacology,* 386(8), 721-732. doi: 10.1007/S00210-013-0875-Y

[3] El Malik, A., & Sabahelkhier, M. K. (2019). Changes in lipid profile and heart tissues of wistar rats induces by using monosodium glutamate as food additive. *International of Journal Biochemistry and Physiology,* 4(1), 141-147. doi: 10.23880/ijbp-16000147

[4] Hamad, S. R., & Hamad, H. R. (2020). Modulation of Monosodium Glutamate Induced Histological Injuries, Histomorphometrical Alterations and DNA Damage in the Mice Hepatic and Renal Tissues by Oral Administration Nano-Cerium Oxide and L-arginine and their Combination. *Egyptian Journal of Histology,* 43(4), 1034-1046. doi: 10.21608/EJH.2020.23155.1244

[5] Hammond-Haley, M., Hartley, A., Essa, M., DeLago, A. J., Marshall, D. C., Salciccioli, J. D., & Shalhoub, J. (2021). Trends in Ischemic Heart Disease and Cerebrovascular Disease Mortality in Europe: An Observational Study 1990-2017. *Journal of the American College of Cardiology,* 77(13), 1697-1698. doi: 10.1016/J.JACC.2021.02.013

[6] Hazzaa, S. M., Abdelaziz, S. A. M., Abd Eldaim, M. A., Abdel-Daim, M. M., & Elgarawany, G. E. (2020). Neuroprotective Potential of Allium sativum against Monosodium Glutamate-Induced Excitotoxicity: Impact on Short-Term Memory, Gliosis, and Oxidative Stress. *Nutrients*, 12(4), 1028. doi: 10.3390/NU12041028

[7] Hazzaa, S. M., El-Roghy, E. S., Abd Eldaim, M. A., & Elgarawany, G. E. (2020). Monosodium glutamate induces cardiac toxicity via oxidative stress, fibrosis, and P53 proapoptotic protein expression in rats. *Environmental Science and Pollution Research,* 27(16), 20014-20024. doi: 10.1007/S11356-020-08436-6

[8] Heck, D., & Jost, A. (2021). Carotid stenosis, stroke, and carotid artery revascularization. *Progress in Cardiovascular Diseases,* 65, 49-54. doi: 10.1016/J.PCAD.2021.03.005

[9] Heil, E. M., Al-Bazi, W., & AL-Aameli, M. H. (2020). The Histological Alteration of Proximal Part of Aorta Exposed to (MSG) and Protective Effect of an a Lipoic Acid (ALA) in Male Rabbits. *Indian Journal of Forensic Medicine & Toxicology,* 14(3), 223. doi: 10.37506/ijfmt.v14i3.10493

[10] Imam, R. S. (2019). Genotoxicity of monosodium glutamate: A review on its causes, consequences and prevention. Indian Journal of Pharmaceutical Education and Research, 53(4), S510-517. doi: 10.5530/ijper.53.4s.145

[11] Kraal, A. Z., Arvanitis, N. R., Jaeger, A. P., & Ellingrod, V. L. (2020). Could Dietary Glutamate Play a Role in Psychiatric Distress? Neuropsychobiology, 79(1-2), 13-19. doi: 10.1159/000496294

[12] Krawisz, A. K., Carroll, B. J., & Secemsky, E. A. (2021). Risk Stratification and Management of Extracranial Carotid Artery Disease. Cardiology Clinics, 39(4), 539-549. doi: 10.1016/J.CCL.2021.06.007

[13] Majewski, M., Jurgonski, A., Fotschki, B., & Juskiewicz, J. (2018). The toxic effects of monosodium glutamate (MSG) - The involvement of nitric oxide, prostanoids and potassium channels in the reactivity of thoracic arteries in MSG-obese rats. *Toxicology and Applied Pharmacology,* 359, 62-69. doi: 10.1016/J.TAAP.2018.09.016

[14] Mohamed, M. A., El-Nahrawy, W. A., Zaher, A. M., & Amer, A. S. (2022). Therapeutic Role of Nanocurcumin Versus Monosodium Glutamate Toxicity. *Egyptian Academic Journal of Biological Sciences, B. Zoology,* 14(1), 55-65. doi: 10.21608/EAJBSZ.2022.217532

[15] Niaz, K., Zaplatic, E., & Spoor, J. (2018). Extensive use of monosodium glutamate: A threat to public health?. *EXCLI Journal,* 17, 273. doi: 10.17179/EXCLI2018-1092

[16] Onaolapo, A. Y., Odetunde, I., Akintola, A. S., Ogundeji, M. O., Ajao, A., Obelawo, A. Y., & Onaolapo, O. J. (2019). Dietary composition modulates impact of food-added monosodium

glutamate on behaviour, metabolic status and cerebral cortical morphology in mice. *Biomedicine & Pharmacotherapy,* 109, 417-428. doi: 10.1016/J.BIOPHA.2018.10.172

[17] Sasaki-Hamada, S., Hojyo, Y., Mizumoto, R., Koyama, H., Yanagisawa, S., & Oka, J. I. (2021). Cognitive and hippocampal synaptic profiles in monosodium glutamate-induced obese mice. *Neuroscience Research,* (170), 201-207. doi: 10.1016/J.NEURES.2020.08.005

[18] Wang, Z., Zhang, J., Wu, P., Luo, S., Li, J., Wang, Q., ... & Yang, H. (2020). Effects of oral monosodium glutamate administration on serum metabolomics of suckling piglets. *Journal of Animal Physiology and Animal Nutrition,* 104(1), 269-279. doi: 10.1111/JPN.13212

[19] World Health Organization. (2021). Cardiovascular diseases. Retrieved 11 June 2021, froms https://www.who.int/news-room/fact-sheets/detail/cardiovascular-diseases-(cvds)

СТРУКТУРНА ОРГАНІЗАЦІЯ СОННОЇ ПАЗУХИ ПІД ВПЛИВОМ ГЛУТАМАТУ НАТРІЮ В ЕКСПЕРИМЕНТІ: АНАЛІЗ ЗМІН В ДИНАМІЦІ

Содомора О. О.

Патологія сонних артерій є однією з провідних причин мозкового інсульту. Серед патогенетичних факторів розвитку ушкоджень сонних артерій чільне місце посідають розлади ліпідного обміну, атеросклероз і метаболічний синдром. Аліментарний фактор є надзвичайно істотним у цьому контексті. Глутамат натрію - одна із найпоширеніших харчових добавок, яка часто застосовується неконтрольовано і може спричиняти зміни структури і функцій органів і тканин. Мета дослідження: проаналізувати динаміку морфологічних змін ділянки сонної пазухи під впливом глутамату натрію при пероральному введенні його в експерименті. Досліджено ділянку сонної пазухи 20 лабораторних білих щурів самців, що впродовж 8 тижнів отримували глутамат натрію перорально в дозі 10 мг/кг/добу, морфологічними методами на макро- та мікроструктурному рівнях через 6 і 8 тижнів експерименту. Отримані дані порівняно із результатами морфологічного дослідження цієї ж ділянки у 20 тварин контрольної групи. Статистичну обробку маси тварин проводили за допомогою програмного забезпечення MS Excel 2007 (визначали середню ± середнє квадратичне відхилення). Через 6 тижнів експерименту при оцінці гістологічної будови стінки внутрішньої сонної артерії в зоні, що розташована безпосередньо над біфуркацією при порівнянні із контрольною групою в дослідній групі виявлено мультиплікацію і складчатість інтими, імовірно пов'язану із проліферацією клітин ендотелію під впливом глутамату натрію, відшарування ендотелію і лізис поодиноких ендотеліоцитів, а також нерівномірне потовщення еластичних волокон медії і порушення їх структури. Звертали на себе увагу накопичення білого жиру перивазально і в зоні сонного гломуса, а також дозорганізація нервів і розширення судин мікроциркуляторного русла. Через 8 тижнів експерименту була помітна негативна динаміка структурних змін: ознаки збільшення запальної інфільтрації, деформація судин мікроциркуляторного русла із потовщенням їх стінок і звуженням просвіту, стаз, помітна дегрануляція клітин сонного гломуса I типу, поява в інфільтраті поодиноких лаброцитів (мастоцитів). Помітно збільшилася також кількість жирової тканини (білий жир) в зоні сонної пазухи і біфуркації сонних артерій перивазально, а також в безпосередній близькості до каротидного гломуса, відмічалася тенденція до ущільнення жирової тканини. Таким чином, глутамат натрію при систематичному пероральному вживанні може спричиняти порушення структурної організації сонної пазухи, стінки сонних артерій і сонного гломуса, причому вираженість змін в динаміці наростає. Подальші дослідження необхідні для уточнення характеру структурних змін ділянки сонної пазухи за умов відміни глутамату натрію, а також пошуку можливих способів корекції.

Ключові слова: *глутамат натрію, сонна пазуха, сонний гломус, внутрішня сонна артерія, біфуркація сонних артерій.*

DOI: 10.31393/morphology-journal-2022-28(3)-07 Reports of Morphology, Vol. 28, №3, Pages 45-49

ISSN 1818-1295 eISSN 2616-6194

REPORTS OF MORPHOLOGY

Official Journal of the Scientific Society of Anatomists, Histologists, Embryologists and Topographic Anatomists of Ukraine

journal homepage: https://morphology-journal.com

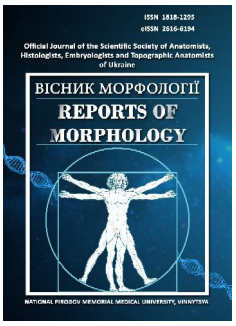

Discriminant models of the possibilities of occurrence and features of the course of benign nevi in men depending on the characteristics of dermatoscopic parameters

Haddad N. B. Yo.[1], Maievskyi O. Ye.[2], Serebrennikova O. A.[1], Khapitska O. P.[1], Vadzyuk S. N.[3]

[1]National Pirogov Memorial Medical University, Vinnytsya, Ukraine
[2]Taras Shevchenko National University of Kyiv, Kyiv, Ukraine
[3]I. Horbachevsky Ternopil National Medical University, Ternopil, Ukraine

ARTICLE INFO
Received: 6 June 2022
Accepted: 8 July 2022

UDC: 616.5-003.829-037-084-07

CORRESPONDING AUTHOR
e-mail: nabil.basim@gmail.com
Haddad N. B. Yo.

CONFLICT OF INTEREST
The authors have no conflicts of interest to declare.

FUNDING
Not applicable.

Human skin is the first barrier to protect the body from external factors. Combinations of certain external and internal (genetically determined) factors can lead to cancer of this organ. One of such pathologies is nevi - still little studied disease. At the same time, modern medicine is interested in inventing mechanisms to predict their occurrence and course. The purpose of the study is to build and analyze discriminant models of the possibility of benign nevi in Ukrainian men depending on the characteristics of dermatoscopic parameters. Ukrainian men aged 22 to 35 years, patients with melanocyte benign simple nevi (n=34), melanocyte benign dysplastic nevi (n=27), melanocyte benign congenital nevi (n=14) and non-melanocyte benign nevi (n=17) get dermatoscopic examination. The possibility of benign nevi occurrence depending on the characteristics of dermatoscopic parameters was carried out using discriminant analysis in the licensed statistical package "Statistica 5.5". With the help of discriminant analysis, reliable models of the possibility of occurrence of benign nevi depending on the characteristics of dermatoscopic parameters are built. It was found that among patients with melanocyte benign simple, dysplastic, congenital and non-melanocyte benign nevi, a reliable interpretation of the obtained classification indicators is possible (discriminant function covers 70.7 % of cases; statistics Wilks' Lambda=0.185; p<0.001). The models include the general dermatoscopic index, the dermatoscopic criterion "Asymmetry" according to the ABCD system, the number of nevi on the body more than 1 cm and the dermatoscopic criterion "Color" according to the ABCD system. Moreover, the general dermatoscopic index and the dermatoscopic criterion "Asymmetry" according to the ABCD system make the greatest contribution to discrimination between Ukrainian men with benign nevi.

Keywords: *skin diseases, benign nevi, dermatoscopy, men, discriminant analysis.*

Introduction

The barrier function of the skin is to protect the human body from a variety of stimuli, namely: mechanical damage (in particular, through the damping function), physical factors (such as ultraviolet radiation), chemical factors, microorganisms, etc.

At the same time, performing such a "piece of work" makes the skin vulnerable to various pathologies. Each of the external factors ultimately acts as a kind of trigger that start a cascade of pathophysiological reactions. However, it should be understood that the activation of such mechanisms also requires an internal factor, which is mostly a genetic predisposition to the occurrence of a pathological condition.

An example of such pathology, in particular, is a nevus. Many studies show that this disease is a combination of exogenous and endogenous factors. Examination of 546 children with nevi revealed that 94.6 % of subjects had a phenotype of II, III categories, 66.7 % had brown eyes, 59.3 % had brown hair and 61.3 % had light skin. At the same time, a higher incidence of sunburn was associated with more nevi [2]. Another group of authors, who also worked with a sample of Spanish children with nevi, performed a multifactor analysis of external factors associated with the number of nevi. If in the group of 4-

year-olds only time spent in the sun was a statistically significant factor, in the group of 14-year-olds such factors were male gender, skin phototype, time spent on the beach and use of sunscreen on the beach [12].

The number of nevi on the human body, as well as their location is completely different. According to Italian scientists, 50 % of children have less than 10 nevi, 45 % have 10 to 30, and only 5 % have 30 to 50 [8]. At the same time, data from a sample of Spanish children showed that the average number of nevi is about 19 units [2].

Examination of more than 9,000 boys aged 18-20, ethnic Jordanians, revealed nevi in 642. Of these: 8.1 % noted their appearance in preschool age, 59.8 % at the age of 12-15 years. In 68.3 % of cases, nevi were observed on the upper torso and shoulders. Most of the representatives with nevi were from the northern regions of Jordan [9].

C. Patruno and co-authors [14] in a sample of 144 children found that the number of nevi is higher in boys than in girls ($p<0.05$), and the highest prevalence of nevi is observed on the torso and neck ($p<0.001$). As in previous studies, a correlation was found between the number of nevi and the time of insolation ($p<0.05$).

The number of nevi is quite volatile. A survey of 90 Puerto Rican children found that 85 % had nevi at the time of the examination. A re-examination a year later revealed new nevi in 62 % of people. The average increase in the number of nevi was 1.8 ($p<0.001$) [20].

However, why is there such an increased interest in the study of nevi? Nevi are often associated with the risk of melanoma. In particular, to a greater extent this risk is associated with the number of nevi on the human body. Particular attention is paid to the presence of congenital, giant or atypical nevi. Although, according to scientists, the mechanism of melanoma is dominated by exogenous components [4]. The annual rate of conversion of a single nevus to is estimated at 0.0005 % or less for patients in the age group less than 40 years [17]. At the same time for a choroidal nevus this indicator makes from 2 to 3 % depending on a race [10].

In addition, we should not forget about the decline in quality of life and deterioration of psycho-emotional state in people with nevi, especially when it comes to congenital nevi of large size or localization in exposed areas of the body [11].

Given the above information, for the needs of practical medicine there is a need to find and study the interdependencies that will predict the risk of benign nevi. The most promising in terms of simplicity and cheapness of data are dermatoscopic indicators, the justification of the use of which can be achieved only by conducting an experimental study, followed by adequate and complete statistical processing of the results.

The purpose of the study is to build and analyze discriminant models of the possibility of benign nevi occurrence in Ukrainian men depending on the characteristics of dermatoscopic parameters.

Materials and methods

On the basis of the Military Medical Clinical Center of the Central Region and the Department of Dermatology and Venereal Diseases with a course of postgraduate education National Pirogov Memorial Medical University, Vinnytsya, Ukrainian men (aged 22 to 35 years) with melanocyte benign simple nevi (n=34), melanocyte benign dysplastic nevi (n=27), melanocyte benign congenital nevi (n=14) and non-melanocyte benign nevi (n=17) were performed clinical-laboratory and pathohistological examinations. The diagnosis of nevi was established according to a two-stage algorithm for the classification of pigmented tumors, which was adopted at the First World Congress of Dermatoscopy (Rome, 2001) [15].

Committee on Bioethics of National Pirogov Memorial Medical University, Vinnytsya (protocol № 10 From 26.11.2020) found that the studies do not contradict the basic bioethical standards of the Declaration of Helsinki, the Council of Europe Convention on Human Rights and Biomedicine (1977), the relevant WHO regulations and laws of Ukraine.

All patients were determined the number of nevi on the body, the number of nevi on the body up to 0.6 cm, the number of nevi on the body up to 1.0 cm, the number of nevi on the body more than 1.0 cm and the number of nevi on the hands more than 0.2 cm.

The dermatoscopic index was calculated according to the so-called "ABCD rule of dermatoscopy":

"A" - Asymmetry. To determine this indicator, the studied neoplasm was visually divided along two asymmetrically favorable lines; in the presence of asymmetry on two axes the index 2 was appropriated;

"B" - Border sharpness. To assess this feature, the tumor was visually divided into eight equal parts, each fate, which has a clear limit, was assigned an index of 1;

"C" - Color. There are 6 dermatoscopic colors (light brown, dark brown, black, gray-blue, white, red). Each color present in the area of the tumor was assigned an index of 1;

"D" - Dermoscopic structures. The dermatoscopic picture distinguished the following structural elements: "pigment network", "stripes" ("radial radiance", "pseudopods"), "points", "granules", "unstructured areas", "blue-white veil", "regression structures", "vascular structures" (areas of milky red color, microvessels are visualized). Each element in the presence of it in the tumor was assigned an index of 1.

The total dermatoscopic index is calculated by the formula "A" + "B" + "C" + "D", where the constant coefficients A=1.3; B=0.1; C=0.5; D=0.5. At the general dermatoscopic index from 4.75 to 5.45 the new growth is regarded as a dysplastic nevus, and at values above 5.45 the preliminary diagnosis of a melanoma of skin is exposed.

The possibility of benign nevi occurrence depending on the characteristics of dermatoscopic parameters was carried out using discriminant analysis in the licensed statistical package "Statistica 5.5".

Results

Taking into account dermatoscopic parameters between men with benign nevi, the discriminant function covers 85.3 % of men with melanocyte simple nevi, 70.4 % of men with melanocyte dysplastic nevi, 21.4 % of men with melanocyte congenital nevi and 82.4 % of men with non-melanocyte nevi. In general, the model in patients with melanocyte simple, dysplastic, congenital and non-melanocyte benign nevi of men is correct in 70.7 % of cases (Table 1).

Among men with benign nevi, the discriminant variables are the general dermatoscopic index (IND), the dermatoscopic criterion "Asymetry" according to the ABCD system (AS), the number of nevi on the body more than 1 cm (BOL_10) and the dermatoscopic criterion "Color" according to the ABCD system (COL) (Table 2). Among the above indicators, the general dermatoscopic index and the dermatoscopic criterion "Asymmetry" have the largest contribution to discrimination between groups of patients with benign nevi by men. The set of all dermatoscopic variables has a pronounced (Wilks' Lambda=0.185; F(12.23)=16.75; p<0.001) discrimination between groups of patients with benign nevi men (see Table 2).

Table 1. Matrix of percentages of coverage of discriminant function for patients with benign nevi men depending on features of dermatoscopic indicators.

Classification Matrix (nabil-gr.sta)					
Rows: Observed classifications					
Columns: Predicted classifications					
	Percent Correct	G_1:2 p=0.3696	G_2:3 p=0.2935	G_3:4 p=0.1522	G_4:5 p=0.1848
G_1:2	85.3	29	3	0	2
G_2:3	70.4	8	19	0	0
G_3:4	21.4	5	4	3	2
G_4:5	82.4	3	0	0	14
Total	70.7	45	26	3	18

Notes: here and in the following tables, 1:2 - men with melanocyte simple nevi; 2:3 - men with melanocyte dysplastic nevi; 3:4 - men with melanocyte congenital nevi; 4:5 - men with non-melanocyte nevi.

Table 2. Summary of the analysis of discriminant function between men with benign nevi depending on the characteristics of dermatoscopic parameters.

Discriminant Function Analysis Summary (nabil-gr.sta)						
Step 4, N of vars in model: 4; Grouping: DZ_1 (4 grps)						
Wilks' Lambda: 0.185 approx. F (12.23)=16.75 p<0,0000						
	Wilks' Lambda	Partial Lambda	F-remove-3.850	p-level	Toler.	(R-Sqr.)
IND	0.266	0.695	12.41	0.0000	0.087	0.913
AS	0.263	0.703	11.98	0.0000	0.171	0.829
BOL_10	0.233	0.792	7.436	0.0002	0.972	0.028
COL	0.203	0.910	2.787	0.0456	0.234	0.766

Notes: here and in the following tables, Wilks' Lambda - statistics of Wilkes lambda; $F_{(12.23)}$=16.75 - critical ($_{12.23}$) and received (16.75) the value of the Fisher test; p - p-level related to the total value Wilks' Lambda; Partial Lambda - Wilkes statistics lambda single contribution of variable to discrimination between populations; F-remove - the standard F-test is related to the corresponding one Partial Lambda; p-level - p-level related to the corresponding F-remove; Toler. - tolerance values for each variable.

Table 3. Indicators of classification of discriminant variable patients with benign nevi men depending on features of dermatoscopic indicators.

Classification Functions; grouping: DZ_1 (nabil-gr.sta)				
	G_1:2 p=0.3696	G_2:3 p=0.2935	G_3:4 p=0.1522	G_4:5 p=0.1848
IND	6.848	8.087	3.302	1.305
AS	-6.930	-5.784	-2.293	-1.334
BOL_10	-0.005	0.273	0.047	0.033
COL	-3.041	-5.017	0.902	-0.938
Constant	-7.644	-12.31	-5.937	-1.888

For patients with benign nevi men, classification indicators (Df) were determined, by means of which it is possible to classify patients into different groups of benign nevi (Table 3).

Below in the form of equations the definition of indicators of classification where assignment to men of patients with melanocytic simple nevi is possible at value Df close to 7.644 is given; to men patients with melanocyte dysplastic nevi - at a Df value close to 12.31; to men patients with melanocyte congenital nevi - at a Df value close to 5.937; to men with non-melanocyte nevi - with a Df value close to 1.888:

Df (*for men with melanocyte simple nevi*) = IND x 6.848 - AS x 6.930 - BOL_10 x 0.005 - COL x 3.041 - 7.644;

Df (*for men with melanocyte dysplastic nevi*) = IND x 8.087 - AS x 5.784 + BOL_10 x 0.273 - COL x 5.017 -12.31;

Df (*for men with melanocyte congenital nevi*) = IND x 3.302 - AS x 2.293 + BOL_10 x 0.047 + COL x 0.902 - 5.937;

Df (*for men with non-melanocyte nevi*) = IND x 1.305 - AS x 1.334 + BOL_10 x 0.033 - COL x 0.938 - 1.888.

The obtained results of the χ^2 test indicate that, taking into account the established dermatoscopic parameters, a reliable interpretation of the obtained classification indicators between men with patients with all groups of benign nevi is possible (see Table 4).

Table 4. Test report χ^2 with removed consecutive roots in patients with benign nevi men, depending on the characteristics of dermatoscopic parameters.

Chi-Square Tests with Successive Roots Removed (nabil-gr.sta)						
	Eigen-value	Canonicl R	Wilks' Lambda	Chi-Sqr.	df	p-level
0	2.074	0.821	0.185	146.9	12	0.0000
1	0.577	0.605	0.568	49.17	6	0.0000
2	0.116	0.323	0.896	9.559	2	0.0084

Notes: Eigenvalue - root values for each discriminant function; Canonicl R - the canonical value of R for different roots; Chi-Sqr. - standard criterion χ^2 of successive roots; Df - number of degrees of freedom; p-level - p-level of the corresponding χ^2.

Discussion

Dermatoscopic method of research occupies a key place in the primary diagnosis and differential diagnosis of nevi. The most popular in terms of differential diagnosis is the exclusion of melanoma. Dermatoscopy allows to perform differential diagnosis 27 % more effectively than the usual examination with the naked eye [16]. However, it should be noted that the effectiveness of this method directly correlates with the experience of the dermatovenerologist who conducts the examination [21].

T. Alendar and H. Kittler [1] analyzed dermatoscopic studies to identify nevi most often associated with melanoma. Of the 357 cases of melanoma, the occurrence of nevus was recorded in 8.7 % of cases. At the same time, in 11.8 % an unambiguous conclusion could not be made. Most melanoma formation occurred on the background of superficial or superficial-deep congenital nevus.

A group of researchers performed a dermatoscopic examination of 3823 atypical nevi in 541 individuals. Pathomorphological examination was subsequently performed for 264 samples taken during dermatoscopy. In 30.5 % the pathomorphological conclusion was melanoma [13].

Analysis of the results of dermatoscopy revealed signs that distinguish nevi from melanoma. The most characteristic criteria for melanoma were pattern asymmetry (OR, 4.9; 95 % CI, 4.1-5.8), contour asymmetry (OR, 3.2; 95 % CI, 2.7-3.7), disorganized pattern (OR, 3.3; 95 % CI, 2.9-3.7), pronounced disorder of architecture (OR, 6.6; 95 % CI, 5.6-7.8) ($p<0.001$). Also as criteria it is possible to apply absence of vessels (ICC, 0,46; 95 % CI, 0,42-0,51), dark brown color (ICC, 0,40; 95 % CI, 0,35-0,44), vessels with a coma (ICC, 0.44; 95% CI, 0.40-0.49) ($p<0.001$). In total, the ABCD rule had the highest specificity (59.4 %) [3].

The effectiveness of the ABCD rule is also indicated by other studies [16].

A group of researchers led by Di Cesare A. [5] found features of the dermatoscopic picture for blue nevus. For the study, 95 cases of blue nevus and 190 melanoma and basal cell carcinoma were selected for comparison. In all 95 cases of dermatoscopy of the blue nevus, the phenomenon of homogeneous pigmentation was observed, in 84.2 % there was a homogeneous pattern (blue, black or brown) or a mixture of two colors (blue and black, brown or blue). 15.8 % had combinations of more than 2 colors. In 49.5 %, pigmentation was observed against the background of the absence of a pigment network, and in 50.5 % local dermatoscopic patterns were detected.

Patients with more than 100 nevi are 7 times more likely to develop melanoma than individuals with fewer nevi (combined RR 6.89; 95 % CI, 4.63, 10.25). In general, people with more than 40 nevi also have a high chance of developing melanoma (combined RR 1.47; 95 % CI, 1.36, 1.59) and people with more than 15 nevi have a 5-fold higher risk of melanoma than persons without nevi (combined RR 4.82; 95 % CI, 3.05, 7.62) [16].

In the analysis of discriminant equations of patients with benign nevi of Ukrainian men depending on dermatoscopic indicators, we found that a reliable interpretation of the obtained classification indicators between patients with melanocyte benign simple, dysplastic, congenital and non-melanocyte benign nevi is possible (discriminant function covers 70.7% of cases; Wilks' Lambda=0.185; $p<0.001$). The discriminant models include the general dermatoscopic index, the dermatoscopic criterion "Asymmetry" according to the ABCD system, the number of nevi on the body more than 1 cm and the dermatoscopic criterion "Color" according to the ABCD system. Moreover, the greatest contribution to discrimination between men with benign nevi is made by the general dermatoscopic index and the dermatoscopic criterion "Asymmetry" according to the ABCD system.

It should be noted that the world scientific community has also achieved significant success in predicting the occurrence of oncopathology, in particular dermatooncopathology, through the use of anthropometric indicators, including height, weight, body mass index, body circumference, etc. [6, 7, 18, 19].

Given the above data, it is encouraging to apply different approaches to predicting the occurrence or course of a nevus, in particular both dermatoscopic and constitutional. This area of research can be considered in subsequent publications.

Conclusions

1. Reliable discriminant models developed on the basis of dermatoscopic indicators allow to predict with high probability the possibility of melanocyte benign simple, dysplastic, congenital and non-melanocyte benign nevi occurrence in Ukrainian men.

2. The composition of discriminant equations in patients with benign nevi Ukrainian men includes the general dermatoscopic index, dermatoscopic criteria "Asymmetry" and "Color" according to the ABCD system and the number of nevi on the body more than 1 cm.

References

[1] Alendar, T., & Kittler, H. (2018). Morphologic characteristics of nevi associated with melanoma: a clinical, dermatoscopic and histopathologic analysis. *Dermatology Practical & Conceptual,* 8(2), 104-108. doi:10.5826/dpc.0802a07

[2] Buendia-Eisman, A., Palau-Lazaro, M. C., Arias-Santiago, S., Cabrera-Leon, A., & Serrano-Ortega, S. (2012). Prevalence of melanocytic nevi in 8- to 10-year-old children in Southern Spain and analysis of associated factors. *Journal of the European Academy of Dermatology and Venereology,* 26(12), 1558-1564. doi: 10.1111/j.1468-3083.2011.04342.x

[3] Carrera, C., Marchetti, M. A., Dusza, S. W., Argenziano, G., Braun, R. P., Halpern, A. C., ... & Marghoob, A. A. (2016). Validity and reliability of dermoscopic criteria used to differentiate nevi from melanoma: a web-based international dermoscopy society study. *JAMA dermatology,* 152(7), 798-806. doi: 10.1001/jamadermatol.2016.0624

[4] Conforti, C., & Zalaudek, I. (2021). Epidemiology and Risk Factors of Melanoma: A Review. *Dermatology Practical & Conceptual,* 11(Suppl 1), e2021161S. doi: 10.5826/dpc.11S1a161S

[5] Di Cesare, A., Sera, F., Gulia, A., Coletti, G., Micantonio, T., Fargnoli, M. C., & Peris, K. (2012). The spectrum of dermatoscopic patterns in blue nevi. *Journal of the American Academy of Dermatology,* 67(2), 199-205. doi: 10.1016/j.jaad.2011.08.018

[6] Dusingize, J. C., Olsen, C. M., An, J., Pandeya, N., Law, M. H., Thompson, B. S., ... & Whiteman, D. C. (2020). Body mass index and height and risk of cutaneous melanoma: Mendelian randomization analyses. *International journal of epidemiology,* 49(4), 1236-1245. doi: 10.1093/ije/dyaa009

[7] Kontautiene, S., Stang, A., Gollnick, H., & Valiukeviciene, S. (2015). The role of phenotype, body mass index, parental and sun exposure factors in the prevalence of melanocytic nevi among schoolchildren in Lithuania. *Journal of the European Academy of Dermatology and Venereology,* 29(8), 1506-1516. doi: 10.1111/jdv.12905

[8] Lanna, C., Tartaglia, C., Caposiena Caro, R. D., Mazzilli, S., Ventura, A., Bianchi, L., ... & Diluvio, L. (2020). Melanocytic lesion in children and adolescents: an Italian observational study. *Scientific Reports*, 10(1), 1-5. doi: 10.1038/s41598-020-65690-x

[9] Males, Y. J. (2013). Prevalence and Clinical Characteristics of Becker's Nevi in Young Jordanian Males. *Journal of the royal medical services,* 20(4), 57-62. doi: 10.12816/0001551

[10] Marous, C. L., Shields, C. L., Michael, D. Y., Dalvin, L. A., Ancona-Lezama, D., & Shields, J. A. (2019). Malignant transformation of choroidal nevus according to race in 3334 consecutive patients. *Indian Journal of Ophthalmology,* 67(12), 2035-2042. doi: 10.4103/ijo.IJO_1217_19

[11] Masnari, O., Neuhaus, K., Aegerter, T., Reynolds, S., Schiestl, C. M., & Landolt, M. A. (2019). Predictors of health-related quality of life and psychological adjustment in children and adolescents with congenital melanocytic nevi: analysis of parent reports. *Journal of Pediatric Psychology,* 44(6), 714-725. doi: 10.1093/jpepsy/jsz017

[12] Moreno, S., Soria, X., Martinez, M., Marti, R. M., & Casanova, J. M. (2016). Epidemiology of melanocytic naevi in children from Lleida, Catalonia, Spain: protective role of sunscreen in the development of acquired moles. *Acta Dermato-Venereologica,* 96(4), 479-484. doi: 10.2340/00015555-2277

[13] Moscarella, E., Tion, I., Zalaudek, I., Lallas, A., Kyrgidis, A., Longo, C., ... & Argenziano, G. (2017). Both short-term and long?term dermoscopy monitoring is useful in detecting melanoma in patients with multiple atypical nevi. *Journal of the European Academy of Dermatology and Venereology,* 31(2), 247-251. doi: 10.1111/jdv.13840

[14] Patruno, C., Scalvenzi, M., Megna, M., Russo, I., Gaudiello, F., & Balato, N. (2014). Melanocytic nevi in children of southern Italy: dermoscopic, constitutional, and environmental factors. *Pediatric dermatology,* 31(1), 38-42. doi: 10.1111/pde.12119

[15] Potekayev, N. N., Shuginina, Y. K., Kuzmina, T. S., & Arutyunyan, L. S. (2011). *Дерматоскопия в клинической практике. Руководство для врачей [Dermatoscopy in clinical practice. A guide for doctors].* M: МДВ, 144 - M: MDV, 144.

[16] Puig, S., & Malvehy, J. (2013). Monitoring patients with multiple nevi. *Dermatologic clinics,* 31(4), 565-577. doi: 10.1016/j.det.2013.06.004

[17] Rork, J. F., Hawryluk, E. B., & Liang, M. G. (2012). Literature update on Melanocytic Nevi and pigmented lesions in the pediatric population. *Current Dermatology Reports,* 1(4), 195-202. doi: 10.1007/s13671-012-0023-9

[18] Sergentanis, T. N., Antoniadis, A. G., Gogas, H. J., Antonopoulos, C. N., Adami, H. O., Ekbom, A., & Petridou, E. T. (2013). Obesity and risk of malignant melanoma: a meta-analysis of cohort and case-control studies. *European journal of cancer,* 49(3), 642-657. doi: 10.1016/j.ejca.2012.08.028

[19] Smith, L. K., Arabi, S., Lelliott, E. J., McArthur, G. A., & Sheppard, K. E. (2020). Obesity and the impact on cutaneous melanoma: Friend or foe?. *Cancers,* 12(6), 1583. doi: 10.3390/cancers12061583

[20] Sosa-Seda, I. M., Valentin-Nogueras, S., Figueroa, L. D., Sanchez, J. L., & Mercado, R. (2014). Clinical and dermoscopic patterns of melanocytic nevi in Hispanic adolescents: a descriptive study. *International Journal of Dermatology*, 53(3), 280-287. doi: 10.1111/j.1365-4632.2012.5784.x

[21] Tschandl, P., Hofmann, L., Fink, C., Kittler, H., & Haenssle, H. A. (2017). Melanomas vs. nevi in high-risk patients under long-term monitoring with digital dermatoscopy: do melanomas and nevi already differ at baseline?. *Journal of the European Academy of Dermatology and Venereology,* 31(6), 972-977. doi: 10.1111/jdv.14065

ДИСКРИМІНАНТНІ МОДЕЛІ МОЖЛИВОСТІ ВИНИКНЕННЯ ТА ОСОБЛИВОСТЕЙ ПЕРЕБІГУ ДОБРОЯКІСНИХ НЕВУСІВ У ЧОЛОВІКІВ ЗАЛЕЖНО ВІД ОСОБЛИВОСТЕЙ ДЕРМАТОСКОПІЧНИХ ПОКАЗНИКІВ

Хаддад Н. Б. Ю., Маєвський О. Є., Серебреннікова О. А., Хапіцька О. П., Вадзюк С. Н.

Шкіра людини є найпершим бар'єром захисту організму від зовнішніх чинників. Комбінації дії певних зовнішніх та внутрішніх (генетично детермінованих) чинників можуть призводити до виникнення онкологічних захворювань даного органу. Однією з таких патологій є невуси - досі мало вивченого захворювання. В той же час сучасна медицина зацікавлена у винайденні механізмів передбачення їх виникнення та перебігу. Мета дослідження - побудувати та провести аналіз дискримінантних моделей можливості виникнення доброякісних невусів в українських чоловіків залежно від особливостей дерматоскопічних показників. Українським чоловікам віком від 22 до 35 років, хворим на меланоцитарні доброякісні прості невуси (n=34), меланоцітарні доброякісні диспластичні невуси (n=27), меланоцітарні доброякісні вроджені невуси (n=14) та немеланоцитарні доброякісні невуси (n=17) проведено дерматоскопічне обстеження. Можливість виникнення доброякісних невусів залежно від особливостей дерматоскопічних показників проведено за допомогою дискримінантного аналізу в ліцензійному статистичному пакеті "Statistica 5.5". За допомогою дискримінантного аналізу побудовані достовірні моделі можливості виникнення доброякісних невусів в залежності від особливостей дерматоскопічних показників. Встановлено, що між хворими на меланоцитарні доброякісні прості, диспластичні, вроджені та немеланоцитарні доброякісні невуси можлива достовірна інтерпретація отриманих показників класифікації (дискримінантна функція охоплює 70,7 % випадків; статистика Wilks' Lambda=0,185; p<0,001). До складу моделей входять загальний дерматоскопічний індекс, дерматоскопічний критерій "Asymmetry" по системі ABCD, кількість невусів на тілі більше 1 см та дерматоскопічний критерій "Color" по системі ABCD. Причому, загальний дерматоскопічний індекс і дерматоскопічний критерій "Asymmetry" по системі ABCD вносять найбільший внесок у дискримінацію між хворими на доброякісні невуси українськими чоловіками.

Ключові слова: *захворювання шкіри, доброякісні невуси, дерматоскопія, чоловіки, дискримінантний аналіз.*

DOI: 10.31393/morphology-journal-2022-28(3)-08 Reports of Morphology, Vol. 28, №3, Pages 50-55

ISSN 1818-1295 eISSN 2616-6194

REPORTS OF MORPHOLOGY

Official Journal of the Scientific Society of Anatomists, Histologists, Embryologists and Topographic Anatomists of Ukraine

journal homepage: https://morphology-journal.com

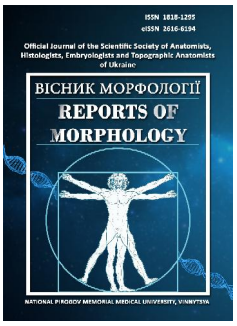

Modeling of appropriate spirometric indicators in practically healthy young women from Podillia with ectomorphic somatotype

Sarafyniuk L. A., Kyrychenko Yu. V.
National Pirogov Memorial Medical University, Vinnytsya, Ukraine

ARTICLE INFO
Received: 9 June 2022
Accepted: 11 July 2022

UDC: 616.24-073.173-053.7(477.44)

CORRESPONDING AUTHOR
e-mail: lsarafinyuk@gmail.com
Sarafyniuk L. A.

CONFLICT OF INTEREST
The authors have no conflicts of interest to declare.

FUNDING
Not applicable.

Many researchers emphasize the practical importance of using mathematical modeling to determine the reference values of spirographic parameters, but unfortunately, there are no works that study the complex influence of anthropometric and somatotypological indicators on spirometric parameters in healthy young people. The purpose of the work was to build regression models to determine the proper indicators of external breathing in practically healthy young women (YW) ectomorphs and to establish the total influence of the constitutional characteristics of the body on spirographic parameters. We conducted a spirographic examination of 109 practically healthy YW (from 16 to 20 years inclusive) according to the American Pulmonology Association and the European Respiratory Society (2019) method on the Medgraphics Pulmonary Function System 1070 series. The anthropometric examination was carried out according to the method of Bunak V. V. as modified by Shaparenko P. P. (2000). The component composition of body weight was assessed according to Matiegka method (1921), muscle mass according to the method of the American Institute of Nutrition (1991). Somatotypological research was carried out according to the Heath-Carter (1990) method. After somatotyping, it was found that 31 YW had an ectomorphic type of constitution. For them, we conducted a direct step-by-step regression analysis in the "STATISTICA 5.5" package. On the basis of multivariate regression analysis, the total influence of anthropometric, somatotypological and dynamometric indicators on the variability of spirographic parameters of the body was determined. Mathematical modeling was carried out to determine the appropriate individual spirographic indicators in practically healthy YW of the Podillia ectomorphic somatotype. 11 reliable regression linear models were built with the accuracy of the description of the feature in the range of 57.63-94.44 %. To the greatest extent, the value of the spirometric parameters was determined by the girth of the body (most often the girth of the hand), the diameters of the pelvis (most often the external conjugate and intercristal distance), the width of the distal epiphyses (most often the shins), the skinfold thickness (most often under the shoulder blade).

Keywords: *spirography, young women, youth, ectomorphic somatotype, regression models.*

Introduction

At present, the conditionality of the macro- and microstructure of individual organs of various systems of the human body does not cause objections [8, 19]. In addition, modern studies have proven the existence of a mutually determined relationship between the features of the external structure of the body and functional parameters [3]. But it should be noted that the majority of such studies focus on the cardiovascular system [10, 11, 13, 18, 20, 23]. Although recently, scientists emphasize the need to study the interrelationships and interdependencies between indicators of respiratory organs and body structure parameters [1, 9, 15]. The relevance and practical importance of studying this issue is determined by the prevalence and progression of respiratory diseases among different population cohorts [6, 16, 17, 25] and the need for an individual approach to determining normative indicators [1, 14].

The practical importance of using mathematical modeling to determine the reference values of spirographic parameters is emphasized by many researchers who draw attention to the need to take into account the factor of sex and age [4, 7, 15]. Unfortunately, there are no works that

study the complex influence of all anthropometric and somatotypological indicators on spirometric parameters in healthy young people.

It is interesting that a certain number of studies related to the relationship between the indicators of pulmonary ventilation and the characteristics of fat deposition, such as fat and lean body mass, sagittal diameter of the abdomen, and the total amount of water in the body [4, 15, 24]. It has been proven that obesity, even in the absence of disease, is the cause of a decrease in external respiration, which is considered a predictor of mortality and a risk factor for diseases [7]. From our point of view, it is interesting to determine the dependence of spirometric indicators on the total influence of parameters of the external structure of the body in young women of the ectomorphic somatotype, which are characterized by minimal development of subcutaneous adipose tissue.

The purpose of the study was to build regression models to determine the proper parameters of external breathing in practically healthy young women ectomorphs and to establish the total influence of the constitutional characteristics of the body on spirographic parameters.

Materials and methods

On the basis of the research center of the National Pirogov Memorial Medical University, Vinnytsya, as a result of a comprehensive survey of the urban population, 109 practically healthy young women (from 16 to 20 years inclusive) were selected, who in the third generation lived in the territory of the Podillia region of Ukraine. Their state of health was assessed on the basis of a preliminary comprehensive clinical and laboratory examination.

Committee on Bioethics of National Pirogov Memorial Medical University, Vinnytsya (protocol № 6 From 8.06.2020) found that the studies do not contradict the basic bioethical standards of the Declaration of Helsinki, the Council of Europe Convention on Human Rights and Biomedicine (1977), the relevant WHO regulations and laws of Ukraine.

A spirographic examination was conducted according to the methodology of the American Pulmonology Association and the European Respiratory Society [5] on the Medgraphics Pulmonary Function System 1070 series. Anthropometric examination was performed according to Bunak's V. V. method, modified by Shaparenko P. P. [21]. This study included the assessment of total body dimensions: length (cm), mass (kg), body surface area (m2) and partial: longitudinal, girth, transverse and sagittal body dimensions and the width of the distal epiphyses - determined in cm, the skinfold thickness measured in mm. The assessment of the component composition of body weight was carried out according to the Matiegka method [12], the amount of muscle, fat and bone mass of the body was determined in kg. In addition, body muscle mass (kg) was determined according to the method of the American Institute of Nutrition [22]. The strength of the hand flexor muscles was determined using a hand dynamometer (kg). The somatotypological study was carried out according to the Heath-Carter method [2], the value of mesomorphic, endomorphic and ectomorphic components was estimated in points. After somatotyping, it was found that 31 girls had an ectomorphic type of constitution. For them, we conducted a direct step-by-step regression analysis in the "STATISTICA 5.5" package.

Results

On the basis of multivariate regression analysis, we performed mathematical modeling of spirographic parameters in practically healthy YW ectomorphic somatotype of the Podillia region of Ukraine, depending on the characteristics of indicators of external body structure. Constructed linear regression models provide an opportunity to determine appropriate individual spirographic indicators on the basis of anthropometric and somatotypological characteristics of each person of young female age.

In particular, we found that the volumetric exhalation rate, respectively, at 50 % of the forced vital capacity of the lungs (FIF 50 %) was 81.00 % dependent on the combined effect of 9 anthropometric and 1 dynamometric indicators. Most of the coefficients of the independent variables included in this regression polynomial had high reliability, with the exception of the free member and the skinfold thickness on the chest and under the shoulder blade. Fisher's criterion of this mathematical model (F=8.50) was greater than its calculated value ($F_{cr.}$=10.20). Accordingly, we could claim that the constructed regression polynomial is highly significant (p<0.001), which was also confirmed by the results of variance analysis. The built model had the form of the following linear equation:

FIF 50 % (l/s) = 3.388 + 3.916 x width of the distal epiphysis of the shoulder on the left - 0.261 x circumference of the waist - 3.805 x width of the distal epiphysis of the shoulder on the right - 0.066 x dynamometry of the right hand + 0.655 x circumference of the forearm in the upper third + 0.203 x transverse middle chest size - 0.200 x skinfold thickness on the shin + 0.197 x skinfold thickness on the chest - 0.093 x shoulder width + 0.113 x skinfold thickness under the shoulder blade.

We found that the variability of the forced vital capacity of the lungs (FVC) in YW ectomorphic somatotype was 95.55 % dependent on 13 anthropometric parameters, which were correlated with each other. To reduce multicollinearity, we used the ridge regression method, where a constant (lambda) equal to 0.1 was added to the correlation matrix. Ridge regression in this case reduced the coefficient of determination (R^2=72.42) and the number of independent variables of the regression polynomial, the vast majority of whose coefficients were reliable, with the exception of the inter-ridge pelvic distance. Fisher's criterion of this model (F=13.11) more than doubled its calculated value ($F_{cr.}$=5.25). Accordingly, we could claim that the constructed regression polynomial is highly significant

(p<0.001), which was also confirmed by the results of variance analysis. The model had the form of the following linear equation:

FVC (l) = -3.578 + 0.047 x chest girth at rest + 0.119 x transverse average chest size - 0.155 x external conjugate + 0.036 x muscle body weight according to the American Institute of Nutrition + 0.103 x intercristal distance.

Forced expiratory volume in the first second (FEV1) in YW ectomorphs was 91.70 % dependent on the combined effect of 14 anthropometric indicators. The vast majority of the coefficients of the independent variables of this model were significant, except for the free members and sagittal chest size. Fisher's criterion of this model (F=12.64) was slightly lower than its calculated value ($F_{cr.}$=14.16). The constructed regression polynomial was reliable (p<0.001), which was also confirmed by the results of variance analysis. The model had the form of the following linear equation:

FEV1 (l) = 0.879 + 0.100 x circumference of the chest on exhalation - 1.264 x width of the distal femoral epiphysis on the left + 0.317 x circumference of the shin in the lower third - 0.239 x external conjugate - 0.134 x height of the pubic point + 0.095 x thigh circumference - 0.122 x skinfold thickness on the abdomen - 2.600 x width of the distal epiphysis of the right shin + 1.739 x width of the distal epiphysis of the left shin + 0.127 x skinfold thickness on the side - 0.107 x skinfold thickness on the front surface of the shoulder + 0.680 x width of the distal epiphysis of the right forearm + 0.971 x width of the distal femoral epiphysis on the right + 0.038 x sagittal chest size.

In YW ectomorphs, almost all coefficients of the model of forced inspiratory flow, which is 50 % expiratory from forced vital capacity (FEF50FIF), had high reliability, with the exception of shoulder width. The coefficient of determination R^2 by 78.24 % determined admissibly this dependent variable. The regression linear polynomial was reliable (p<0.001), which was also confirmed by the results of variance analysis. Based on the fact that Fisher's criterion of 9.21 was greater than the calculated value ($F_{cr.}$=8.39), it was possible to assert the significance of the constructed equation:

FEF50FIF (l/s) = -17.77 - 2.959 x width of the distal epiphysis of the left shoulder + 0.589 x sagittal size of the chest + 0.742 x foot circumference - 0.480 x muscle body mass - 0.134 x shoulder width - 0.277 x skinfold thickness under the scapula + 0.108 x height of the acetabular point + 0.687 x external conjugate + 1.636 x width of the distal epiphysis of the forearm on the right.

The variability of maximum voluntary lung ventilation (MVV) depended on 77.44 % of the total complex of 10 parameters of the external structure of the body and 1 dynamometric index. Most of the coefficients of the independent variables that were included in the polynomial had high reliability, except for the free member, the intertrochanteric distance of the pelvis, and the chest circumference at expiration. Fisher's criterion of this model (F=5.92) was smaller than its calculated value ($F_{cr.}$=11.19). The constructed regression polynomial was reliable (p<0.001), which was also confirmed by the results of variance analysis. The model had the form of the following linear equation:

MVV (l) = 212.5 + 4.805 x sagittal size of the chest - 36.06 x width of the distal epiphysis of the tibia on the right + 1.351 x dynamometry of the left hand + 4.700 x skinfold thickness under the scapula - 1.636 x height of the acetabular point - 7.663 x girth of the hand + 16.25 x bone body weight + 8.454 x neck circumference - 2.669 x hip circumference + 6.166 x intertrochanteric distance - 1.045 x chest circumference on exhalation.

The Tiffeneau-Pinelli index, reflecting the ratio of the one-second volume of forced exhalation to the forced vital capacity, in YW of the ectomorphic somatotype had a dependence of 66.33 % on the total complex of constitutional indicators. The vast majority of the coefficients of the independent variables of this model are reliable; except for the girth of the neck. The Fisher criterion of this model (F=7.88) is greater than the calculated value of the F-criterion ($F_{cr.}$=6.24). Accordingly, we could claim that the constructed regression polynomial is highly significant (p<0.001), which was also confirmed by the results of variance analysis. The model had the form of the following linear equation:

Tiffeneau-Pinelli index (%) = 182.8 - 4.791 x bone mass of the body + 6.907 x interspinous distance - 7.621 x intercristal distance - 0.654 x dynamometry of the left hand + 3.945 x shin circumference in the lower third - 2.895 x neck circumference.

Expiratory volume rate, respectively, at 25 % of the forced vital capacity of the lungs (FEF 25 %) in YW ectomorphs depended by 57.63 % on the influence of only 4 anthropometric indicators that were included in the linear polynomial. All coefficients of independent variables and the free term of this model were reliable. Fisher's test (F=8.81) was greater than its calculated value ($F_{cr.}$=8.81). The constructed regression polynomial was reliable (p<0.001). The model had the form of the following linear equation:

FEF 25 % (l/s) = -20.06 + 0.934 x forearm girth in the upper third - 0.522 x external conjugate + 0.815 x intercristal distance - 0.137 x body weight.

The value of the vital capacity of the lungs (SVC) is determined by 79.73 % of the complex influence of anthropometric and somatotypological indicators, which were included in the regression polynomial. Most of the coefficients of the independent variables of this model had high reliability, with the exception of the free member and skinfold thickness under the scapula. Fisher's criterion of this model (F=12.90) was greater than its calculated value ($F_{cr.}$=7.23). The constructed regression polynomial was reliable (p<0.001), which was also confirmed by the results of variance analysis and comb regression. The model had the form of the following linear equation:

SVC (l) = 0.026 + 0.073 x thigh girth - 0.249 x

mesomorphic component + 0.039 x muscle body mass according to the American Institute of Nutrition + 0.080 x interspinous distance - 0.294 x width of the distal epiphysis of the ipшт on the left + 0.053 x skinfold thickness on the abdomen - 0.042 x skinfold thickness under the scapula.

Inhalation capacity (IC) in YW ectomorphs by 91.84 % is due to the complex influence of constitutional indicators that were included in the polynomial. All coefficients of independent variables of this model were reliable. Fisher's criterion of this model (F=19.32) was greater than its calculated value ($F_{cr.}$=11.19). The constructed regression polynomial was highly significant (p<0.001), which was also confirmed by the results of variance analysis. The model had the form of the following linear equation:

IC (l) = -1.817 - 0.020 x dynamometry of the right hand + 0.155 x intertrochanteric distance + 0.060 x skinfold thickness on the chest - 0.204 x hand circumference + 0.280 x forearm circumference in the lower third - 0.175 x foot circumference + 0.094 x shin circumference in upper third - 0.100 x thickness of the fat fold under the scapula + 0.021 x height of the acetabular point - 0.114 x ectomorphic component - 0.036 x sagittal chest size.

Most of the coefficients of the expiratory residual volume (ERV) model had high reliability, except for free member, sagittal chest size, and body length. The coefficient of determination R^2 determined this dependent variable by 79.61 %. Based on the fact that F=10.73, which is greater than the calculated value ($F_{cr.}$=8.22), it was possible to claim that the regression linear polynomial is highly significant (p<0.001), as evidenced by the results of the variance analysis. The model looked like this:

ERV (l) = -2.259 + 0.197 x foot circumference + 0.097 x intercristal distance - 0.386 x width of distal femoral epiphysis on the right - 0.122 x transverse mid-chest size + 0.150 x hand circumference - 0.213 x forearm circumference in the lower third + 0.047 x sagittal chest size cells + 0.014 x body length.

The maximum peak expiratory flow (FEF MAX) in YW ectomorphic somatotype depended on 94.44 % of the total complex 1 dynamometric and 13 indicators of external body structure. Most of the coefficients of the independent variables of this regression polynomial had high reliability, with the exception of the free member, neck circumference and the thickness of the fold under the shoulder blade. Fisher's criterion of this model (F=19.28) is greater than its calculated value ($F_{cr.}$=14.16). Accordingly, we had grounds to claim that the constructed regression polynomial is highly significant (p<0.001), which was also confirmed by the results of variance analysis. The model had the form of the following linear equation:

FEF MAX (l/s) = -4.910 + 0.665 x interspinous distance - 1.049 x external conjugate + 0.519 x body length - 0.274 x height of the pubic point + 0.690 x shin circumference in the lower third + 1.346 x forearm circumference in the upper third - 0.558 x hand circumference - 0.369 x height of the suprasternal point - 0.284 x skinfold thickness on the shin + 0.631 x skinfold thickness on the chest - 0.100 x dynamometry of the left hand - 3.455 x width of the distal epiphysis of the right forearm - 0.411 x neck circumference - 0.146 x skinfold thickness under the shoulder blade.

Discussion

The use of regression analysis makes it possible to create mathematical equations for determining the appropriate parameters of various organs and systems [3, 11, 18], in particular for spirometric forecasting, where predictors are anthropometric and somatotypological variables [4, 7]. Despite the fact that there are separate works in which mathematical modeling of external breathing indicators is performed [1, 8, 15], this does not negate the expediency of such studies, especially for certain ethno-territorial population groups of a certain age, sex, health status, constitutional type, because it will make it possible to establish reference values of spirometric parameters. The main predictors of lung function are most often height while sitting, body length and weight, component composition of body weight [9]. Unfortunately, there are no works that study the complex influence of all anthropometric and somatotypological indicators on spirometric parameters in practically healthy YW of a particular somatotype. We conducted such a study for the first time, where the combined influence of 55 constitutional parameters and 3 dynamometry indicators on the functional state of the lungs was studied. Therefore, let's dwell in more detail on the predictors of indicators of external breathing in female representatives of the ectomorphic constitutional type.

Thus, we have built mathematical models with the accuracy of the sign description in the range of 57.63 - 94.44 % for only 11 spirometric indicators, out of 16 possible parameters of external breathing that we determined. These mathematical models, or polynomials, included 99 constitutional indicators. Among them, girth sizes of the body were most often presented, included in 11 out of 11 models (100 %). They accounted for 29.29 % of the other predictors included in the models, while hand girth was the most frequent predictor (5.05 % of all parameters and 17.24 % of girth sizes). The dimensions of the pelvis were included in 10 out of 11 models (90.9 %). They accounted for 14.14 % of the other predictors included in the models, among them external conjugate and intercristal distance were most frequently represented.

Indicators of the width of the distal epiphyses of the long tubular bones of the limbs were included in 7 out of 11 models (63.63 %), accounted for 13.13 % of other variable polynomials, while the width of the epiphysis of the shin was the predictor most often (4.04 % of all parameters and 30.76 % of other indicators of this groups). The skinfold thickness was also included in 63.63 % of the models and accounted for 15.15 % of the other predictors that were included in the regression polynomials, while the fold under the scapula was the most common (6.06 % of all

parameters and 40.0 % of the indicators that indicate subcutaneous fat).

5 models (45.45 %) included the heights of the acetabulum, pubic and suprasternal points, they accounted for 6.06 % of the other predictors included in the regression polynomials. It is noteworthy that in YW ectomorphs, the main difference of which is a large longitudinal elongation of the body, body length (18.18 %) was found in only 2 models, which, according to the results of research by individual authors, was the main predictor of respiratory volumes [1, 15, 24].

In 45.45 % of the models of spirometric parameters, the sagittal size of the chest, body weight components (muscle, bone, fat mass), and dynamometry indicators were presented. All of them accounted for 5.05 % of the other predictors included in the models.

The transverse dimensions of the body were included in 4 out of 11 models (36.36 %). They accounted for 5.05 % of other variable polynomials, with transverse mean chest size being the predictor most often (3.00 % of all parameters and 60.00 % of transverse dimensions).

The obtained results provide an opportunity in further studies to conduct an analysis and determine the appropriate individual spirographic parameters in YW ectomorphic somatotype.

Conclusions

1. 11 mathematical models were built to determine the appropriate spirometric parameters with the accuracy of character description in the range of 57.63 - 94.44 % for practically healthy YW ectomorphic somatotype of the Podillia region of Ukraine.

2. To the greatest extent, the value of spirometric parameters in YW ectomorphs was determined by girth sizes (29.29 % of other predictors included in the models), skinfold thickness (15.15 %), pelvis sizes (14.14 %), width of distal epiphyses (13.13 %).

References

[1] Bajo, J. M. (2010). Relationship Between the Lung Function and Anthropometric Measures and Indexes in Adolescents from Cordoba, Argentina. *American Journal of Human Biology,* 22(6), 823-829. doi: 10.1002/ajhb.21090

[2] Carter, J. L., & Heath, B. H. (1990). *Somatotyping - development and applications.* Cambridge University Press.

[3] Cherkasov, V. G., Ustymenko, O. S., Shayuk, A. V., Prokopenko, S. V., & Gunas, I. V. (2018). Modeling of sonographic parameters of the kidneys in practically healthy women of the middle intermediate somatotype depending on the constitutional parameters of the body. *Reports of Morphology,* 24(3), 5-10. doi: 10.31393/morphology-journal-2018-24(3)-01

[4] Fahmy, W. A., Khairy, S. A., & Anwar, G. M. (2013). The effects of obesity on pulmonary function tests among children and adolescents. *Researcher*, 5(1), 55-59. doi: 10.7813/2075-4124.2013/5-6/A.23

[5] Graham, B. L., Steenbruggen, I., Miller, M. R., Barjaktarevic, I. Z., Cooper, B. G. & Hall, G. L. (2019). Standardization of Spirometry 2019 Update. An Official American Thoracic Society and European Respiratory Society Technical Statement. *Am J Respir Crit Care Med*, 200(8), 70-88. doi: 10.1164/rccm.201908-1590S

[6] Imad, H., & Yasir, G., (2015). Epidemiological and clinical characteristics, spirometric parameters and response to budesonide/formoterol in patients attending an asthma clinic: an experience in a developing country. *Pan African Medical Journal*, 21(1), 154. doi: 10.11604/pamj.2015.21.154.5404

[7] Ishikawa, C., Barbieri, M. A, Bettiol, H., Bazo, G., Ferraro, A. A., & Vianna, E. O. (2021). Comparison of body composition parameters in the study of the association between body composition and pulmonary function. *BMC Pulm Med,* 21(1), 178. doi: 10.1186/s12890-021-01543-1

[8] Jaroszynski, A., Derezinski, T., Jaroszynska, A., Zapolski, T.,Wasikowska, B., Wysokinski, A., ... & Horoch, A. (2016). Association of anthropometric measures of obesity and chronic kidney disease in elderly women. *Ann. Agric. Environ. Med.,* 23(4), 636-640. doi: 10.5604/12321966.1226859

[9] Jibril, M., Saadatu, M., & Farida, S. (2015). Relationship between anthropometric variables and lung function parameters among primary school children. *Annals of Nigerian Medicine,* 9(1), 20.

[10] Khapitska, O. P. (2017). Interactions between rheographic indicators of shin with somatometric characteristics of the athletes with mesomorphic somatotype. *Bulletin of the problems of biology and medicine,* 4(2), 205-207.

[11] Khapitska, O. P. (2017). Modeling appropriate indicators peripheral hemodynamics depending on the peculiarities of body structure from volleyball players with mesomorphic somatotype. *Reports of Morphology,* 23(2), 315-320.

[12] Matiegka, J. (1921). The testing of physical effeciecy. *Amer. J. Phys. Antropol.,* 2(3), 25-38. doi: org/10.1002/ajpa.1330040302

[13] Moroz, V. M., Khapitska, O. P., Lisyuk, S. P., & Kachan, V. V. (2016). The relationship reovasographic parameters of the tibia with anthropometric dimensions, components of somatotype and weight of wrestlers, athletes and volleyball players. *Bulletin of the problems of biology and medicine,* 4(134), 224-229.

[14] Mozun, R., Berger, F., & Singer, F. (2022). One size does not fit all-Why do pediatric spirometry estimates vary across populations "down under"? *Pediatric Pulmonology,* 57(2), 345-346. doi: 10.1002/ppul.25751

[15] Ogunlana, M. O., Oyewole, O. O., Lateef, A. I., & Ayodeji, A. F. (2021). Anthropometric determinants of lung function in apparently healthy individuals. *S Afr J Physiother,* 77(1), 1509. doi: 10.4102/sajp.v77i1.1509

[16] Raghavan, D., & Jain, R. (2016). Increasing awareness of sex differences in airway diseases. *Respirology,* 21(3), 449-459.doi: 10.1111/resp.12702

[17] Raghavan, D., Varkey, A., & Bartter, T. (2017). Chronic obstructive pulmonary disease: the impact of gender. *Curr Opin Pulm Med.,* 23(2), 117-123. doi: 10.1097/MCP.0000000000000353

[18] Sarafyniuk, L. A., Syvak, A. V., Piliponova, V. V., Dus, S. V., & Lezhnova, O. V. (2019). The variation pulsometry correct indicators` modeling in volleyball players with mesomorphic somatotype depending on the anthropometric features of the organism. *Reports of Vinnytsia National Medical University,* 23(4), 567-572. doi: 10.31393/reports-vnmedical-2019-23(4)-01

[19] Sarafyniuk, L. A., Khapitska, O. P., Yakusheva, Yu. I., Ivanytsia, A. O., & Sarafyniuk, P. V. (2018). Somatotypological features of acrobat girl in different periods of ontogenesis. *Biomedical and Biosocial Anthropology*, 32, 43-47, doi: 10.31393/bba32-2018-06

[20] Semenchenko, V. V. (2018). Correlation of anthropo-somatometric parameters of the body of practically healthy women of the ectomorphic somatotype with cerebral blood circulation indicators. *Biomedical and Biosocial Anthropology,* 30, 27-35. doi: 10.31393/bba30-2018-04

[21] Shaparenko, P. P. (2000). *Anthropometry.* Vinnytsya: [w. p.].

[22] Shephard, R. J. (1991). *Body composition in biological anthropology.* Cambridge.

[23] Syvak, A. V. (2019). Relationships of heart rate variability parameters with indicators of external body structure in highly qualified juvenile mesomorph volleyball players. *Biomedical and Biosocial Anthropology,* 37, 49-54, doi: 10.31393/bba37-2019-08

[24] Yildiran, H., Koksal, E., Ayyildiz, F., & Ayhan, B. (2021). Relationship between pulmonary function and anthropometric measurements and body composition in young women. *Cukurova Medical Journal Cilt,* 46(4), 1379-1386. doi: 10.17826/cumj.978037

[25] Zakaria, R., Harif, N., Al-Rahbi, B., Aziz, C. B. A., & Ahmad, A. H. (2019). Gender Differences and Obesity Influence on Pulmonary Function Parameters. *Oman medical journal,* 34(1), 44-48. doi: 10.5001/omj.2019.07

МОДЕЛЮВАННЯ НАЛЕЖНИХ СПІРОМЕТРИЧНИХ ПОКАЗНИКІВ У ПРАКТИЧНО ЗДОРОВИХ ДІВЧАТ ПОДІЛЛЯ ЕКТОМОРФНОГО СОМАТОТИПУ

Сарафинюк Л. А., Кириченко Ю. В.

На практичному значенні використання математичного моделювання для визначення референтних значень спірографічних параметрів наголошують багато дослідників, але робіт, у яких би вивчався комплексний вплив антропометричних та соматотипологічних показників на спірометричні параметри у здорових осіб юнацького віку, нажаль, немає. Метою роботи було побудувати регресійні моделі для визначення належних показників зовнішнього дихання у практично здорових дівчат ектоморфів та встановити сумарний вплив конституціональних характеристик організму на спірографічні параметри. Нами було проведено спірографічне обстеження 109 практично здорових дівчат юнацького періоду онтогенезу (від 16 до 20 років включно) за методикою Американської асоціації пульмонологів та Європейського респіраторного товариства (2019) на апараті Medgraphics Pulmonary Function System 1070 series. Антропометричне обстеження виконано за методикою Бунака В. В. в модифікації Шапаренко П. П. (2000). Оцінку компонентного складу маси тіла провели за методом Матейко (1921), м'язову масу тіла - за методом Американського інституту харчування (1991). Соматотипологічне дослідження проводили за методом Heath-Carter (1990). Після соматотипування було виявлено, що 31 дівчина мала ектоморфний тип конституції. Для них нами був проведений прямий покроковий регресійний аналіз в пакеті "STATISTICA 5.5". На основі багатофакторного регресійного аналізу визначили сумарний вплив антропометричних, соматотипологічних і динамометричних показників на варіабельність спірографічних параметрів тіла. Провели математичне моделювання для визначення належних індивідуальних спірографічних показників у практично здорових дівчат Поділля юнацького віку ектоморфного соматотипу. Було побудовано 11 достовірних регресійних лінійних моделей з точністю опису ознаки у межах 57,63-94,44 %. У найбільшій мірі величина спірометричних параметрів детермінувалася обхватними розмірами тіла (найчастіше обхватом кисті), діаметрами таза (найчастіше зовнішньою кон'югатою та міжгребеневою відстанню), шириною дистальних епіфізів (найчастіше гомілки), товщиною шкірно-жирових складок (найчастіше під лопаткою).

Ключові слова: *спірографія, дівчата, юнацький вік, ектоморфний соматотип, регресійні моделі.*

DOI: 10.31393/morphology-journal-2022-28(3)-09 Reports of Morphology, Vol. 28, №3, Pages 56-61

ISSN 1818-1295 eISSN 2616-6194

REPORTS OF MORPHOLOGY

Official Journal of the Scientific Society of Anatomists, Histologists, Embryologists and Topographic Anatomists of Ukraine

journal homepage: https://morphology-journal.com

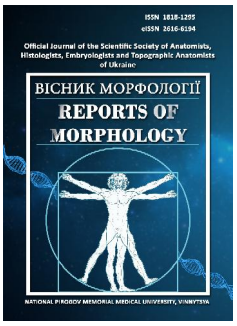

Cephalometric characteristics of the upper respiratory tract in Ukrainian young men and young women with an orthognathic bite without and with the type of face taken into account

Kostiuchenko-Faifor O. S., Gunas I. V., Belik N. V., Shapoval O. M., Veretelnyk S. P.
National Pirogov Memorial Medical University, Vinnytsya, Ukraine

ARTICLE INFO
Received: 13 June 2022
Accepted: 15 July 2022

UDC: 616.21:616.314.26-053.81-073.75

CORRESPONDING AUTHOR
e-mail: kostyuchenko.olha.91@gmail.com
Kostiuchenko-Faifor O. S.

CONFLICT OF INTEREST
The authors have no conflicts of interest to declare.

FUNDING
Not applicable.

The upper respiratory tract is a component of the respiratory system, which ensures the performance of several key human functions at once. The variability of cephalometric indicators of this structure of the human body, depending on the peculiarities of body structure, nationality, sex, and other factors, is one of the current topics of discussion among modern scientists. The purpose of the study is to establish the peculiarities of the cephalometric characteristics of the upper respiratory tract in young people without pathology of the upper respiratory tract with an orthognathic bite without and taking into account the type of face. For 72 Ukrainian young women and 46 young men with an orthognathic bite and the absence of pathology of the upper respiratory tract, taken from the database of the research center and the pediatric dentistry department of National Pirogov Memorial Medical University, Vinnytsya, determination of cephalometric parameters of the upper respiratory tract itself was carried out. The face type of young women and young men was determined using Garson's morphological index. The statistical analysis of the obtained results was carried out in the licensed statistical package "Statistica 6.0" using non-parametric estimation methods. In Ukrainian young women and young men without and taking into account the type of face, the percentile range of cephalometric parameters of the upper respiratory tract proper was established (distance PASmin - the size of the retroglossal oropharyngeal airway space, distance PM-UPW - the size of the nasopharyngeal airway space, distance U-MPW - the size of the retropalatal oropharyngeal airway space, distance V-LPW - the size of the hypopharyngeal airway space, area UAA - the size of the upper airway area). Sex differences (significantly greater, or a tendency towards greater values in young men) of distance V-LPW values were found in representatives without taking into account the face type by 13.8 %, with a wide face type - by 11.6 % and with a narrow face type - by 15.9 %; as well as the size of the UAA area in representatives without taking into account the face type by 20.6%, with a very wide face type - by 21.2 %, with a wide face type - by 21.6 % and with an average face type - by 23.1 %. Both in young women and in young men, no reliable differences or trends in the magnitude of the cephalometric parameters of the upper respiratory tract between representatives with different types of faces were established.

Keywords: *teleroentgenography, cephalometry, upper respiratory tract, young men, young women, orthognathic bite, facial types.*

Introduction

The affiliation of certain structures of the respiratory tract to the upper respiratory tract is still debatable by anatomists, morphologists and ENT specialists. There are views according to which only the nasal cavity and nasopharynx belong to the upper respiratory tract [15], but the majority of researchers also include the oropharynx and larynx and even the paranasal sinuses [19].

The multifunctionality of this part of the respiratory tract is related to the variety of anatomical structures that form it and, accordingly, their morphological structure. Among the key functions, it is worth noting the heating and humidification of air, its filtration, the performance of protective, vocal, and olfactory functions [15].

In this regard, any pathology affecting this system will

cause a corresponding disorder of the above functions, each of which has a certain value in maintaining the homeostasis of the body [19].

Cephalometric indicators are an important indicator that can indicate the existence or threat of pathology of the upper respiratory tract. Cephalometry has found wide use both for assessing the state of the jaw-dental system and for assessing the structures of the upper respiratory tract. In addition, this method of research allowed scientists to understand the existence and power of the influence of various external and internal factors on the peculiarities of the parameters of the cephalometric indicators of this part of the respiratory tract, and vice versa - its influence on other structures of the body.

For example, let's take into account the influence of nasal and mouth breathing in children on especially cephalometric indicators. A study by Mu?oz I. C. L. and Orta P. B. [12] showed that mouth-breathing children have higher values of SNB, NS-Go Gn and NS-O Pl ($p<0.05$) than nose-breathing children. At the same time, nose-breathing children often have a high position of the hyoid bone and significantly smaller values of the air space of the nasopharynx ($p<0.001$). Changes in cephalometric indicators depending on the type of breathing have also been confirmed in older age groups of children [20].

Craniofacial structures change in case of upper respiratory tract obstruction [3].

All these factors cause the increased interest of researchers in the study of cephalometric indicators of the upper respiratory tract. Work is being carried out on comparing the effectiveness of two- and three-dimensional studies [21], creating artificial neural networks for identifying the main anatomical landmarks in these structures [22].

Among the most promising directions of research, it is worth considering the study of normative cephalometric indicators of the upper respiratory tract in groups of different nationalities, sex and age, taking into account the peculiarities of odontological indicators and facial type.

The purpose of the study is to establish the peculiarities of the cephalometric characteristics of the upper respiratory tract in young people without pathology of the upper respiratory tract with an orthognathic bite without and taking into account the type of face.

Materials and methods

Primary lateral radiographs of 72 Ukrainian young women (YW) (aged 16 to 20 years) and 46 Ukrainian young men (YM) (aged 17 to 21 years) with an orthognathic bite and the absence of upper respiratory tract pathology were taken from the database of the National Pirogov Research Center and Department of Pediatric Dentistry Memorial Medical University, Vinnytsia.

All YW and YM in the private dental clinic "Vinintermed" underwent a teleradiographic examination (effective radiation dose up to 0.001 mSv) using a dental cone-beam tomograph Veraviewepocs 3D Morita (Japan). The licensed

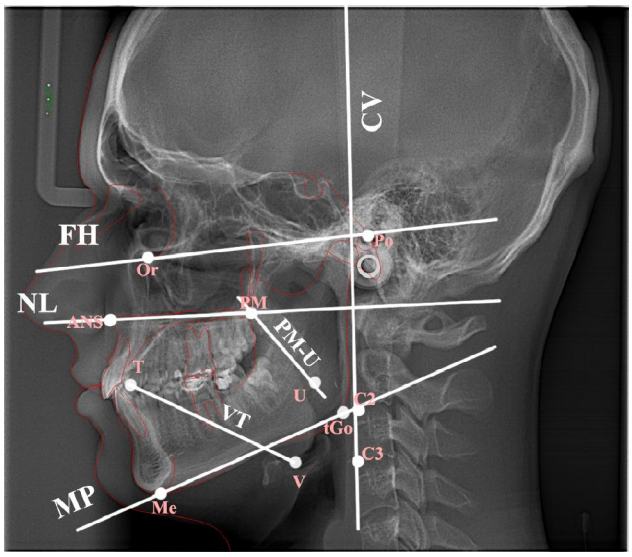

Fig. 1. Cephalometric lines used in cephalometric examination of the upper respiratory tract. CV - cervical plane (passes through points C2 and C3); FH - Frankfurt plane (passes through points Or and Po); MP - mandibular plane (passes through points Me and tGo); NL - nasal plane (passes through the ANS and PNS points); PM-U - longitudinal axis of the soft palate (passes through points PM and U); VT - longitudinal axis of the tongue (passes through points V and T).

medical software OnyxCeph$^{3™}$, version 3DPro (Image Instruments GmbH, Germany) and the "UniqCeph" diagnostic program created at the National Pirogov Memorial Medical University, Vinnytsya were used for cephalometric analysis.

Committee on Bioethics of National Pirogov Memorial Medical University, Vinnytsya (protocol № 8 From 30.09.2021) found that the studies do not contradict the basic bioethical standards of the Declaration of Helsinki, the Council of Europe Convention on Human Rights and Biomedicine (1977), the relevant WHO regulations and laws of Ukraine.

The cephalometric lines used in the cephalometric study of the upper respiratory tract [16] are shown in Figure 1.

The following cephalometric parameters of the upper respiratory tract itself were determined (Fig. 2, 3):

- distance PASmin (also known as Retroglossal oropharyngeal airway space) - distance between points TB and TB` (mm);
- distance PM-UPW (also known as Nasopharyngeal airway space) - distance between the points PM and UPW (mm);
- distance U-MPW (also known as Retropalatal oropharyngeal airway space) - the distance between the points U and MPW (mm);
- distance V-LPW (also known as Hypopharyngeal airway space) - distance between points V and LPW (mm);
- area UAA (also known as Upper airway area) - outlined by a contour through the points: PM - UPW - MPW - TB` - LPW - V - PM (mm^2);

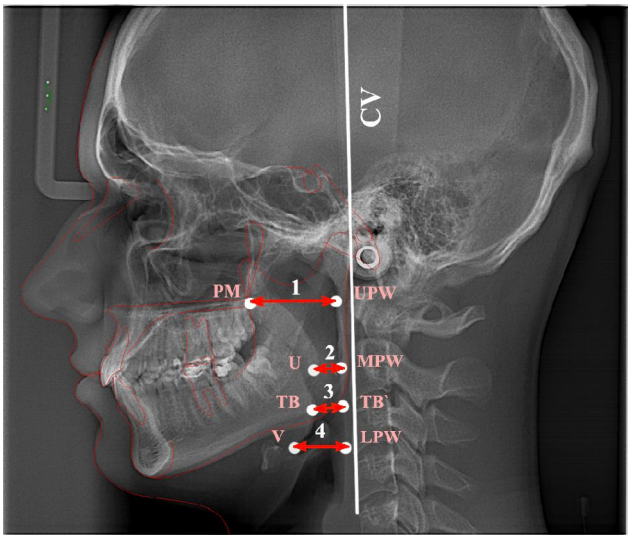

Fig. 2. Linear parameters used in the cephalometric study of the upper respiratory tract itself: 1 - distance PASmin, 2 - distance PM-UPW, 3 - distance U-MPW, 4 - distance V-LPW.

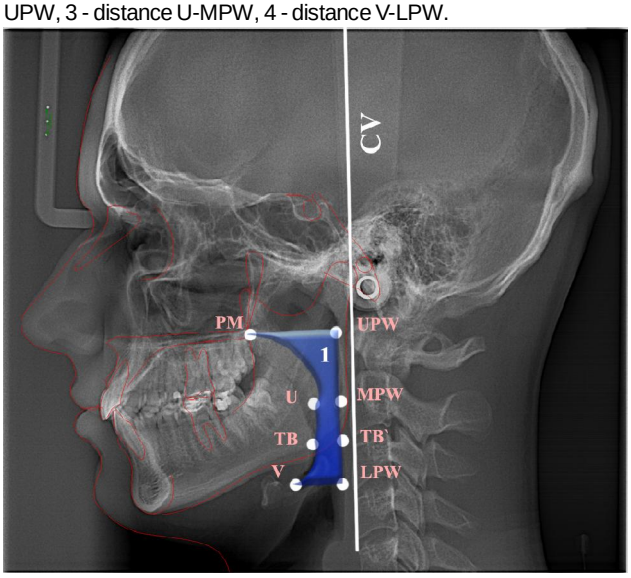

Fig. 3. Upper airway area (area UAA).

The type of face was determined using Garson's morphological index [14]. The following distribution by face types of YW and YM was established: YW - with a very wide face 25, with a wide face 25, with an average face 10, with a narrow face 12; YM - with a very wide face 5, with a wide face 22, with an average face 11, with a narrow face 8.

The statistical analysis of the obtained results was carried out in the licensed statistical package "Statistica 6.0" using non-parametric estimation methods. An assessment of the nature of distributions for each of the obtained variation series, the average for each characteristic being studied, the standard square deviation, and the percentile range of indicators was carried out. The significance of the difference in values between independent quantitative values was determined using the Mann-Whitney U-test.

Results

The percentile range of cephalometric parameters of the upper respiratory tract in Ukrainian YW and YM without pathology of the upper respiratory tract with an orthognathic bite without and taking into account the type of face are shown in Table 1.

When comparing the values of the cephalometric parameters of the upper respiratory tract proper between Ukrainian YW and YM with an orthognathic bite without and taking into account the type of face, it was established:

- the value of the V-LPW distance in YM regardless of face type (16.91±3.04 mm), with a wide face (16.51± 3.05 mm) and with a narrow face type (17.53±2.77 mm) is significantly greater or tends to greater values than in YW regardless of face type (14.58±3.03 mm, $p<0.001$), with a wide face (14.60±3.44 mm, $p<0.05$) and narrow face type (14.75±2.55 mm, $p=0.076$);
- the size of the UAA area in YM regardless of face type (734.7±179.8 mm^2), with a very wide face (718.0±100.3 mm^2), wide face (761.6±207.3 mm^2) and with an average face type (719.3±166.1 mm^2) is significantly greater than in YW regardless of face type (583.5±144.8 mm^2, $p<0.001$), with a very wide face (566.1±131.4 mm^2, $p<0.05$), wide face (597.0±166.9 mm^2, $p<0.01$) and with an average face type (553.4±171.8 mm^2, $p<0.05$).

When comparing the values of the cephalometric parameters of the upper respiratory tract proper in Ukrainian YW or YM with an orthognathic bite between different facial types, no reliable or trend differences in these parameters were established.

Discussion

Thus, as a result of the research conducted by us in Ukrainian YW and YM without pathology of the upper respiratory tract with an orthognathic bite without and taking into account the type of face, the percentile range of cephalometric parameters of the indicators of the upper respiratory tract itself was established. As a result of the analysis of the obtained results, pronounced manifestations of sexual dimorphism (larger values in YM) of the size of the lower oropharyngeal space were found in representatives without taking into account the type of face by 13.8 %, with a wide face - by 11.6 % and with a narrow face type - by 15.9 %; as well as the size of the area of the upper respiratory tract in representatives without taking into account the type of face by 20.6 %, with a very wide face - by 21.2 %, with a wide face - by 21.6 % and with an average face type - by 23.1 %. No significant differences or trends in cephalometric parameters of the upper respiratory tract proper in Ukrainian YW or YM with orthognathic bite between different facial types were established.

In children with different types of skeletal pattern (I group $2° \leq ANB \leq 5°$; II group $ANB>5°$), statistically significant differences in the size of the pharyngeal space of the respiratory tract were found (larger sizes were found in children of group I). Statistically significant differences were

Table 1. Percentile range (25.0th - 75.0th percentl) of cephalometric characteristics of the proper upper respiratory tract in Ukrainian YW and YM without and taking into account the type of face.

Indicator	Sex	Total	Face type			
			Very wide	Wide	Average	Narrow
Distance PASmin (mm)	YW	7.4 - 11.5	8,9 - 12,2	7.6 - 11.8	7.2 - 10.2	6.7 - 11.1
	YM	8.3 - 11.2	9.5 - 11.0	8.2 - 11.0	8.3 - 13.7	8.2 - 12.6
Distance PM-UPW (mm)	YW	21.6 - 26.4	21.1 - 25.5	22.5 - 26.5	19.8 - 25.9	21.6 - 26.7
	YM	22.4 - 26.5	23.1 - 26.9	22.3 - 26.3	19.3 - 26.2	23.2 - 27.5
Distance U-MPW (mm)	YW	8.6 - 11.9	7.2 - 11.4	8.9 - 12.7	7.1 - 12.8	8.7 - 12.3
	YM	8.2 - 12.3	10.6 - 11.0	9.2 - 12.3	7.7 - 12.9	6.9 - 13.4
Distance V-LPW (mm)	YW	12.2 - 16.2	11.8 - 16.5	13.1 - 15.8	12.2 - 15.3	13.0 - 16.4
	YM	14.8 - 19.1	14.7 - 17.2	15.0 - 18.1	15.0 - 20.1	14.7 - 19.8
Area UAA (mm^2)	YW	480 - 663	481 - 624	469 - 639	385 - 614	565 - 684
	YM	622 - 855	636 - 770	611 - 890	595 - 855	584 - 826

Notes: YW - young women; YM - young men.

found for the indicators of airway area ($p<0.01$), airway volume ($p<0.01$), minimum axial area ($p<0.05$) and the minimal space of the pharyngeal airway between the uvula and the back wall of the pharynx ($p<0.05$) [1].

According to the cephalometric analysis according to McNamara, for individuals with different types of facial growth, features of the indicators of the upper respiratory tract were revealed. Individuals with a hyperdivergent type of growth had smaller values of the width of the upper and lower part of the pharynx compared to other groups ($p<0.05$) [2].

The parameters of the upper respiratory tract are strikingly different in individuals with open bite, open skeletal and dental bite. So, people with an open bite have an anteroposterior narrowing of the upper respiratory tract. This is especially noted in the nasopharynx and oropharynx. A forward displacement of the hyoid bone is also noted. The same narrowing was noted in persons with an open skeletal bite. At the same time, an increase in the vertical dimensions of the respiratory tract was found in persons with a dental open bite [8].

Age-related changes in the development of the respiratory tract differ between men and women. R. D. C. Goncalves and others [5] found that in the period from 6 to 18 years the width of the respiratory tract increases, but if in general their width is greater in women, then for the upper respiratory tract it is the same for both sexes. Sharp increases in the width of the upper respiratory tract are noted in the period from 9 to 16 years.

The analysis of indicators of two age groups (the first 7-11 and the second 12-17 years) showed that the average value of the adenoid-nasopharynx ratio (A/N) was 0.45 and 0.44, PNS-ad1 and PNS-ad2 24 and 18.7 mm for age groups 1 and 2, respectively. The highest correlation with age was the length of the upper respiratory tract ($r=0.557$, $p<0.001$) [10].

B. Mislik and others [11] studied the effect of age on the distance "p" (the shortest distance between the soft palate and the back wall of the pharynx) and "t" (the shortest distance between the tongue and the back wall of the pharynx). The results of statistical data processing revealed an insignificant effect of age only on the "p" distance ($p=0.034$) and statistically significant correlations between both distances and anterior-posterior cephalometric data.

Studies devoted to the determination of normative indicators of the respiratory tract within different populations have a wide geographical distribution. So, the normative indicator of Chinese boys and girls was determined and compared with European data. In contrast to their European peers, Chinese children showed signs of sexual dimorphism - boys had a thicker soft palate ($p=0.008$), a smaller depth of the retropalatal ($p=0.011$), posterior lingual ($p=0.034$) and hypopharyngeal ($p<0.001$) parts of the pharynx. In addition, differences with European data were found regarding the depth of the posterior lingual part of the oropharynx and the position of the hyoid bone [6].

Significant manifestations of sexual dimorphism and features of indicators of the upper respiratory tract have also been established for the Indian population of various ages [7, 17].

According to McNamara's cephalometric analysis, normative indicators were established for the upper and lower respiratory tracts of children of European origin: PNS-Ad1 23.2 mm, Ad1-Ba 24.7 mm, PNS-Ba 47.6 mm, Ptm-Ba 45.7 mm, PNS-H 30.0 mm [13].

The increased interest of international scientists is growing in the study of the peculiarities of the respiratory tract in persons with different types of faces. Thus, the largest indicators of the width of the nasopharynx are found in brachyfacial individuals [4].

The existence of a statistically significant difference in the indicators of the posterior palatine space in brachyfacial and dolichofacial individuals was confirmed in the study of 45 teleroentgenograms using the Tweed analysis [18].

Also, a statistically significant negative correlation between the width of the upper part of the pharynx and the ANB angle was found during the cephalometric analysis [9].

Conclusions

1. The percentile range of cephalometric parameters of the upper respiratory tract proper in Ukrainian YW and YM with orthognathic bite without and taking into account the type of face was established.

2. Pronounced manifestations of sexual dimorphism of the size of the lower oropharyngeal space were revealed (larger values in YM without taking into account the type of face, with wide and with narrow types of face) and the size of the area of the upper respiratory area (larger values in YM without taking into account the type of face, with very wide, with wide and with medium face types).

References

[1] Alves Jr, M., Franzotti, E. S., Baratieri, C., Nunes, L. K. F., Nojima, L. I., & Ruellas, A. C. O. (2012). Evaluation of pharyngeal airway space amongst different skeletal patterns. *International journal of oral and maxillofacial surgery,* 41(7), 814-819. doi: 10.1016/j.ijom.2012.01.015

[2] Ansar, J., Singh, R. K., Bhattacharya, P., Agarwal, D. K., Verma, S. K., & Maheshwari, S. (2015). Cephalometric evaluation of the airway dimensions in subjects with different growth patterns. *Journal of Orthodontic Research*, 3(2), 108-112. doi: 10.4103/2321-3825.149051

[3] Ardehali, M. M., Zarch, V. V., Joibari, M. E., & Kouhi, A. (2016). Cephalometric assessment of upper airway effects on craniofacial morphology. *Journal of Craniofacial Surgery,* 27(2), 361-364. doi: 10.1097/SCS.0000000000002388

[4] Flores-Blancas, A. P., Carruitero, M. J., & Flores-Mir, C. (2017). Comparison of airway dimensions in skeletal Class I malocclusion subjects with different vertical facial patterns. *Dental press journal of orthodontics,* 22, 35-42. doi: 10.1590/2177-6709.22.6.035-042.oar

[5] Goncalves, R. D. C., Raveli, D. B., & Pinto, A. D. S. (2011). Effects of age and gender on upper airway, lower airway and upper lip growth. *Brazilian oral research,* 25, 241-247. doi:10.1590/S1806-83242011000300009

[6] Gu, M., McGrath, C. P., Wong, R. W., Hagg, U., & Yang, Y. (2014). Cephalometric norms for the upper airway of 12-year-old Chinese children. *Head & face medicine*, 10(1), 38. doi: 10.1186/1746-160X-10-38

[7] Guttal, K. S., & Burde, K. N. (2013). Cephalometric evaluation of upper airway in healthy adult population: a preliminary study. *Journal of Oral and Maxillofacial Radiology,* 1(2), 55-60. doi: 10.4103/2321-3841.120115

[8] Laranjo, F., & Pinho, T. (2014). Cephalometric study of the upper airways and dentoalveolar height in open bite patients. *International orthodontics,* 12(4), 467-482. doi: 10.1016/j.ortho.2014.10.005

[9] Lopatiené, K., Šidlauskas, A., Vasiliauskas, A., Čečyté, L., Švalkauskiene, V., & Šidlauskas, M. (2016). Relationship between malocclusion, soft tissue profile, and pharyngeal airways: A cephalometric study. *Medicina,* 52(5), 307-314. doi: 10.1016/j.medici.2016.09.005

[10] Masoud, A. I., & Alwadei, F. H. (2022). Two-dimensional upper airway normative values in children aged 7 to 17 years. *CRANIO®*, 1-8. 10.1080/08869634.2021.1943137

[11] Mislik, B., Hänggi, M. P., Signorelli, L., Peltomäki, T. A., & Patcas, R. (2014). Pharyngeal airway dimensions: a cephalometric, growth-study-based analysis of physiological variations in children aged 6-17. *European journal of orthodontics,* 36(3), 331-339. doi: 10.1093/ejo/cjt068

[12] Munoz, I. C. L., & Orta, P. B. (2014). Comparison of cephalometric patterns in mouth breathing and nose breathing children. *International journal of pediatric otorhinolaryngology,* 78(7), 1167-1172. doi: 10.1016/j.ijporl.2014.04.046

[13] Perez-Rodriguez, L. M., Dieguez-Perez, M., Millon-Cruz, A., & Arcos-Palomino, I. (2021). Airways cephalometric norms from a sample of Caucasian Children. *Journal of Clinical and Experimental Dentistry*, 13(9), e941-e947. doi: 10.4317/jced.58105

[14] Proffit, U. R., Fildz, G. U., & Saver, D. M. (2006). *Современная ортодонтия* (перевод с английского Д. С. Персина) [*Modern orthodontics* (translation from English by D. S. Persina)]. M.: МЕДпресс-информ - M.: MEDpress-inform.

[15] Sahin-Yilmaz, A., & Naclerio, R. M. (2011). Anatomy and physiology of the upper airway. *Proceedings of the American Thoracic Society*, 8(1), 31-39.

[16] Savoldi, F., Xinyue, G., McGrath, C. P., Yang, Y., Chow, S. C., Tsoi, J. K., & Gu, M. (2020). Reliability of lateral cephalometric radiographs in the assessment of the upper airway in children: A retrospective study. *The Angle Orthodontist*, 90(1), 47-55. doi: 10.2319/022119-131.1

[17] Shastri, D., Tandon, P., Nagar, A., & Singh, A. (2015). Cephalometric norms for the upper airway in a healthy North Indian population. *Contemporary clinical dentistry*, 6(2), 183-188. doi: 10.4103/0976-237X.156042

[18] Sprenger, R., Martins, L. A. C., Dos Santos, J. C. B., de Menezes, C. C., Venezian, G. C., & Degan, V. V. (2017). A retrospective cephalometric study on upper airway spaces in different facial types. *Progress in orthodontics,* 18(1), 25. doi:10.1186/s40510-017-0180-2

[19] Strohl, K. P., Butler, J. P., & Malhotra, A. (2012). Mechanical properties of the upper airway. *Comprehensive Physiology,* 2(3), 1853-1872. doi: 10.1002/cphy.c110053

[20] Ucar, F. I., & Uysal, T. (2012). Comparision of orofacial airway dimensions in subject with different breathing pattern. *Progress in orthodontics*, 13(3), 210-217. doi: 10.1016/j.pio.2012.02.005

[21] Vizzotto, M. B., Liedke, G. S., Delamare, E. L., Silveira, H. D., Dutra, V., & Silveira, H. E. (2012). A comparative study of lateral cephalograms and cone-beam computed tomographic images in upper airway assessment. *The European Journal of Orthodontics,* 34(3), 390-393. doi: 10.1093/ejo/cjr012

[22] Yoon, H. J., Kim, D. R., Gwon, E., Kim, N., Baek, S. H., Ahn, H. W., ... & Kim, S. J. (2022). Fully automated identification of cephalometric landmarks for upper airway assessment using cascaded convolutional neural networks. *European Journal of Orthodontics,* 44(1), 66-77. doi:10.1093/ejo/cjab054

ОСОБЛИВОСТІ ЦЕФАЛОМЕТРИЧНИХ ХАРАКТЕРИСТИК ВЕРХНІХ ДИХАЛЬНИХ ШЛЯХІВ В УКРАЇНСЬКИХ ЮНАКІВ І ДІВЧАТ ІЗ ОРТОГНАТИЧНИМ ПРИКУСОМ БЕЗ ТА З УРАХУВАННЯМ ТИПУ ОБЛИЧЧЯ

Костюченко-Файфор О. С., Гунас І. В., Белік Н. В., Шаповал О. М., Веретельник С. П.

Верхні дихальні шляхи є складовою респіраторної системи, що забезпечує виконання одразу кількох ключових функцій

людини. Мінливість цефалометричних показників даної структури тіла людини в залежності від особливостей тілобудови, національності, статі та інших факторів є одним з актуальних предметів дискусій сучасних вчених. Мета дослідження - встановити особливості цефалометричних характеристик власно верхніх дихальних шляхів у осіб юнацького віку без патології верхніх дихальних шляхів із ортогнатичним прикусом без та з урахуванням типу обличчя. 72 українським дівчатам і 46 юнакам із ортогнатичним прикусом і відсутністю патології верхніх дихальних шляхів, взятих із бази даних науково-дослідного центру та кафедри стоматології дитячого віку Вінницького національного медичного університету ім. М. І. Пирогова, проведено визначення цефалометричних параметрів власно верхніх дихальних шляхів. Тип обличчя дівчат і юнаків визначали за допомогою морфологічного індексу Гарсона. Статистичний аналіз отриманих результатів проведений у ліцензійному статистичному пакеті "Statistica 6.0" з використанням непараметричних методів оцінки. В українських дівчат та юнаків без та з урахуванням типу обличчя встановлено процентильний розмах цефалометричних параметрів показників власно верхніх дихальних шляхів (distance PASmin - величина заязикового ротоглоткового простору, distance PM-UPW - величина носоглоткового простору, distance U-MPW - величина запіднебінного ротоглоткового простору, distance V-LPW - величина нижнього ротоглоткового простору, ділянка UAA - величина площі верхньої дихальної ділянки). Виявлені статеві розбіжності (достовірно більші, або тенденція до більших значень в юнаків) величини distance V-LPW у представників без урахування типу обличчя на 13,8 %, з широким типом обличчям - на 11,6 % і з вузьким типом обличчя - на 15,9 %; а також величини ділянки UAA у представників без урахування типу обличчя на 20,6 %, з дуже широким типом обличчям - на 21,2 %, з широким типом обличчям - на 21,6 % і з середнім типом обличчя - на 23,1 %. Як у дівчат, так і в юнаків не встановлено достовірних або тенденцій відмінностей величини цефалометричних параметрів власно верхніх дихальних шляхів між представниками з різними типами обличчя.

Ключові слова: *телерентгенографія, цефалометрія, верхні дихальні шляхи, юнаки, дівчата, ортогнатичний прикус, типи обличчя.*

DOI: 10.31393/morphology-journal-2022-28(3)-10 Reports of Morphology, Vol. 28, №3, Pages 62-73

ISSN 1818-1295 eISSN 2616-6194

REPORTS OF MORPHOLOGY

Official Journal of the Scientific Society of Anatomists, Histologists, Embryologists and Topographic Anatomists of Ukraine

journal homepage: https://morphology-journal.com

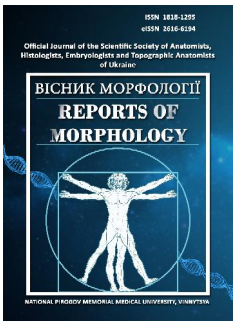

Shape of cerebral hemispheres: structural and spatial complexity. Quantitative analysis of skeletonized MR images

Maryenko N. I., Stepanenko O. Yu.
Kharkiv National Medical University, Kharkiv, Ukraine

ARTICLE INFO
Received: 17 June 2022
Accepted: 20 July 2022

UDC: 611.813:57.086:517:530.191

CORRESPONDING AUTHOR
e-mail: maryenko.n@gmail.com
Maryenko N. I.

CONFLICT OF INTEREST
The authors have no conflicts of interest to declare.

FUNDING
Not applicable.

For quantitative characterization of the complexity of the spatial configuration of anatomical structures, including cerebral hemispheres, fractal analysis is the most often used method, in addition to which, other methods of image analysis are quite promising, including quantitative analysis of skeletonized images. The purpose of the study was to determine the features of the structural and spatial complexity of the cerebral hemispheres shape using quantitative analysis of skeletonized magnetic resonance images of the cerebral hemispheres. Magnetic resonance brain images of 100 conditionally healthy individuals (who did not have structural changes in the brain) of both sexes (56 women, 44 men) aged 18-86 years (average age 41.72±1.58 years) were studied, 5 tomographic sections (4 coronal sections and 1 axial section) were selected from the set of tomographic images of each brain. During preprocessing, image segmentation was performed to obtain a binary silhouette image, after which silhouette skeletonizing was carried out. Quantitative analysis of skeletonized images included determination of the following parameters: branches, junctions, end-point voxels, junction voxels, slab voxels, triple points, quadruple points, average branch length, maximum branch length. We divided quantitative parameters of skeletonized images into two groups. The first group included branches, junctions, end-point voxels, junction voxels, slab voxels, triple points, quadruple points. These parameters were related to each other and to the values of the fractal dimension by positive correlations. The second group of parameters included average branch length, maximum branch length. These parameters were positively correlated, but they had negative correlations with most of the parameters of the first group and with fractal dimension values. Quantitative parameters and fractal dimension turned out to be better parameters for characterizing the spatial and structural complexity of the cerebral hemispheres shape than traditional morphometric parameters (area, perimeter and their derivatives). It was found that the values of most of the investigated quantitative parameters decreased with age; coronal sections were the most representative for characterizing age-related changes. Quantitative assessment of the brain shape, including spatial and structural complexity, can become an informative tool for the diagnosis of some nervous diseases and the differentiation of pathological and normal age-related changes.

Keywords: *brain, cerebral hemispheres, morphometry, skeletonizing, fractal dimension.*

Introduction

One of the urgent tasks of modern neuroscience and neuromorphology is the development and improvement of methods of objective assessment of various morphological parameters of nervous system structures. Most of the morphometry methods used in modern neuromorphology and medicine in general provide determination of basic geometric parameters - linear dimensions, area, volume and various indices that are derivatives of these parameters [1, 20]. The informativeness of these indicators is quite high when studying structures whose shape is close to the shape of simple geometric figures - a sphere, a prism, a cylinder, etc. However, for the assessment of some natural structures that have an irregular shape, such parameters are not enough, so the search for morphometric algorithms continues.

The shape of the cerebral hemispheres is irregular,

which is due to many factors, including the number, size and complexity of the configuration of convolutions and sulci. These parameters determine such an important characteristic of the shape of the cerebral hemispheres as spatial and structural complexity - the greater the number of convolutions and sulci and the more complex their configuration, the more complex the spatial configuration of the brain as a whole.

For the quantitative characterization of spatial and structural complexity, such a quantity as the fractal dimension is used, which is determined by means of fractal analysis [14]. Using this method, research was carried out on the cortex of the cerebral hemispheres [4, 10, 24] and its outer surface [8, 11], as well as the white matter of the cerebral hemispheres [3, 5, 19, 21, 22, 26-28] and cerebellar white matter [13, 15].

A fairly common image preprocessing method used for fractal analysis is skeletonization [9]. This processing method involves eroding the silhouette image with the formation of its digital skeleton [7, 9, 17, 18]. During the construction of a digital skeleton, an automatic algorithm detects all the vertices of the figure being skeletonized (in the case of cerebral hemispheres, such points are the vertices of the gyri) and connects them using the smallest possible number of short straight segments, forming a network inside the silhouette.

In the works of various researchers, skeletonization was used as a method of image preprocessing for fractal analysis of the white matter of the cerebral hemispheres [3, 5, 21, 22, 26-28]. Skeletonization was also used to analyze magnetic resonance imaging of the cerebral hemispheres using the "Peak Width of Skeletonized Mean Diffusivity" method [2, 6, 13, 23].

In addition to fractal analysis itself, in some cases quantitative analysis of digital skeletons of various biological structures is performed, which can be used both as an independent morphometric method and in combination with fractal analysis [7, 9, 17, 18]. Quantitative analysis of skeletonized images was used in the study of tree-like structures (most often - the dendritic tree of neurons) [7, 17, 18]. Previously, we performed a quantitative analysis of skeletonized images of human cerebellar white matter [15]. However, according to the scientific literature available to us, quantitative analysis of skeletonized images of the cerebral hemispheres has not been performed before. In our previous work [16], we performed a fractal analysis of skeletonized magnetic resonance (MR) images of the cerebral hemispheres. This work is a continuation of the previous one and includes quantitative analysis of skeletonized images.

The purpose of the study is to determine the features of the structural and spatial complexity of the shape of the cerebral hemispheres using quantitative analysis of skeletonized magnetic resonance images of the cerebral hemispheres.

Materials and methods

The study was conducted in compliance with the basic bioethical provisions of the Council of Europe Convention on Human Rights and Biomedicine (from 04.04.1997), the Helsinki Declaration of the World Medical Association on Ethical Principles of Scientific Medical Research with Human Participation (1964-2008), as well as the Order of the Ministry of Health of Ukraine № 690 from 23.09.2009. The conclusion of the Committee on Ethics and Bioethics of the Kharkiv National Medical University confirms that the research was conducted in compliance with human rights, in accordance with the legislation in force in Ukraine, meets international ethical requirements and does not violate ethical norms in science and standards for conducting biomedical research (minutes of the meeting of the Committee on of ethics and bioethics of the Kharkiv National Medical University № 10 dated November 7, 2018).

Magnetic resonance (MR) tomograms of the brain of 100 conditionally healthy individuals (who did not have structural changes in the brain) of both sexes (56 women, 44 men) aged 18-86 years (average age 41.72±1.58 years) were used as the research material.

Selection and pre-processing of images was carried out according to the algorithm described in our previous work [16]. From the set of tomographic images of each brain, 5 tomographic slices were selected (4 in the coronal projection, 1 in the axial projection). The sections had the following localization: the 1st coronal section was located at the level of the most anterior points of the temporal lobes, the 2nd - at the level of the corpus mamillare, the 3rd - at the level of the lamina quadrigemina, the 4th - at the level of the splenium corpori callosi, the axial tomographic section was located at the level of the thalamus.

The parameters of the investigated images were as follows: the size for examining coronal sections - 512x400 pixels, for axial sections - 512x800 pixels; resolution is 128 pixels per inch. The absolute scale of a digital image is 3 pixels (voxels) = 1 mm. During preprocessing, image segmentation was performed to obtain a binary silhouette image (Fig. 1B), after which the silhouette was skeletonized using the "skeletonize" tool of the Image J program (see Fig. 1C). Fractal analysis of skeletonized images was then carried out using the box counting method, for which the "fractal box count" tool of the Image J program was used. The same stages of image processing and analysis were used in our previous work [16].

The next stage of research, to which this work is devoted, was the quantitative analysis of skeletonized images, for which the "analyze skeleton" tool of the Image J program was used (Fig. 2). The following parameters were determined in each of the digital skeletons: branches, junctions, end-point voxels, junction voxels, slab voxels, triple points, quadruple points, average branch length, maximum branch length. The branches parameter characterizes the number of branches, the junctions parameter characterizes the number of branch connections.

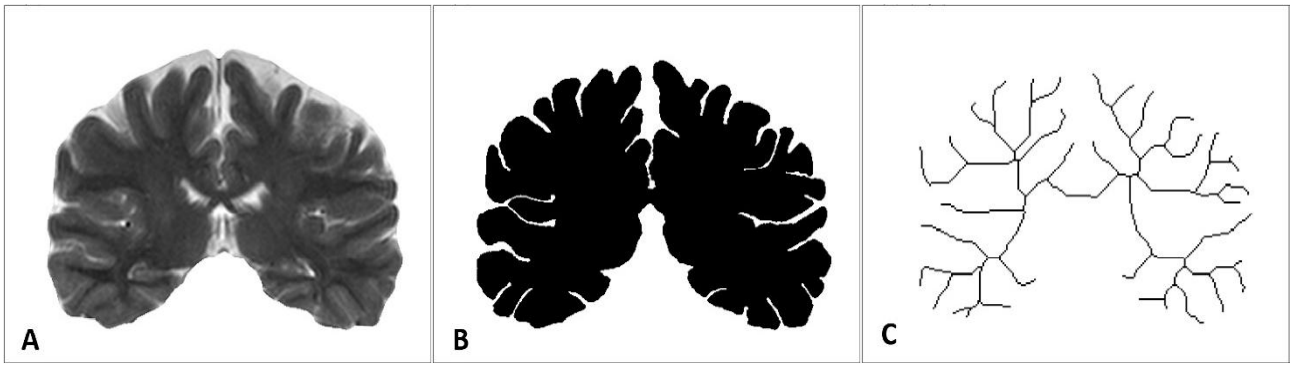

Fig. 1. Pre-processing of the magnetic resonance image of the brain: A - non-segmented coronal section after removal of background structures, B - binary silhouette image after segmentation, C - skeletonized image.

The end-point voxels parameter corresponds to the number of end points of the branches of the digital skeleton, junction voxels - the number of voxels forming the junction of branches, slab voxels - the number of voxels forming the branches. The triple points parameter characterizes the number of connections connecting three branches, quadruple points - four branches. The average branch length parameter is the arithmetic average value of the absolute length of all branches, and the maximum branch length parameter is the maximum among the values of the absolute length of all branches of the digital skeleton.

Traditional morphometric parameters belonging to Euclidean geometry were also determined: These parameters were determined on two types of images. The 1st type of images are tomographic sections as a whole (see Fig. 1, A), the perimeter of which corresponds to the contour of the visible surface of the cerebral hemispheres, and the area corresponds to the brain tissue as a whole, including the content of the sulci. The following indicators were determined on these images: P_0 (perimeter), S_0 (area), P_0/S_0 (ratio of perimeter to area), SF_0 (form factor). The 2nd type of images are segmented silhouette images (see Fig. 1, B), the perimeter of which corresponds to the contour of the pial surface of the cerebral hemispheres (including the contour of the depth of the furrows), and the area corresponds to the brain tissue as a whole (not including the contents of the sulci). The following indicators were determined on these images: P_s (perimeter), S_s (area), P_s/S_s (perimeter to area ratio), SF_s (form factor). The formula $SF=(4\pi \times A)/P^2$ was used to determine the form factor for both types of images. The ratio of the perimeter and area of the segmented silhouette image to the corresponding parameters of the section as a whole (P_s/P_0 and S_s/S_0) were also calculated.

Statistical processing of the data was carried out using the Microsoft Excel 2016 program. The data was processed using the tools of variational statistics. The following statistical parameters were calculated for each variation series: arithmetic mean (M), its error (mM), minimum (Min) and maximum (Max) values. The significance of statistical differences between the values of the fractal dimension of tomographic sections of different localization was assessed using the Kruskal-Wallis KW test with Bonferroni correction and Dunn's post-hoc test for multiple comparisons. To determine the relationship between the obtained values, the Pearson correlation coefficient (r) was calculated, the significance of which was assessed using the Student's test.

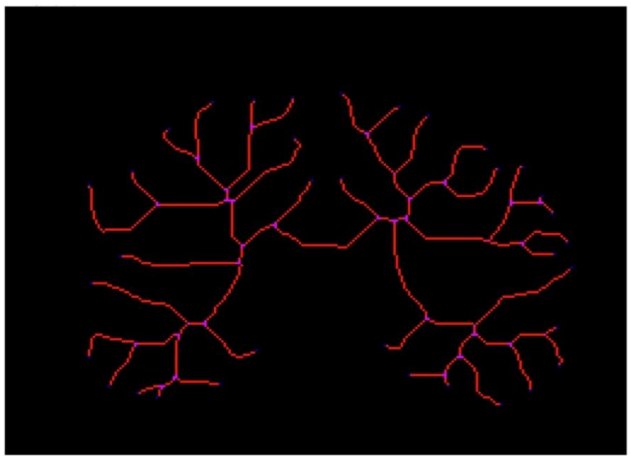

Fig. 2. Quantitative analysis of the skeleton image of the cerebral hemispheres: end-point voxels are highlighted in blue, junction voxels are in pink, slab voxels are in red.

Results

The statistical parameters and the distribution of the values of the quantitative parameters of the skeletonized images of the cerebral hemispheres are shown in Table 1 and Figure 3. When comparing the values of the quantitative parameters of the skeletonized images of five different tomographic sections, it was determined that the values of all parameters, except quadruple points, were statistically significantly different in sections of different localization ($p<0.001$), the number of quadruple points in different tomographic sections did not differ statistically significantly ($p=0.191$). When comparing the values in pairs, it was found that the values of the parameters branches, junctions, junction voxels, slab voxels and triple points of the 1st coronal section and axial section were statistically significantly different from each other and differed from the corresponding values of the rest of the tomographic

Table 1. Statistical parameters of the distribution of the values of the quantitative parameters of cerebral hemispheres skeletonized images.

Parameter		Tomographic section				
		Coronal 1	Coronal 2	Coronal 3	Coronal 4	Axial
Branches (N)	M	95.30	125.08	120.57	116.47	150.18
	m	1.58	2.73	2.53	2.21	4.41
	Min	61	69	70	77	86
	Max	146	202	224	208	317
Junctions (N)	M	48.62	63.94	62.01	59.80	77.13
	m	0.91	1.54	1.47	1.26	2.41
	Min	30	34	34	37	43
	Max	76	108	124	109	168
End-point voxels (N)	M	41.85	54.73	52.35	50.48	65.61
	m	0.54	0.85	0.71	0.71	1.49
	Min	29	36	36	38	42
	Max	58	80	72	79	114
Junction voxels (N)	M	156.4	199.3	193.5	186.0	234.5
	m	3.3	5.5	5.1	4.3	8.3
	Min	94	100	102	116	127
	Max	260	364	396	344	578
Slab voxels (N)	M	1755	2655	2680	2651	4209
	m	20	32	28	26	60
	Min	1337	1998	2116	2185	3090
	Max	2214	3359	3418	3235	6398
Triple points (N)	M	45.51	60.29	58.98	56.56	73.41
	m	0.80	1.36	1.34	1.16	2.17
	Min	30	34	32	35	42
	Max	65	95	115	99	153
Quadruple points (N)	M	2.300	3.060	2.440	2.460	3.137
	m	0.173	0.251	0.179	0.173	0.311
	Min	0	0	0	0	0
	Max	8	15	9	10	18
Average branch length (mm)	M	8.342	9.372	9.754	10.03	12.50
	m	0.095	0.094	0.104	0.10	0.17
	Min	6.71	7.42	6.74	7.01	8.23
	Max	13.14	12.05	12.50	12.61	16.14
Maximum branch length (mm)	M	27.26	33.90	37.44	40.33	50.88
	m	0.51	0.55	0.61	0.62	0.91
	Min	17.76	24.01	20.82	26.75	32.26
	Max	39.80	50.69	57.25	51.96	82.51

sections ($p<0.001$); the values of the 2nd, 3rd and 4th coronal sections did not differ statistically significantly from each other ($p>0.05$). The values of the end-point voxels and average branch length parameters of the 1st coronal section and axial section were statistically significantly different from each other and differed from the corresponding values of the rest of the tomographic sections ($p<0.001$); the values of the 2nd and 3rd coronal sections, as well as the 3rd and 4th coronal sections did not differ statistically significantly from each other ($p>0.05$), however, the values of the 2nd and 4th coronal sections differed statistically significantly from each other ($p<0.05$). No statistically significant difference was found between the values of the "maximum branch length" parameter of the 3rd and 4th coronal sections ($p=0.017$, the level of statistical significance $\alpha=0.050$ with Bonferroni correction was $\alpha=0.005$); the values of the remaining tomographic pairs were statistically significantly different from each other ($p<0.01$).

At the first stage of the correlation analysis, we determined the nature and strength of correlation relationships between the values of similar parameters of the digital skeleton determined on different tomographic sections (Fig. 4). We established that the values of most of the quantitative parameters of the four coronal sections were connected by a statistically significant positive correlation (except for the values of maximum branch length), while the strongest correlation was found between the values of the adjacent coronal sections - 1st and 2nd, 2nd and 3rd, 3rd and 4th. The values of most parameters of the axial section did not have a statistically significant correlation with the similar parameters of the coronal sections. The strongest correlation between adjacent coronal sections was found when conducting a correlation analysis of the following parameters: branches, junctions, end-point voxels, junction voxels, slab voxels, triple points. At the same time, the correlation between adjacent sections was not detected or was weak when conducting a correlation analysis of the values of the following parameters: quadruple points, average branch length, maximum branch length.

At the second stage of the correlation analysis, we investigated the correlation relationships between the values of various quantitative parameters of skeletonized images; we calculated the values of the correlation coefficients both for all the examined sections and separately for each tomographic section (Fig. 5). It turned out that there are significant positive correlations between the values of most parameters, these are the following parameters: branches, junctions, end-point voxels, junction voxels, slab voxels, triple points, quadruple points (at the same time, correlations between the parameters branches and junctions were close to functional). However, the values of average branch length and maximum branch length, which are positively correlated in all sections, are in most cases negatively correlated with the rest of the parameters (at the same time, average branch length has stronger correlation connections, and correlations between maximum branch length and values of other parameters are in many cases weak and not statistically significant).

At the third stage of the correlation analysis, we investigated the relationships between the values of the

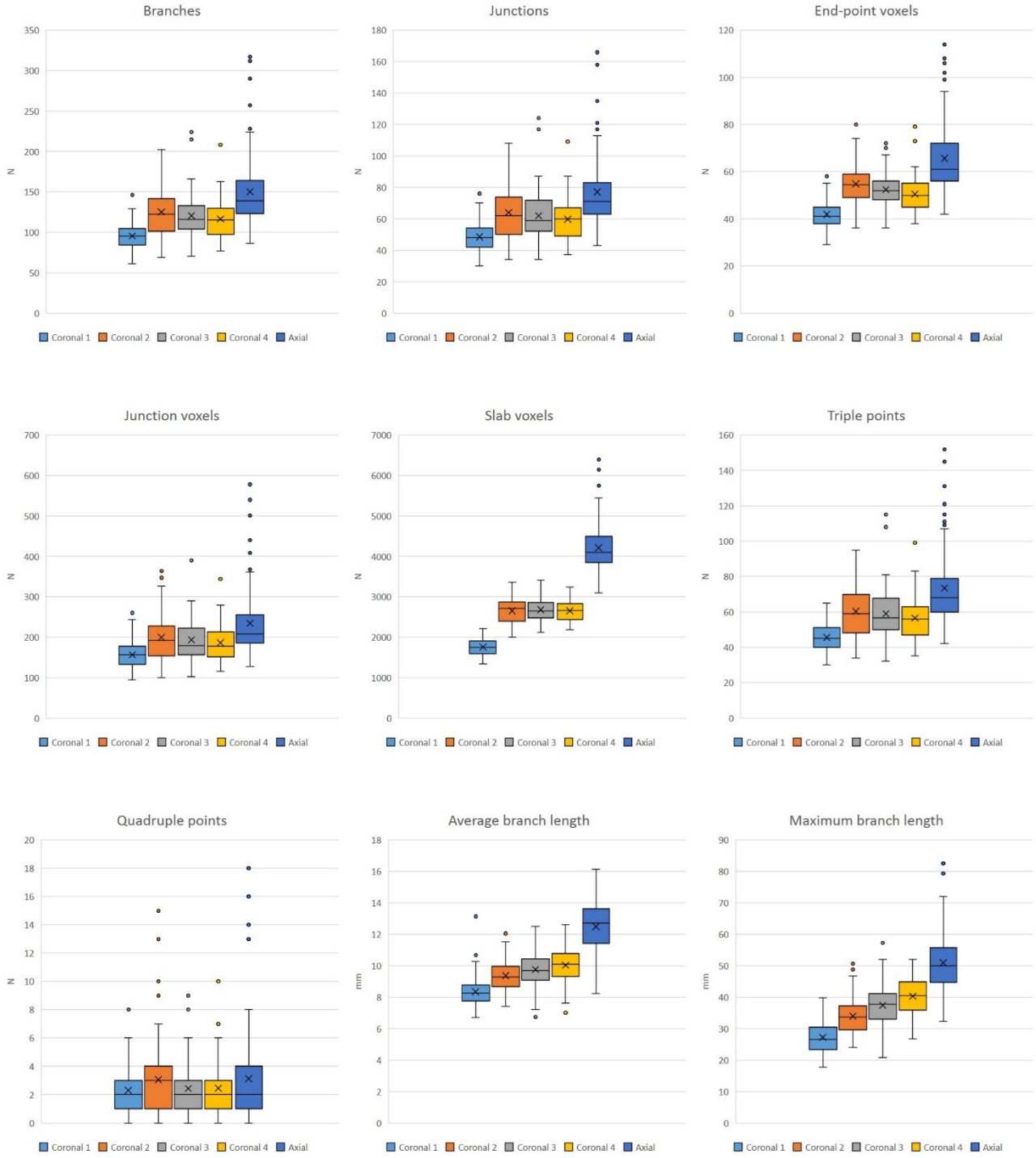

Fig. 3. Distributions of values of quantitative parameters of cerebral hemispheres skeletonized images.

quantitative parameters of the skeletonized images and the traditional morphometric characteristics of the cerebral hemispheres (Fig. 6). It was established that the values of perimeters (P_0, P_s), area (S_0, S_s) of non-segmented and segmented images, as well as their ratio (P_s/P_0, S_s/S_0) are related to most quantitative parameters (with the exception of average branch length and maximum branch length) by positive correlations, while parameters P_0/S_0 and SF_s are related to the same parameters by negative correlations. Attention is also drawn to exceptions from the general regularity: S_s/S_0 parameter of axial sections, unlike coronal sections, is related to the values of the quantitative parameters of the digital skeleton by negative, not positive, correlations; and when examining the sample, which

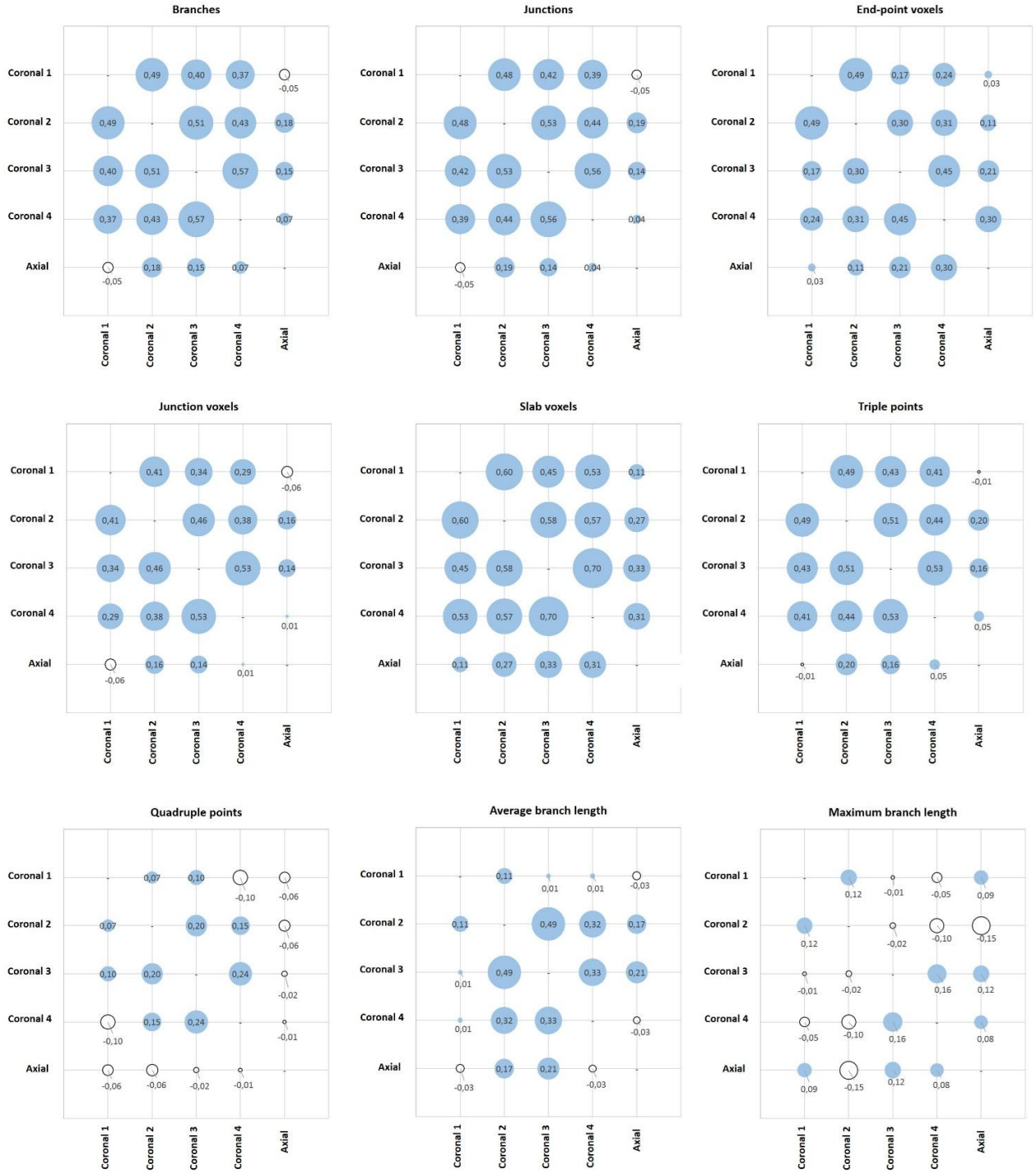

Fig. 4. Correlations of the values of quantitative parameters of skeletonized images of different localization tomographic sections; values of Pearson's correlation coefficients (r) are given.

includes all sections, negative correlations between the P_s/S_s parameter and most of the studied quantitative parameters are revealed. The rest of the morphometric parameters are related to the values of the quantitative parameters by correlations of different strength and direction, which differ in different tomographic sections (see Fig. 6).

At the fourth stage of the correlation analysis, we investigated the correlations between the values of the fractal dimension, the quantitative parameters of the skeletonized images, and the traditional morphometric characteristics (Table 2). The parameters branches,

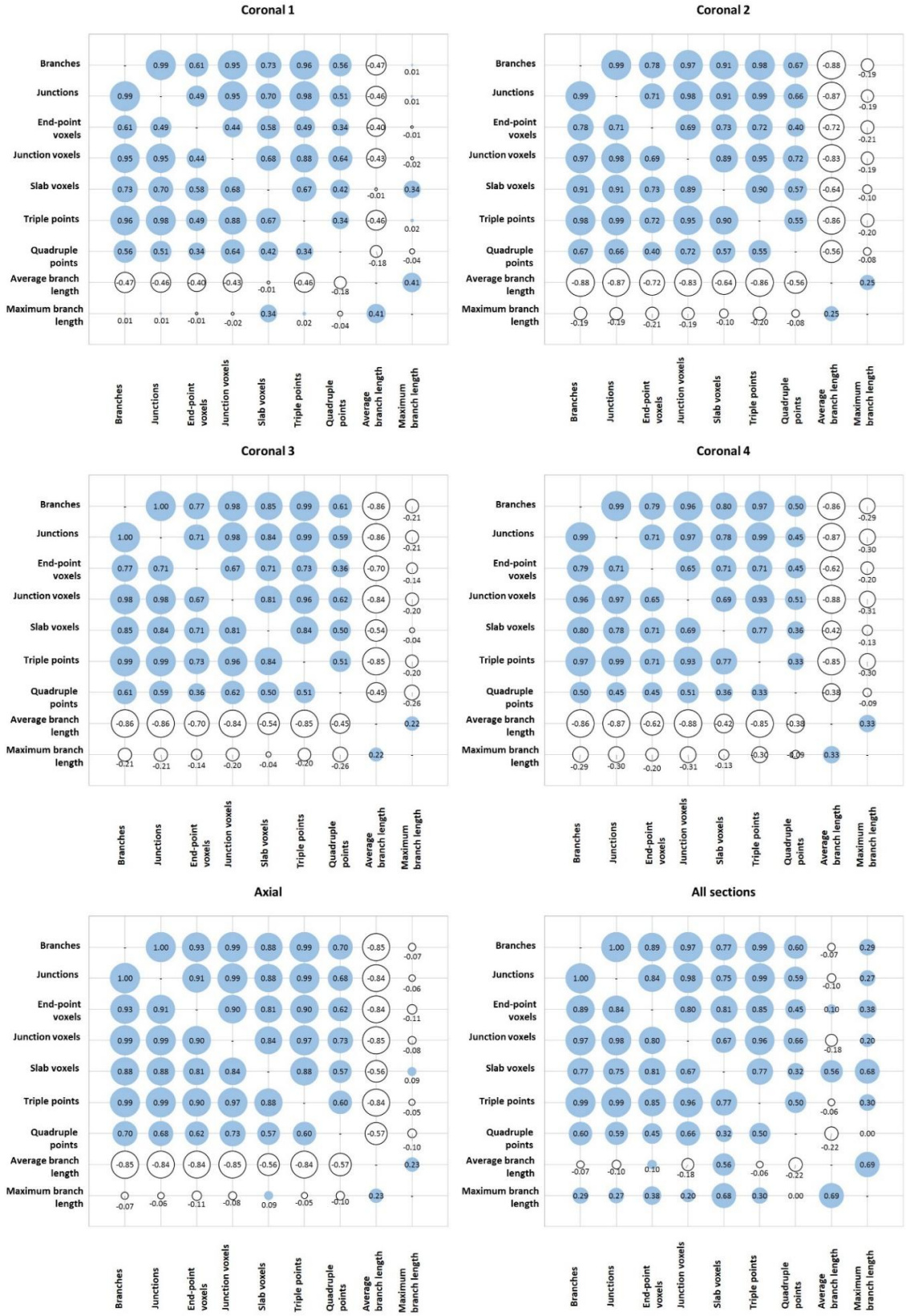

Fig. 5. Correlations of the values of quantitative parameters of skeletonized images of the cerebral hemispheres; values of Pearson's correlation coefficients (r) are given.

Fig. 6. Correlations of the values of quantitative parameters of skeletonized images and traditional morphometric parameters of the cerebral hemispheres; values of Pearson's correlation coefficients (r) are given.

Table 2. Correlation relationships of fractal dimension values with the values of quantitative parameters of skeletonized images and traditional morphometric parameters of the cerebral hemispheres.

Parameter of skeletonized image	Tomographic section					
	Coronal 1	Coronal 2	Coronal 3	Coronal 4	Axial	All sections
Branches	0.668***	0.871***	0.867***	0.834***	0.821***	0.229***
Junctions	0.677***	0.869***	0.871***	0.851***	0.822***	0.261***
End-point voxels	0.276**	0.631***	0.604***	0.521***	0.736***	-0.015
Junction voxels	0.678***	0.851***	0.858***	0.812***	0.813***	0.327***
Slab voxels	0.339***	0.811***	0.743***	0.668***	0.743***	-0.271***
Triple points	0.628***	0.843***	0.857***	0.830***	0.806***	0.217***
Quadruple points	0.414***	0.656***	0.560***	0.456***	0.630***	0.364***
Average branch length	-0.403***	-0.759***	-0.770***	-0.699***	-0.757***	-0.724***
Maximum branch length	-0.063	-0.203*	-0.162	-0.205*	0.013	-0.469***
P_0	-0.305**	-0.102	-0.166	-0.244*	-0.036	-0.605***
S_0	-0.348***	-0.025	-0.209*	-0.211*	0.060	-0.505***
P_0/S_0	0.315***	-0.078	0.177	0.137	-0.126	0.311***
SF_0	-0.171	0.172	-0.029	0.116	0.081	0.191***
P_s	-0.085	0.355***	0.041	0.062	0.395***	-0.433***
S_s	-0.201*	0.064	-0.136	-0.110	-0.182	-0.511***
P_s/S_s	0.125	0.261**	0.138	0.149	0.526***	0.582***
SF_s	-0.002	-0.341***	-0.070	-0.095	-0.468***	-0.185***
P_s/P_0	0.059	0.462***	0.137	0.221*	0.476***	0.234***
S_s/S_0	0.256*	0.203*	0.133	0.236*	-0.146	-0.111**

Notes: the table shows the values of Pearson's correlation coefficients (r); * - p<0.05; ** - p<0.01; *** - p<0.001.

Table 3. Correlation relationships between age and the values of quantitative parameters of skeletonized images of the cerebral hemispheres.

Parameter of skeletonized image	Tomographic section					
	Coronal 1	Coronal 2	Coronal 3	Coronal 4	Axial	All sections
Branches	-0.502***	-0.386***	-0.248*	-0.387***	0.151	-0.160***
Junctions	-0.507***	-0.384***	-0.269**	-0.414***	0.153	-0.175***
End-point voxels	-0.301**	-0.291**	-0.058	-0.162	0.145	-0.057
Junction voxels	-0.435***	-0.385***	-0.246*	-0.411***	0.140	-0.178***
Slab voxels	-0.508***	-0.452***	-0.312**	-0.370***	0.010	-0.093*
Triple points	-0.522***	-0.374***	-0.274**	-0.415***	0.166	-0.168***
Quadruple points	-0.167	-0.255**	-0.046	-0.059	0.007	-0.097*
Average branch length	0.120	0.231*	0.128	0.307**	-0.290**	0.040
Maximum branch length	-0.114	-0.185	-0.151	0.098	-0.025	-0.038

Notes: the table shows the values of Pearson's correlation coefficients (r); * - p<0.05; ** - p<0.01; *** - p<0.001.

junctions, end-point voxels, junction voxels, slab voxels, triple points, quadruple points were associated with the values of the fractal dimension by positive correlations; the parameters average branch length, maximum branch length were related to the values of the fractal dimension of most slices by negative correlations. Traditional morphometric parameters, in comparison with the quantitative parameters of skeletonized images, had a lower correlation strength with the values of the fractal dimension, the strength and directionality of which differed depending on the tomographic section (see Table 2).

At the fifth stage of the correlation analysis, we determined the presence and nature of correlation relationships between age and the values of quantitative parameters of skeletonized images of the cerebral hemispheres (Table 3). It turned out that most of the quantitative characteristics (except for quadruple points and maximum branch length and partially average branch

length) of all coronal sections had statistically significant negative correlations with age (however, the corresponding parameters of the axial section did not have significant relationships with age).

Discussion

Structural and spatial complexity is an important parameter that allows you to qualitatively add to the arsenal of morphological characteristics for the study of structures of irregular shape, including cerebral hemispheres. In most meanings, structural complexity and spatial complexity are very close and practically synonymous concepts and characterize the complexity of the spatial configuration. In addition to this value, structural complexity describes the complexity of not only the form, but also the actual internal structure of certain anatomical formations and can characterize the number and variety of elements that make up the studied structure (for example, the branches of the digital skeleton). An increase in structural complexity leads to an increase in the complexity of the spatial configuration (form), and therefore to an increase in spatial complexity.

Despite the relative novelty of fractal analysis as a morphometric method, the fractal dimension has become the "gold standard" for evaluating the structural and spatial complexity of the configuration of various natural structures, including the cerebral hemispheres [3-5, 8, 10, 11, 16, 19, 21, 22, 24, 26-28].

The spatial and structural complexity and, accordingly, the value of the fractal dimension of the cerebral hemispheres can be influenced by various factors. In this paper, we analyzed the correlations of fractal dimension values of skeletonized images of the cerebral hemispheres with two groups of parameters: with traditional morphometric parameters (perimeter, area, and their derivatives), and with quantitative parameters of skeletonized images. Most traditional morphometric parameters had no statistically significant correlations or weak correlations with fractal dimension values. Most of the quantitative parameters of skeletonized images had statistically significant strong or moderate correlations with fractal dimension values. Therefore, it can be considered that the quantitative parameters of skeletonized images are representative for evaluating the spatial and structural complexity of the cerebral hemispheres, in contrast to traditional morphometric parameters.

We divided the quantitative parameters of skeletonized images into two groups. The first included branches, junctions, end-point voxels, junction voxels, slab voxels, triple points, quadruple points. These parameters were related to each other and to the values of the fractal dimension by positive correlations. The second group of parameters includes average branch length, maximum branch length. These parameters are connected with each other by positive correlations, but with most of the parameters of the first group and with the values of the fractal dimension, they had negative correlations. Therefore, the increase in the spatial and structural complexity of the shape of the cerebral hemispheres, which is reflected in the increase in the values of the fractal dimension, is accompanied by an increase in the number and decrease in the length of the branches of the digital skeleton, an increase in the number of connections and end points of the branches, and the number of voxels forming the skeleton. Therefore, the digital skeletons of the hemispheres, which have more convolutions and a more complex shape, are characterized by higher values of the fractal dimension and consist of a relatively large number of relatively short branches. Conversely, the digital skeletons of the hemispheres, which have a less complex configuration, have smaller values of fractal dimension and consist of a small number of relatively long branches. Similar regularities were also revealed as a result of quantitative analysis of skeletonized images of cerebellar white matter [15].

The relatively large age range of the studied sample allowed us to analyze correlations between age and quantitative parameters of skeletonized images. We found that the values of most of the studied parameters decrease with age. This is consistent with a decrease in the values of the fractal dimension and other morphometric parameters of the brain as a result of atrophic changes during normal aging [5, 16, 20, 27] and caused by neurodegenerative diseases [10]. Reducing the volume, smoothing the surface and expanding the grooves of the brain in the complex can lead to a simplification of the spatial configuration of the brain, which in turn will lead to a simplification of the configuration of digital skeletons. However, the described changes were not detected when analyzing the parameters of axial slices and when examining the sample that includes all slices. Therefore, it can be considered that coronal sections are more representative for characterizing age-related changes. A similar regularity was found in our previous work in the study of age-related dynamics of fractal dimension [16].

The number of endpoints of the digital skeleton allows us to indirectly characterize the number of convolutions forming the studied silhouette of the hemispheres. The number of gyri after the completion of their formation is an invariable anatomical characteristic, so the number of endpoints almost does not change during life. The existing weak negative correlations with age can be explained by the fact that sometimes gyri with a complex shape can form not one, but several points of the digital skeleton. Simplifying the shape of the convolutions and the overall silhouette may in some cases lead to a slight reduction in the number of endpoints.

Conclusion

Quantitative analysis of skeletonized images of allows to supplement the arsenal of morphometric methods of both morphology and clinical neuroscience. Quantitative parameters and fractal dimension of skeletonized images

are the most relevant morphological parameters for characterizing the spatial and structural complexity of the shape of the cerebral hemispheres. Quantitative assessment of the shape of the brain, including spatial and structural complexity, can become an informative tool for the diagnosis of some nervous diseases and the differentiation of pathological and normal age-related changes.

References

[1] Avtandilov, G. G. (1990). *Медицинская морфометрия [Medical morphometry].* Москва: Медицина - Moscow: Medicina.

[2] Baykara, E., Gesierich, B., Adam, R., Tuladhar, A. M., Biesbroek, J. M., Koek, H. L., … & Duering, M. (2016). A Novel Imaging Marker for Small Vessel Disease Based on Skeletonization of White Matter Tracts and Diffusion Histograms. *Annals of neurology,* 80(4), 581-592. doi: 10.1002/ana.24758

[3] Esteban, F. J., Sepulcre, J., de Mendizabal, N. V., Goni, J., Navas, J., de Miras, J. R., … & Villoslada, P. (2007). Fractal dimension and white matter changes in multiple sclerosis. *NeuroImage,* 36(3), 543-549. doi: 10.1016/j.neuroimage.2007.03.057

[4] Esteban, F. J., Sepulcre, J., de Miras, J. R., Navas, J., de Mendizabal, N. V., Goni, J., … & Villoslada, P. (2009). Fractal dimension analysis of grey matter in multiple sclerosis. *Journal of the neurological sciences,* 282(1-2), 67-71. doi: 10.1016/j.jns.2008.12.023

[5] Farahibozorg, S., Hashemi-Golpayegani, S. M., & Ashburner, J. (2015). Age- and sex-related variations in the brain white matter fractal dimension throughout adulthood: an MRI study. *Clinical neuroradiology,* 25(1), 19-32. doi: 10.1007/s00062-013-0273-3

[6] Frey, B. M., Petersen, M., Schlemm, E., Mayer, C., Hanning, U., Engelke, K., … & Cheng, B. (2021). White matter integrity and structural brain network topology in cerebral small vessel disease: The Hamburg city health study. *Human brain mapping,* 42(5), 1406-1415. doi: 10.1002/hbm.25301

[7] Greenblum, A., Sznitman, R., Fua, P., Arratia, P. E., Oren, M., Podbilewicz, B., & Sznitman, J. (2014). Dendritic tree extraction from noisy maximum intensity projection images in C. elegans. *Biomedical engineering online,* 13, 74. doi: 10.1186/1475-925X-13-74

[8] Ha, T. H., Yoon, U., Lee, K. J., Shin, Y. W., Lee, J. M., Kim, I. Y., … & Kwon, J. S. (2005). Fractal dimension of cerebral cortical surface in schizophrenia and obsessive-compulsive disorder. *Neuroscience letters,* 384(1-2), 172-176. doi: 10.1016/j.neulet.2005.04.078

[9] Jelinek, H. F., & Fernandez, E. (1998). Neurons and fractals: how reliable and useful are calculations of fractal dimensions?. *Journal of neuroscience methods,* 81(1-2), 9-18. doi: 10.1016/s0165-0270(98)00021-1

[10] King, R. D., George, A. T., Jeon, T., Hynan, L. S., Youn, T. S., Kennedy, D. N., … & the Alzheimer's Disease Neuroimaging Initiative (2009). Characterization of Atrophic Changes in the Cerebral Cortex Using Fractal Dimensional Analysis. *Brain imaging and behavior*, 3(2), 154-166. doi: 10.1007/s11682-008-9057-9

[11] Lee, J. M., Yoon, U., Kim, J. J., Kim, I. Y., Lee, D. S., Kwon, J. S., & Kim, S. I. (2004). Analysis of the hemispheric asymmetry using fractal dimension of a skeletonized cerebral surface. *IEEE transactions on bio-medical engineering,* 51(8), 1494-1498. doi: 10.1109/TBME.2004.831543

[12] Liu, J. Z., Zhang, L. D., & Yue, G. H. (2003). Fractal dimension in human cerebellum measured by magnetic resonance imaging. *Biophysical journal,* 85(6), 4041-4046. doi: 10.1016/S0006-3495(03)74817-6

[13] Low, A., Mak, E., Stefaniak, J. D., Malpetti, M., Nicastro, N., Savulich, G., … & O'Brien, J. T. (2020). Peak Width of Skeletonized Mean Diffusivity as a Marker of Diffuse Cerebrovascular Damage. *Frontiers in neuroscience*, 14, 238. doi: 10.3389/fnins.2020.00238

[14] Mandelbrot, B. B. (1983). *The fractal geometry of nature.* N.Y.: W. H. Freeman&Co.

[15] Maryenko, N., & Stepanenko, O. (2021). Characterization of white matter branching in human cerebella: quantitative morphological assessment and fractal analysis of skeletonized MR images. *Biomedical Research and Therapy,* 8(5), 4345-4357. doi: 10.15419/bmrat.v8i5.673

[16] Maryenko, N. I., & Stepanenko, O. Y. (2022). Fractal dimension of skeletonized MR images as a measure of cerebral hemispheres spatial complexity. *Reports of Morphology,* 28(2), 40-47. doi: 10.31393/morphology-journal-2022-28(2)-06

[17] Milosevic, N. T., & Ristanovic, D. (2006). Fractality of dendritic arborization of spinal cord neurons. *Neurosci Lett,* 396(3), 172-176. doi: 10.1016/j.neulet.2005.11.031

[18] Orlowski, D., & Bjarkam, C. R. (2012). A simple reproducible and time saving method of semi-automatic dendrite spine density estimation compared to manual spine counting. *J Neurosci Methods,* 208(2), 128-133. doi: 10.1016/j.jneumeth.2012.05.009

[19] Pantoni, L., Marzi, C., Poggesi, A., Giorgio, A., De Stefano, N., Mascalchi, M., … & Diciotti, S. (2019). Fractal dimension of cerebral white matter: A consistent feature for prediction of the cognitive performance in patients with small vessel disease and mild cognitive impairment. *NeuroImage Clinical*, 24, 101990. doi: 10.1016/j.nicl.2019.101990

[20] Podgorski, P., Bladowska, J., Sasiadek, M., & Zimny, A. (2021). Novel Volumetric and Surface-Based Magnetic Resonance Indices of the Aging Brain - Does Male and Female Brain Age in the Same Way?. *Frontiers in neurology,* 12, 645729. doi: 10.3389/fneur.2021.645729

[21] Rajagopalan, V., Das, A., Zhang, L., Hillary, F., Wylie, G. R., & Yue, G. H. (2019). Fractal dimension brain morphometry: a novel approach to quantify white matter in traumatic brain injury. *Brain imaging and behavior,* 13(4), 914-924. doi: 10.1007/s11682-018-9892-2

[22] Rajagopalan, V., Liu, Z., Allexandre, D., Zhang, L., Wang, X. F., Pioro, E. P., & Yue, G. H. (2013). Brain white matter shape changes in amyotrophic lateral sclerosis (ALS): a fractal dimension study. *PloS one,* 8(9), e73614. doi: 10.1371/journal.pone.0073614

[23] Raposo, N., Zanon Zotin, M. C., Schoemaker, D., Xiong, L., Fotiadis, P., Charidimou, A., … & Viswanathan, A. (2021). Peak Width of Skeletonized Mean Diffusivity as Neuroimaging Biomarker in Cerebral Amyloid Angiopathy. *AJNR. American journal of neuroradiology,* 42(5), 875-881. doi: 10.3174/ajnr.A7042

[24] Roura, E., Maclair, G., Andorra, M., Juanals, F., Pulido-Valdeolivas, I., Saiz, A., … & Villoslada, P. (2021). Cortical fractal dimension predicts disability worsening in Multiple Sclerosis patients. *NeuroImage. Clinical,* 30, 102653. doi: 10.1016/j.nicl.2021.102653

[25] Schneider, C. A., Rasband, W. S., & Eliceiri, K. W. (2012). NIH

Image to ImageJ: 25 years of image analysis. *Nature methods,* 9(7), 671-675. doi: 10.1038/nmeth.2089

[26] Zhang, L., Butler, A. J., Sun, C. K., Sahgal, V., Wittenberg, G. F., & Yue, G. H. (2008). Fractal dimension assessment of brain white matter structural complexity post stroke in relation to upper-extremity motor function. *Brain research,* 1228, 229-240. doi: 10.1016/j.brainres.2008.06.008

[27] Zhang, L., Dean, D., Liu, J. Z., Sahgal, V., Wang, X., & Yue, G. H. (2007). Quantifying degeneration of white matter in normal aging using fractal dimension. *Neurobiology of aging,* 28(10), 1543-1555. doi: 10.1016/j.neurobiolaging.2006.06.020

[28] Zhang, L., Liu, J. Z., Dean, D., Sahgal, V., & Yue, G. H. (2006). A three-dimensional fractal analysis method for quantifying white matter structure in human brain. *Journal of neuroscience methods,* 150(2), 242-253. doi: 10.1016/j.jneumeth.2005.06.021

ФОРМА ВЕЛИКИХ ПІВКУЛЬ ГОЛОВНОГО МОЗКУ: СТРУКТУРНА ТА ПРОСТОРОВА СКЛАДНІСТЬ. КІЛЬКІСНИЙ АНАЛІЗ СКЕЛЕТОНОВАНИХ МР-ЗОБРАЖЕНЬ

Мар'єнко Н. І., Степаненко О. Ю.

Для кількісного характеризування складності просторової конфігурації анатомічних структур, у тому числі великих півкуль головного мозку, найчастіше використовується фрактальний аналіз, крім якого досить перспективними є й інші методи аналізу зображень, у тому числі кількісний аналіз скелетонованих зображень. Мета дослідження - визначити особливості структурної та просторової складності форми великих півкуль головного мозку за допомогою кількісного аналізу скелетонованих магнітно-резонансних зображень великих півкуль головного мозку. У якості матеріалу дослідження було використано магнітно-резонансні томограми головного мозку 100 умовно здорових осіб (які не мали структурних змін головного мозку) обох статей (жінок 56, чоловіків 44) віком 18-86 років (середній вік 41,72±1,58 років). Із набору томографічних зображень кожного мозку було відібрано 5 томографічних зрізів (4 - у корональній проекції, 1 - у аксіальній). Під час попередньої обробки проводилася сегментація зображень із отриманням бінарного силуетного зображення, після чого проводилося скелетонування силуету. Кількісний аналіз скелетонованих зображень включав визначення таких параметрів: branches, junctions, end-point voxels, junction voxels, slab voxels, triple points, quadruple points, average branch length, maximum branch length. Ми розділили кількісні параметри скелетонованих зображень на дві групи. До першої увійшли branches, junctions, end-point voxels, junction voxels, slab voxels, triple points, quadruple points. Ці параметри були пов'язані між собою та зі значеннями фрактальної розмірності позитивними кореляційними зв'язками. До другої групи параметрів увійшли average branch length, maximum branch length. Ці параметри були пов'язані між собою позитивними кореляційними зв'язками, але з більшістю параметрів першої групи та зі значеннями фрактальної розмірності вони мали негативні кореляційні зв'язки. Кількісні параметри та фрактальна розмірність виявилися кращими параметрами для характеризування просторової та структурної складності форми великих півкуль головного мозку, ніж традиційні морфометричні параметри (площа, периметр та їх похідні). Виявлено, що значення більшості досліджених кількісних параметрів зменшуються з віком, корональні зрізи виявилися найбільш репрезентативними для характеризування вікових змін. Кількісне оцінювання форми головного мозку, у тому числі просторової та структурної складності, може стати інформативним інструментом для діагностики деяких нервових захворювань та диференціювання патологічних та нормальних вікових змін.

Ключові слова: *головний мозок, великі півкулі головного мозку, морфометрія, скелетонування, фрактальна розмірність.*

REQUIREMENTS FOR ARTICLES

For publication, scientific articles are accepted only in English only with translation on Ukrainian, which contain the following necessary elements: UDC code; title of the article (in English and Ukrainian); surname, name and patronymic of the authors (in English and Ukrainian); the official name of the organization (institution) (in English and Ukrainian); city, country (in English and Ukrainian); structured annotations (in English and Ukrainian); keywords (in English and Ukrainian); introduction; purpose; materials and methods of research; research results; discussion; conclusions; bibliographic references.

The title of the article briefly reflects its contents and contains no more than 15 words.

Abstract. The volume of the annotation is 1800-2500 characters without spaces. The text of an annotation in one paragraph should not contain general phrases, display the main content of the article and be structured. The abstract should contain an introductory sentence reflecting the relevance of the study, the purpose of the study, a brief description of the methods of conducting research (2-3 sentences with the mandatory provision of the applied statistical methods), a description of the main results (50-70% of the volume of the abstract) and a concise conclusion (1 sentence). The abstract should be clear without familiarizing the main content of the article. Use the following expressions: "Detected ...", "Installed ...", "Fixed ...", "Impact assessed ...", "Characterized by regularities ...", etc. In an annotation, use an active rather than passive state.

Keywords: 4-6 words (or phrases).

"Introduction"

The introduction reflects the state of research and the relevance of the problem according to the world scientific literature (at least 15 references to English articles in international journals over the past 5 years). At the end of the entry, the purpose of the article is formulated (contains no more than 2-3 sentences, in which the problem or hypothesis is addressed, which is solved by the author).

"Materials and methods"

The section should allow other researchers to perform similar studies and check the results obtained by the author. If necessary, this section may be divided into subdivisions. Depending on the research objects, the ethical principles of the European Convention for the protection of vertebrate animals must be observed; Helsinki Declaration; informed consent of the surveyed, etc. (for more details, see "Public Ethics and its Conflict"). At the end of this section, a "statistical processing of results" section is required, which specifies the program and methods for processing the results obtained by the automobile.

"Results"

Requirements for writing this section are general, as well as for all international scientific publications. The data is presented clearly, in the form of short descriptions, and must be illustrated by color graphics (no more than 4) or drawings (no more than 8) and tables (no more than 4), the information is not duplicated.

"Discussion"

In the discussion, it is necessary to summarize and analyze the results, as possible, compare them with the data of other researchers. It is necessary to highlight the novelty and possible theoretical or practical significance of the results of the research. You should not repeat the information already listed in the "Introduction" section. At the end of the discussion, a separate paragraph should reflect the prospects for using the results obtained by the author.

"Conclusion"

5-10 sentences that summarize the work done (in the form of paragraphs or solid text).

"Acknowlegements"

Submitted after conclusion before bibliographic references.

"References"

References in the text are indicated by Arabic numerals in square brackets according to the numerology in the list of references. The list of references (made without abbreviations) sorted by alphabet, in accordance with the requirements of APA Style (American Psychological Association Style): with the obligatory referencing of all authors, work titles, journal names, or books (with obligatory publication by the publishing house, and editors when they are available), therefore, numbers or releases and pages. In the Cyrillic alphabets references, give the author's surnames and initials in English (Cyrillic alphabet in brackets), the title of the article or book, and the name of the magazine or the publisher first to be submitted in the original language of the article, and then in square brackets in English. If available, doi indexes must be provided on www.crossref.org (at least 80% of the bibliographic references must have their own doi indexes). Links to online publications, abstracts and dissertations are not welcome.

After the list of references, it is necessary to provide information about all authors (in English, Ukrainian and Russian): last name, first name and patronymic of the author, degree, place of work and position, **ORCID number** (each of the authors of the ORCID personal number if absence - free creation on the official website http://www.orcid.org) to facilitate the readers of this article to refer to your publications in other scientific publications.

The last page of the text should include the surname, name and patronymic of the author, degree, postal address, telephone number and e-mail of the author, with which the editors will maintain contact.

Concluding remarks

The manuscript should be executed in such a way that the number of refinements and revisions during the editorial of the article was minimal.

When submitting the article, please observe the following requirements. The volume of the article - not less than 15 and not more than 25 pages, Times New Roman, 14 pt, line spacing - one and a half, fields - 2 cm, sheet A4. Text materials should be prepared in the MS Word editor (* .docx), without indentations. Math formulas and equations to prepare in the embedded editor; graphics - in MS Excel. Use the units of the International Measurement System. Tables and drawings must contain the name, be numbered, and references to them in the text should be presented as follows: (fig. 1), or (table 1). The drawings should be in the format "jpg" or "tif"; when scanned, the resolution should be at least 800 dpi; when scanning half-tone and color images, the resolution should be at least 300 dpi. All figures must be represented in the CMYK palette. The statistical and other details are given below the table in the notes. Table materials and drawings place at the end of the text of the manuscript. All elements of the text in images (charts, diagrams, diagrams) must have the Times New Roman headset.

Articles are sent to the editorial board only in electronic form (one file) at the e-mail address nila@vnmu.edu.ua

Responsible editor - Gunas Igor Valeryovich (phone number: + 38-067-121-00-05; e-mail: igor.v.gunas@gmail.com).

Signed for print 05.09.2022
Format 60x84/8. Printing offset. Order № 2917. Circulation 100.
Vinnytsia. Printing house “TVORY”, Nemyrivske shose St., 62a,
Vinnytsya, 21034
Phone: 0 (800) 33-00-90, (096) 97-30-934, (093) 89-13-852,
(098) 46-98-043
e-mail: tvory2009@gmail.com
http://www.tvoru.com.ua